SEISMIC STABILITY EVALUATIONS OF CHESBRO, LENIHAN, STEVENS CREEK, AND UVAS DAMS (SSE2)

PHASE A: STEVENS CREEK AND LENIHAN DAMS

LENIHAN DAM

SITE CHARACTERIZATION, MATERIAL PROPERTIES, AND GROUND MOTIONS
(REPORT No. LN-3)

Prepared for

SANTA CLARA VALLEY WATER DISTRICT
5750 Almaden Expressway
San Jose, CA 95118

April 2012

TERRA / GeoPentech
a Joint Venture

TABLE OF CONTENTS

TABLE OF CONTENTS

Tables

TABLE OF CONTENTS

Figures

1.1 GENERAL

In May 2010, the Santa Clara Valley Water District (District) retained Terra / GeoPentech (TGP), a joint venture of Terra Engineers, Inc. and GeoPentech, Inc., to complete seismic stability evaluations of Chesbro, Lenihan, Stevens Creek and Uvas Dams. These evaluations were required by the Division of Safety of Dams (DSOD) in June 2008 as part of their Phase III screening process of the State's dams located in highly seismic environments. The evaluations are also a vital part of the District's Dam Safety Program (DSP). Phase A of the project includes work on Stevens Creek and Lenihan Dams and has a planned completion date of 2012. Phase B of the project includes work on Chesbro and Uvas Dams and is scheduled to begin in 2012 and to finish by the end of 2013. The general scope of the project consists of the field, laboratory, and office studies required to evaluate the seismic stability of the four referenced dams.

This document contains the results of our site characterization at James J. Lenihan Dam (Lenihan Dam) based on the data available from the dam construction records, the field investigations and laboratory tests completed by prior investigators, and the results of supplemental site investigations and laboratory testing completed in 2011 (Terra/GeoPentech, 2011b).

The purpose of the site characterization is to:

1. summarize the geology of the site;
2. describe the conditions of the dam and foundation, and characterize the material properties to be used in the engineering analyses for the seismic evaluation of the dam; and
3. provide ground motions to be used in the seismic deformation analyses of the dam.

The scope of the site characterization includes the following activities:

1. Review of design and construction history including modifications and previous evaluations;
2. Review and evaluation of engineering geology data;
3. Review and evaluation of information on faulting;
4. Review and evaluation of construction data;
5. Review and evaluation of dam monitoring data;
6. Review and evaluation of ground motion data;
7. Evaluation of laboratory data and development of static and dynamic engineering properties for embankment, foundation soils, and rock; and
8. Selection of earthquake ground motions for use in the seismic deformation analyses of the dam.

1.2 ORGANIZATION OF DOCUMENT

This document contains eight sections, including this introduction. Section 2.0 describes the site and the history of Lenihan Dam including its construction, its documented performance during earthquakes, and the various investigations and studies that were conducted at the dam by a number of investigators. Section 3.0 discusses the site geology, including regional and local

conditions, and Section 4.0 addresses the foundation conditions at the dam. The various zones incorporated into the dam embankment and the characterization of the embankment material properties within these zones are discussed in Section 5.0. Section 6.0 documents the development of ground motions for use in the dynamic analyses and Section 7.0 provides a summary of the key findings of the site characterization. Section 8.0 is a list of references.

2.1 GENERAL

James J. Lenihan Dam (formerly called Lexington Dam) is located in Santa Clara County, California, about 1 mile south of the City of Los Gatos, as shown on Figure 2-1. The dam is an earthfill structure that was constructed across Los Gatos Creek in 1952. The dam impounds Lexington Reservoir, which has a maximum capacity of 19,044 acre-feet at the spillway elevation of 653 feet[1]. DSOD has classified Lenihan Dam as a "High Hazard" dam because of the "extensive urban development in close proximity of the dam" (DSOD, 1981), with a DSOD Hazard Classification Total Class Weight of 30.

Appurtenant structures include a concrete-lined ogee type spillway located in the left abutment and an outlet tunnel through the right abutment connected to an inclined inlet structure in the reservoir, on the upstream side of the right abutment, and to an outlet structure that allows reservoir water to discharge into Los Gatos Creek approximately 150 feet beyond the toe of the dam. The outlet tunnel and inclined inlet structure were completed in 2009 and replaced the original outlet pipe that generally followed the preconstruction thalweg of Los Gatos Creek beneath the dam. The original outlet pipe was filled with grout and abandoned in place in 2009.

2.2 DAM AND APPURTENANT STRUCTURES

Figure 2-2A is an aerial photograph of Lenihan Dam that shows the outline of the embankment, the limits of Figures 2-2B and 2-2C, and an overview of the locations of previous explorations that are discussed in Section 2.4. Figures 2-2B and 2-2C provide larger scale location plans that include labels with the identifying name of the exploration (boring, test pit, or Cone Penetrometer Test [CPT] probe). Figure 2-2D shows the location and labels of instruments (piezometers and inclinometers) that were installed in the borings. Borings that extended to rock are identified using larger symbols, as shown in the legend on Figures 2-2B to 2-2D.

Figure 2-3 contains transverse sections through the current configuration of the dam at Stations 14+10 and 15+95 that are representative of dam zoning and conditions near the center of the valley. The locations of the two sections are shown on Figures 2-2 (A through D). These sections have been heavily instrumented with piezometers, and the piezometer locations are shown on the sections. In some cases (e.g., LVP-19), it was necessary to project the location of piezometers installed at nearby dam stations onto the sections shown and, in the case of LVP-19, this caused a piezometer that was actually installed in the embankment to be shown as located in rock on Section B-B' of Figure 2-3. The location of previous borings are not shown on the cross-sections of Figure 2-3 for clarity but their plan locations are shown on Figures 2-2B and 2-2C, and the information from these borings on depth to rock is presented and discussed in Section 4.0.

As shown on Figure 2-3, Lenihan Dam was constructed as a compacted earth dam with upstream and downstream shells, core and drainage zones. The core is further divided into the upper core and lower core to reflect significant differences in material properties above and below elevation 590 feet. The dam is about 195 feet high as measured from the lowest point in the

[1] Unless otherwise noted in this document, all elevations are referenced to NAVD88 vertical datum.

foundation beneath the axis to the crest, and about 207 feet high as measured from the lowest point of the downstream toe to the crest.

Following the Loma Prieta Earthquake, it was determined that the crest of the dam had settled about 2.3 feet since construction because of a combination of long-term consolidation and seismically-induced deformation from the earthquake. The crest was subsequently raised by up to 4.5 feet, and the spillway chute walls raised by up to 6 feet, during the 1996-1997 freeboard restoration project. Thus, the crest is currently at nominal elevation 673 feet and is about 40 feet wide, 830 feet long, and cambered. In general, the upstream face is inclined at 5.25 to 5.5 Horizontal to 1 Vertical (5.25 to 5.5H:1V). The downstream slope is inclined at 2.5 to 3H:1V. The concrete-lined, un-gated ogee crest spillway is located on the left abutment, with a nominal spillway crest elevation of 653 feet.

The original low level outlet pipe was extensively investigated after it experienced several partial collapses of the steel liner. The investigation showed that this occurred because of excess external pressure combined with vacuum pressures, corrosion, and out of roundness, and the outlet was subsequently repaired. The low level outlet was replaced by an outlet tunnel through the right abutment in 2009. The low level outlet pipe was filled with grout after completion of the outlet tunnel.

2.3 DESIGN AND CONSTRUCTION HISTORY

2.3.1 Initial Design and Construction

A relatively complete summary of the initial design and construction history of the dam and spillway was presented in the Phase 1 Inspection Report prepared by DSOD for the US Army Corps of Engineers (DSOD, 1981). The reader is referred to this document for construction details that are not repeated herein.

The following milestone dates associated with the original design and construction have been selected based on a review of DSOD files by TGP in order to allow discussion of some of the unusual features of the dam construction that may be relevant to understanding subsequent site exploration and dam monitoring data.

February 1948	District submits Application for Approval of Plans and Specifications to DSOD.
December 1951	District begins stripping of abutments and excavation for outlet pipe using District forces, after California Department of Highways completed relocation of Highway 17 adjacent to dam site.
April 1952	District submits amended Application for Approval of Plans and Specifications to DSOD.

May 1952	District awards contract for construction of dam and spillway to Guy F. Atkinson Construction Company.
June 13, 1952	DSOD Consulting Board recommends relocation of dam axis 60 feet upstream at the right abutment and 60 feet downstream at the left abutment. The move on the right abutment would allow avoiding contact of core materials with large rock masses exposed on that abutment. The move on the left abutment would better align the upstream face of the dam and spillway with sound material in that area.
June 1952	Placement of fill in upstream shell (Zone 1) begins.
July 11, 1952	Slide of 250,000 yd^3 occurs at left abutment in vicinity of upstream shell, near a smaller slide mapped prior to construction.
August 11, 1952	Construction of outlet conduit is essentially complete.
August 14, 1952	Cleanup of slide is completed and placement of fill in Upstream Shell (Zone 1) resumes and construction of Core (Zone 2) begins.
October 3, 1952	Upstream shell (Zone 1) and Core (Zone 2) are at elevation 605 feet while Inclined Drain (Zone 3) and Downstream Shell (Zone 4) are at elevation 510 feet. Construction of Zone 4 required the use of materials excavated for construction of the spillway and was delayed because the spillway excavation was delayed due to design changes, and did not begin until end of September. Zone 3 is discovered to be misaligned at elevation 510 feet and corrective action is taken as described below.
November 1, 1952	Zones 3 and Zones 4 reach elevation 600 feet where Zone 3 is terminated. DSOD inspection reports indicate quality of materials and control of thickness and continuity of Zone 3 are not always satisfactory.
November 12, 1952	Zone 4 reaches elevation 643 feet.
November 30, 1952	Dam embankment is completed.
December 29, 1952	Construction of spillway is completed.

TGP made the following observations based on our review of the DSOD construction records:

1. DSOD required stripping of the abutments to rock prior to placement of embankment fill and had DSOD inspectors monitor and enforce this requirement. This requirement was also applied to removal of materials that were involved in landslides during construction.
2. The relocation of the dam axis in order to accommodate conditions observed after initial stripping of the abutments (combined with the landslide activity on the left abutment, the proximity of relocated Highway 17, and the geometry of the approach channel to the spillway) delayed completion of the redesign of the spillway location and alignment until November 6, 1952. Excavation in the area of the spillway produced most of the material for Zone 4 and this excavation did not produce substantial amounts of material until early October.
3. The lack of material for construction of Zone 4 until October 1952, and the need to finish the project before the winter rains, required the construction of Zone 1 and Zone 2 fills (without placement of Zone 3 and Zone 4 materials) until Zones 1 and 2 reached elevation 605 feet. The downstream edge of Zone 2 was temporarily terminated at a slope of 1 1/4 H:1V and the portions of Zone 2 immediately adjacent to the temporary downstream slope were not compacted for safety reasons. The width of the zone that was not compacted was approximately 15 feet.
4. The correction of the misalignment of the Zone 3 inclined drain that was discovered in October 1952 is illustrated in the sketch by A. D. Morrison dated October 3, 1952 that is included as Figure 2-4. The corrections included placement of a 5 foot-thick layer of gravel that linked the misaligned portions of the inclined drain that were 25 feet apart. Figure 2-4 shows the width of the Zone 3 inclined drain is 15 feet but the note on this figure and the as-built drawings indicate the minimum width of the drain is 4 feet. This is further discussed in Section 5.5.6 – Permeability.
5. Once Zone 4 material became available, construction of the downstream section of the dam required removal of the uncompacted portions of the Zone 2 materials described in Item 3 above, and placement of additional Zone 2 materials in a transition fillet fill between the temporary downstream slope of Zone 2 and the design slope of Zone 2, as well as placement of Zone 3 drain material and Zone 4 downstream shell material. This is illustrated in the sketch by DSOD inspector D. Dresselhaus dated September 30, 1952 and included as Figure 2-5.
6. A consistent and reliable source of Zone 3 material for the inclined drain was not available. The limited amounts of materials provided from on-site borrow areas varied and were sometimes muddy. Delivery of materials procured from off-site commercial quarries lagged behind the need for drain material, particularly during the night shift when truck traffic on public roads was not allowed. Although the contractor was cautioned by DSOD to maintain the Zone 3 inclined drain fill well above the Zone 4 fill and was able to do so through mid October, the inspection report dated October 15, 1952 indicates that the contact of the drain was lost in one place and that placement of drain material was difficult because of the differences in elevation between Zones 2 and 4. The contractor was required to correct this situation. By the end of October, the placement of Zone 3 inclined drain material lagged

behind the placement of Zone 2 and 4 fills and drain material contacts were lost every night. The fill was at approximately elevation 580 feet at the time and the placement of the Zone 3 inclined drain material was stopped once it reached elevation 600 feet.

7. From the above observations we have concluded that the offset in the inclined Zone 3 drain material at elevation 510 feet may have significantly impacted the hydraulic capacity of the drain and that the continuity and permeability of the Zone 3 inclined drain above this elevation is variable and sometimes severely compromised, particularly near the top of the layer between approximate elevations 575 feet and 600 feet. In addition, there are no construction records on the gradation of the Zone 3 drain materials.

2.3.2 Modifications

The following modifications were made to the dam and appurtenant structures after the facility was initially completed in December 1952:

1. The spillway was modified to protect the Highway 17 fill in accordance with an agreement reached between the District and the State of California in December 1953. Construction of the spillway modifications was completed in March 1955 and a Certificate of Approval for the dam and reservoir was issued on December 24, 1956.
2. In 1958, gunite reinforcement was placed beneath the downstream end of the spillway as a precaution to prevent undermining of the spillway by Trout Creek that enters Los Gatos Canyon immediately downstream of the end of the spillway.
3. In 1960, the intake structure was raised.
4. In 1961, gunite lining was placed in erosion gullies at the right downstream groin of the dam.
5. In 1966, the County built a bridge across the spillway approach channel (currently used for Alma Bridge Road).
6. In 1971, gunite lining was again placed in erosion gullies at the right downstream groin of the dam.
7. In 1975, the District did some maintenance work on the intake structure.
8. In 1989, the outlet pipe was extended upstream and a new intake structure was constructed on the right abutment of the dam.
9. In October 1989, following the Loma Prieta earthquake, an inspection of the outlet pipe revealed that a partial collapse of the pipe had occurred (however, the exact timing of the collapse is not known) and a 30-foot long section of the pipe was repaired by installing a new steel lining.
10. In 1997, the crest of the dam was raised by as much as 4.5 feet and the spillway walls were raised 2 to 6 feet during the freeboard restoration project.
11. Also in 1997, three additional sections of the outlet pipe were found to have partially collapsed; these were repaired in 1998.

12. In 2009, a new outlet tunnel and inlet structure were completed in the right abutment and the original outlet pipe was abandoned in place by grouting.

2.3.3 Instrumentation

Instrumentation at Lenihan Dam includes the following:

1. Nine survey monuments originally installed along the dam crest and later replaced by ten survey monuments installed as part of the freeboard restoration project in 1997. In addition, five survey monuments were installed along the downstream dam face bike path to measure settlement and horizontal movement;
2. Two pneumatic piezometers (now abandoned) and three open well piezometers were installed in 1975 and three additional pneumatic piezometers (now abandoned) were installed in 1979 (Wahler, 1982);
3. Twenty-two "permanent" piezometers installed in 1998 to monitor piezometric levels adjacent to the outlet pipe that were abandoned when the outlet pipe was grouted in 2009;
4. Two inclinometers and thirty-two vibrating wire piezometers installed in two phases during 1999 and 2001: 23 piezometers in the dam embankment, 2 within the bedrock foundation beneath the dam, and 7 within the bedrock at the right abutment;
5. A strong motion accelerometer installed by the District in the control building on the dam crest in 1999 to record crest acceleration in the event of an earthquake and to trigger a change in the reading frequency of the vibrating wire piezometers after a significant earthquake;
6. Three strong motion accelerographs (two on the dam crest and one on the left abutment) installed in 1975 by the California State Division of Mines and Geology (now called the California Geological Survey);
7. A weir to measure tunnel seepage discharge at the downstream end of the new outlet tunnel; and
8. A partially completed but not yet functional seepage monitoring facility at the toe of the dam installed in 2009.

Maximum piezometric levels (i.e. measured total head at full reservoir level) from the piezometer data within the dam embankment (Item 4) are shown on Figure 2-3.

The location of piezometers along the outlet pipe and the variation of piezometric level with time for all these piezometers are summarized on Figure 2-6. The maximum piezometric level measured during the period from 2005 to 2007, as reported by the District (Nelson and Volpe, 2007), is also shown on the cross section at the top of Figure 2-6. The data from the outlet pipe piezometers show that the piezometric heads along the outlet pipe are very close to the reservoir level until the centerline of the dam crest is reached at which point the total heads drop off rapidly over a distance of about 100 feet.

2.4 CHRONOLOGY AND SCOPE OF PREVIOUS INVESTIGATIONS

There have been a significant number of investigations and studies at Lenihan Dam since the dam was originally built. As discussed in Section 2.2, Figure 2-2A provides an overview of the locations of previous investigations.

The following is a summary of the previous investigations.

1. The first significant field and laboratory investigation at Lenihan Dam was the Seismic Safety Evaluation study by Wahler (1982). This evaluation consisted of three episodes of field investigation in 1975, 1979 and 1981, with the final report prepared in 1982 (the Figures all refer to the 1982 date for these field investigations). In all, Wahler completed:

   - 18 rotary borings in the dam, several of which included frequent Pitcher Barrel sampling with some Standard Penetration Tests (SPTs); 12 of these borings were extended into bedrock;
   - two trenches on the downstream slope, with in-place density testing of the embankment;
   - three sets of cross-hole shear wave tests, with seismic refraction and downhole surveys at each cross-hole site;
   - installation of 5 pneumatic piezometers in the upstream shell and core (now abandoned), and three open well piezometers in the downstream shell (no longer monitored); and
   - a large amount of classification and engineering properties testing including permeability, consolidation, compaction, and triaxial tests (UU, ICU and cyclic).

   Wahler concluded that the dam had high seismic resistance and that catastrophic failure due to the maximum credible earthquake (M8.5 on the San Andreas Fault) was not likely.

2. The second significant study was performed by Earth Sciences Associates (ESA, 1987) for the Outlet Modification Project. All of the explorations for this study were located outside the limits of the embankment for the purpose of designing a relocated intake structure on the lower upstream right abutment. However, as discussed further in Section 3.3, we used some of the exploration data generated from this work to clarify the likely level of the embankment foundation excavation in this area.

3. Following the Loma Prieta Earthquake in 1989, R. L. Volpe & Associates (RLVA) conducted an investigation of earthquake damage at Lenihan Dam (RLVA, 1990); this investigation included mapping and trenching of earthquake-induced cracking at the dam site.

4. The next significant study was conducted by Geomatrix in 1996 for the Lexington Dam Freeboard Restoration Project (Geomatrix, 1996). Geomatrix completed:

   - 7 shallow hollow-stem auger borings along the dam crest;
   - 14 rotary, core and flight auger borings along the sides of the spillway, ranging from 3 feet to 43 feet in depth;
   - 7 test pits, mostly along the spillway; and
   - laboratory testing including index properties, compaction, and unconfined compression (UC) tests on the shallow embankment materials, and limited UU triaxial tests on weathered rock along the spillway.

5. In 1997, Harza conducted a study to model the Loma Prieta Earthquake deformations at the dam using the GEFDYN program (Harza, 1997). Their work included the drilling of three borings along the maximum section of the dam, with Pitcher Barrel sampling, consolidation testing, and triaxial testing (ICU and cyclic).
6. Another significant study was performed in 1999 and in 2001 by RLVA and the District (RLVA, 1999a and 1999b; Frame and Volpe 2001), initially for the purpose of evaluating repeated episodes of outlet conduit damage that were first noted following the Loma Prieta Earthquake and that culminated in a Level One emergency at the dam in 1998. Work completed for these studies included a detailed seepage analysis and extensive installation of instrumentation, including most of the piezometers that are now used for monitoring. This work included:
    - 4 Cone Penetrometer Tests (CPTs);
    - 22 rotary borings with installation of 29 vibrating wire (VW) piezometers and two inclinometer casings with 13 in-place inclinometers;
    - installation of 22 piezometers along the outlet conduit (all now abandoned); and
    - limited laboratory testing including index properties, consolidation, permeability and triaxial tests (UU and ICU).
7. The most recent significant investigation at Lenihan Dam was performed by Geomatrix in 2006, for the design of the new outlet tunnel (Geomatrix, 2006b). The exploration completed as part of that study was concentrated on the right abutment along the alignment of the new outlet tunnel and included:
    - 18 rotary and core borings, some with packer testing and downhole seismic velocity measurements, optical televiewer and acoustic logging, and installation of 5 piezometers;
    - 4 test pits;
    - seismic refraction and electric resistivity lines; and
    - laboratory testing, mostly rock strength properties for tunnel design.

Data from the preceding studies have been consolidated and reviewed by TGP. Other data also reviewed included as-built drawings from the original construction (dated 1956), the intake structure modifications (1989), and the freeboard restoration project (1997), and other reports related to various investigations at Lenihan Dam obtained from a review of District files. In addition, several sets of black and white stereo aerial photographs were reviewed at the District's office, and selected sets were scanned and provided by the District for our later use. We also reviewed the extensive files on Lenihan Dam that are archived at DSOD's offices in Sacramento and scanned memoranda and photos from those files for our project data library. A list of the documents we reviewed is presented in Section 8.0.

2.5 SUPPLEMENTAL SITE INVESTIGATIONS AND LABORATORY TESTING

TGP completed additional site investigations and laboratory testing to supplement the large body of available data from previous investigations and reduce the uncertainties in the seismic stability analyses of the dam. The scope of this supplemental work was based on an interim site characterization at the dam and the results of preliminary engineering analyses using this interim

characterization (Terra / GeoPentech, 2011a). The scope and the results of these supplemental investigations are documented in a separate data report (Terra /GeoPentech, 2011b).

The supplemental site investigations included three mud rotary borings and four CPT probes. Measurements of shear wave velocity within the embankment soils and underlying bedrock were obtained using OYO P-S Borehole Suspension Logging in the mud rotary borings and the "seismic cone" in CPT soundings. The plan locations of these supplemental investigations are shown on Figure 2-7 which also shows the locations of previous investigations.

The supplemental laboratory testing included index and engineering property tests on the embankment materials. The engineering property tests were aimed at providing supplemental information on the undrained strength of the materials and included triaxial compression and direct simple shear tests. They also included consolidation tests to help assess the apparent Over Consolidation Ratio of the materials. The results of these supplemental tests were combined with the data available from previous investigations and interpreted to develop the material properties discussed in Section 5.0.

2.6 PREVIOUS SEISMIC PERFORMANCE

The Loma Prieta earthquake occurred on October 17, 1989 along a branch of the San Andreas Fault. The epicenter of this M_w 6.9-event was located about 13 miles (20 km) from Lenihan Dam.

The effects of the Loma Prieta earthquake on Lenihan Dam were investigated by the District and RLVA in the days following the event as part of an overall investigation of District dams affected by the earthquake. The observed damage at the dam was documented in a report by RLVA (RLVA, 1990).

The dam was found to have sustained about 10 inches of crest settlement along the maximum section and a maximum of about 3 inches of lateral movement downstream, in addition to some localized transverse and longitudinal cracking. Also, about six weeks after the earthquake, a wet area had developed below the footpath near the right abutment, although no flow was reportedly emanating from this area. The mapped locations of the observed cracks and wet area have been highlighted on a copy of the drawing prepared by RLVA (RLVA, 1990) and are presented in Figure 2-8. This figure also includes a summary of the material that was cracked, maximum crack width, and depth of cracking at test trench locations, as reported by RLVA.

3.1 GENERAL

This section describes the geologic and tectonic conditions that characterize the region and local site of Lenihan Dam. Section 3.2 describes the regional geologic and tectonic conditions, and Section 3.3 discusses geology, faulting and seismicity in the vicinity of the site. The foundation conditions are addressed in Section 4.0 along with a discussion of our evaluation concluding that the embankment is founded directly on Franciscan bedrock without any surficial soils having been left in-place within the foundation.

3.2 REGIONAL GEOLOGIC AND TECTONIC STETTING

Lenihan Dam is located in the eastern foothills of the southern Santa Cruz Mountains that border the west side of the Santa Clara Valley, within the northwest-trending California Coast Ranges geomorphic province. The Santa Cruz Mountains are divided into two major fault blocks that are composed of different basement rock and separated by the San Andreas Fault, approximately 2 km southeast of the dam. The San Andreas Fault and associated sub-parallel San Gregorio, Calaveras, and Hayward faults comprise the principal faults of the San Andreas fault system, and accommodate the majority of transverse tectonic motion between the Pacific and North American plates within the region of San Francisco Bay. Principal faults in the region of Lenihan Dam are shown on Figure 3-1.

The fault block basement on the northeast side of the San Andreas Fault consists of an assemblage of rocks that originally formed along the convergent Mesozoic continental margin. These rocks include Jurassic and Cretaceous-age volcanic, sedimentary and meta-sedimentary rocks of the Franciscan Complex, Coast Range ophiolite and Great Valley Sequence. This basement has been broken into several discrete fault-bounded wedges, including the Sierra Azul block that is located between the San Andreas Fault and a complex line of locally merged segments of the Sargent, Berrocal, Sierra Azul and Aldercroft faults (mostly thrust faults), and the New Almaden block that is situated between this latter line of faults and the Hayward Fault on the east side of the Santa Clara Valley. As shown on previous geologic mapping by the United States Geological Survey (USGS) (McLaughlin et al., 2001), Lenihan Dam is located on the New Almaden block near its southwest margin.

The principal fault movement in the region is dominantly right lateral but northeast-vergent (directed) thrusting along a number of reverse faults has resulted in crustal shortening and uplift of the Santa Cruz Mountains and foothills on the northeast side of the San Andreas Fault. This crustal shortening is due to a westward restraining bend in the San Andreas Fault where it passes through the Santa Cruz Mountains. Most of these faults are oriented sub-parallel to the San Andreas Fault and appear to merge with it at depth. These reverse and oblique slip faults include the aforementioned Sargent, Berrocal, Sierra Azul and Aldercroft faults, as well as the Stanford, Monte Vista and Shannon faults that run along the lower foothills/valley margin, about 1.5 miles northeast of the dam.

The Mesozoic basement of the New Almaden block is unconformably overlain by Eocene and Miocene marine deposits, and younger unconformably overlying strata of Pliocene and Pleistocene fluvial deposits including the Santa Clara Formation. Since middle Pleistocene, these Miocene and younger rocks of the New Almaden block have been locally deformed and

faulted along the northeast-vergent Sargent, Berrocal and Shannon fault zones (McLaughlin et al, 2001).

Holocene sediments derived from the Santa Cruz Mountains underlie the relatively flat floor of the Santa Clara Valley, and overlap the lowermost foothills along the west side of the valley as broad alluvial fan deposits. Within the mountains, the Holocene deposits are usually limited to floors of the typically narrow stream valleys draining the range.

3.3 LOCAL GEOLOGY, FAULTING, AND SEISMICITY

3.3.1 Local Geology

Figure 3-2 is excerpted from McLaughlin et al (2001) and depicts the geology of the local region of Lexington Reservoir. Lenihan Dam was constructed across the narrow canyon of Los Gatos Creek about 1.3 miles upstream from where it emerges from the Santa Cruz Mountains onto the floor of Santa Clara Valley. The upper reach of Los Gatos Creek follows the northwest regional trend defined by the San Andreas Fault to the upstream end of Lexington Reservoir, at which point it bends northward, paralleling the Lexington fault and eventually emerging from the mountains at Los Gatos. Lenihan Dam crosses this north-trending downstream reach of the canyon.

The project region is located entirely within the Central Belt of the Franciscan Complex. The Central Belt Franciscan rocks in the area of Lenihan Dam consist mainly of Upper Cretaceous mélange and Jurassic-Cretaceous age sandstone of the Marin Headlands terrane. Mapping by the USGS (McLaughlin et al, 2001) shows the immediate area of the dam site being underlain by the Central Belt mélange, with an area of more massive Marin Headlands terrane sandstone occurring at the upper end of the spillway and under the left upstream side of the dam.

The Plio-Pleistocene-age Santa Clara Formation consists of coarse-grained fluvial and, to a lesser extent, fine-grained lacustrine deposits, now exposed as erosional remnants outcropping on the lowermost foothills of the Santa Cruz Mountains and also locally along the margins of Los Gatos Creek and Lexington Reservoir. Some Santa Clara remnants occur as deformed, steeply and tightly folded fault-bound deposits (e.g., as observed along the Lexington fault "Cove exposure" noted below). No deposits of Santa Clara Formation were cited as having been identified within the immediate as-constructed foundation of Lenihan Dam, although a possible Santa Clara remnant was noted along a cut during construction for the relocated highway, just upstream of the foundation on the left abutment and above the elevation of the dam crest (Marliave, 1951).

Numerous landslides occur throughout the Santa Cruz Mountains region and, in the vicinity of the dam site, are concentrated along the west side of Los Gatos Creek and Lexington Reservoir. Several landslides occurred within the dam foundation during construction, mostly along the left abutment, and have also occurred since construction along the left side of the spillway downstream of the crest. These slides were the result of local over-steepening during excavation of the sheared Franciscan shale mélange, and of a generally weaker and more sheared condition of the shale along that left side of the dam.

As noted previously, younger Holocene alluvial deposits are usually limited to the floors of creek channels within the typically narrow canyons and ravines of the Santa Cruz Mountains and foothills and, at the dam site, were for the most part limited to the very bottom of Los Gatos Creek. As discussed further below, construction records indicate that all surficial deposits, including stream channel and terrace alluvium, colluvium and landslide deposits, were removed from the dam foundation prior to placement of the embankment.

3.3.2 Local Faulting of Consequence to Lenihan Dam (San Andreas, Shannon, Stanford-Monte Vista and Berrocal faults)

As noted above, the significant seismogenic faults affecting seismic hazard at Lenihan Dam are shown on Figure 3-1. The recent Technical Memorandum 3 (TM-3) "Seismotectonic and Ground Motion Study for Seismic Stability Evaluation of DIP Phase 1 Dams" (AMEC, 2009) indicates that the San Andreas, Berrocal, and Stanford-Monte Vista faults are the controlling seismic sources at Lenihan Dam. According to AMEC, the Maximum Credible Earthquake (MCE) on the Stanford-Monte Vista (magnitude M_w 6.9 at 5.5 km map distance northeast of the dam) produces the highest accelerations at short periods whereas the MCE on the San Andreas Fault (M_w 7.9 at 2.1 km southwest of the dam) dominates at longer periods.

The Berrocal and Stanford-Monte Vista faults are both west-dipping reverse faults located northeast of the dam; therefore, they dip directly under Lenihan Dam at fault rupture distances of 2.0 and 4.5 km, respectively. Although the Berrocal Fault is situated closer than the Stanford-Monte Vista Fault (2.3 vs. 5.5 km map distance), its lesser fault length and attendant MCE (M_w 6.8 vs. M_w 6.9) result in marginally lower median and 84th percentile ground motions at the dam (0.69g median and 1.17g 84th percentile for the Berrocal Fault vs. 0.71g median and 1.20g 84th for the Stanford-Monte Vista Fault). Additionally, TM-3 shows the Berrocal Fault as a conditionally active, low to moderate slip rate fault (< 0.1 to 1.0 mm/yr) whereas the Stanford-Monte Vista Fault is shown as an active, moderate slip rate fault (0.1 to 1.0 mm/yr). The San Andreas Fault is a strike-slip fault with a very high slip rate (> 9mm/yr) and was the source of the M_w 7.9 San Francisco earthquake in 1906. A subsidiary oblique-slip fault that is part of the San Andreas system and located on the southwest side of the main trace of the San Andreas Fault, in the region south of Lenihan Dam, was the source of the M_w 6.9 Loma Prieta earthquake in 1989. This fault was unrecognized prior to the Loma Prieta event.

DSOD has indicated in their comments on the SSE-1 Investigations DM-2 and Interim DM-4 for Guadalupe, Almaden, and Calero Dams (DSOD, 2010a) that they have historically considered a combined rupture of the Shannon-Monte Vista Fault, in contrast to the Stanford-Monte Vista Fault rupture scenario of AMEC. The combined Shannon-Monte Vista scenario is consistent with the interpretation of the fault as defined in Appendix A: California Fault Parameters for the National Seismic Hazard Maps and Working Group on California Earthquake Probabilities (Wills et al, 2008). However, TM-3 provides a basis for the segregation of the Shannon Fault from the Stanford-Monte Vista Fault in the vicinity of Blossom Hill, and we are herein utilizing the delineation of the Stanford-Monte Vista Fault as a single fault rupture source separate from the Shannon Fault, as described in TM-3. The maximum moment magnitude of M_w 7 assigned by DSOD to the Shannon-Monte Vista earthquake closely approximates the M_w 6.9 estimate by AMEC for the Stanford-Monte Vista earthquake.

Although the Shannon Fault is not shown in TM-3 as one of the primary faults contributing to the greatest seismic hazard at Lenihan Dam, a strong MCE event on the Shannon Fault (M_w 6.7 as per TM-3) would undoubtedly result in strong shaking at the dam. As noted in Section 3.3.4, earthquake-related damage that occurred in the Los Gatos and Blossom Hill areas as a result of the 1989 Loma Prieta earthquake appears to have been indicative of contractional deformation that was triggered along the Monte Vista-Shannon and Berrocal faults (Bryant, 2000).

3.3.3 Lexington Fault

The Lexington Fault was first named by McLaughlin et al (1992) during geologic mapping studies of the local region by the USGS, following the 1989 Loma Prieta earthquake. However, traces of northward-striking faulting generally paralleling the course of Los Gatos Creek and across, or immediately adjacent to, the dam site had been previously mapped by several different investigators during earlier studies (e.g., Lewis 1951, Rogers and Armstrong 1971, and Rogers and Williams 1974). As part of our review of existing data, we compiled and reviewed various data related to the Lexington Fault, and dam site faulting potential in general. Our initial evaluation of faulting conditions at Lenihan Dam also included some local field mapping, review of site geomorphology, study of pre-construction aerial photos of the area, consideration of local aftershocks of the 1989 Loma Prieta Earthquake, and review of regional and local geodetic data (the latter provided by the District).

In 2006 and 2007, Geomatrix conducted investigations of the Lexington Fault in connection with studies for the new outlet works at Lenihan Dam (Geomatrix; 2006a, 2006b, and 2007). During a period of low reservoir level in 2007, Geomatrix and DSOD were able to examine and map an exposure of the fault that had been previously mapped by the USGS (McLaughlin et al, 1992 and 2004) but that is normally submerged beneath Lexington Reservoir. This exposure, located in a "cove" at the northeastern edge of the reservoir (approximately 1,000 feet southeast of the right end of the dam), was found to be a 30-foot wide shear zone with near-vertically tilted beds of Santa Clara Formation (east side) offset against Franciscan Complex rock (west side), along an 80° east-dipping fault contact. Geomatrix produced a detailed log of the fault exposure and then mapped the northward trace of the fault and found that it did not cross the planned outlet tunnel through the right abutment, but rather extended due north and passed about 200 to 300 feet east of the new tunnel alignment and approximately 600 feet east of the right abutment of the dam (Geomatrix, 2007). This "cove" faulting was reviewed by DSOD who concluded that it did not cross the outlet tunnel but that it was (at that time) considered conditionally active (DSOD, 2007b).

The relatively recent TM-3 (AMEC, 2009) lists the Lexington Fault as low slip rate, conditionally active, oblique-normal fault, consistent with DSOD's designation of the Lexington Fault as a conditionally active fault, at the time TM-3 was prepared. Additionally, TM-3 assigns the Lexington Fault a rupture length of 7.5 km based on its intersections with the Berrocal and San Andreas faults to the north and south, respectively, and a corresponding MCE magnitude of M_w 6.0 at a distance of 0.1 km, with peak ground accelerations of 0.46g (median) and 0.72g (84^{th} percentile). As such, these calculated parameters would not control site ground motions. In addition, DSOD advised the District in November 2010 that DSOD now considers the Lexington Fault to be inactive by their criteria (DSOD, 2010b). Consequently, we are not considering the

Lexington Fault as an independent source for either ground motions or foundation fault rupture in our analysis.

3.3.4 Seismicity of Local Region

The 1906 M_w 7.9 San Francisco and 1989 M_w 6.9 Loma Prieta earthquakes dominate the historical seismicity in the region of Lenihan Dam. The USGS has estimated that approximately 10 feet of horizontal slip occurred at depth along the reach of the fault immediately southwest of Lenihan Dam (USGS, 2011). The 1906 earthquake also produced a number of landslides, at least one of which blocked Los Gatos Creek within the present area of the reservoir; this particular slide occurred on the west side of Los Gatos Creek just to the north of Aldercroft Creek (ibid).

The 1989 earthquake occurred with an epicenter 20 km southeast of the dam along a southwest dipping rupture surface that is separate from the main trace of the San Andreas Fault. The northernmost reach of fault rupture was defined by the distribution of aftershocks and extended to a point about 6 km northwest of the dam. The earthquake produced right-oblique movement along the fault at depth, and uplift and shortening of the overlying crust that, in the local epicentral region, resulted in ridge-top spreading, extensional fissuring and other deformational surface features not directly related to surface faulting (Wells, 2004). Also, localized areas of damage indicating contractional deformation were noted in the Los Gatos and Blossom Hill areas along the southwestern margin of Santa Clara Valley, and appear to have resulted from Loma Prieta-triggered slip along the Monte Vista-Shannon and Berrocal faults (Bryant, 2000).

4.1 GENERAL

Foundation conditions at Lenihan Dam have been described to varying degrees in a number of reports on previous geotechnical investigations conducted in association with construction, modifications, and engineering analyses of the dam and outlet works. In particular, an excellent summary and discussion of essentially everything that was known about the local foundation geology at Lenihan Dam through 1999 was written by geologist Phil A. Frame and was included as "Chapter 2 - Geologic and Seismotectonic Setting" in the "Lenihan Dam Outlet Investigation, Vol. 1 – Final Engineering Report" by RLVA (1999a).

Other informative data that was developed subsequent to the 1999 RLVA report and that can be extrapolated to embankment foundation conditions include 2002 field mapping data by Gilpin Geosciences, presented on a detailed geologic compilation map prepared for Treadwell and Rollo's Geotechnical Feasibility Report for Lenihan Dam New Tunnel Option study (Treadwell and Rollo, 2002). That map presents the most comprehensive compilation of previous subsurface exploration and geologic mapping data that has been produced to date. Other more recent data that can be extrapolated to foundation conditions include selected mapping and rock testing data from the Final Geologic and Geotechnical Data Report, Lenihan Dam Outlet Modification Project, prepared by Geomatrix (2006b).

The rock surface on which the dam is founded was surveyed during construction, after removal of surficial soils. Figure 4-1 shows the original as-built topographic contours from the construction surveys and Figure 4-2 provides a three-dimensional perspective as shaded relief of that bedrock surface. It is unknown how many individual episodes of surveying may have been performed to prepare the as-built topographic surface shown on Figure 4-1; however, as discussed further below, a significant survey error is evident over portions of the right abutment foundation when one compares the as-built rock surface elevations to the original site topographic survey and data on rock elevations from borings. As part of our site characterization work, we have, where possible, re-drawn the dam foundation contours for the portions of the misrepresented right abutment area under the embankment using available boring information in order to provide a more accurate foundation surface model for our engineering analyses. These revised foundation contours are shown in brown on the modified as-built foundation topography presented on Figure 4-3.

Figure 4-4 provides transverse and longitudinal cross-sections through the dam that supplement the primary transverse sections shown on Figure 2-3. It is evident from Figure 4-2 that the bedrock surface has a typical, relatively uniform valley slope configuration on the right side of the dam but includes more irregular topography resulting from the presence of massive rock knobs on the upstream left side of the dam.

4.2 ROCK CONDITIONS

Lenihan Dam was constructed on Franciscan Complex bedrock, without a foundation seepage cutoff or grout curtain. As indicated previously and as shown on Figure 3-2, regional geologic mapping by the USGS (McLaughlin et al, 2001) shows the majority of the dam site being underlain by Franciscan mélange (map unit "fm"), with an area of more massive sandstone occurring at the upper end of the spillway and under the left upstream side of the dam (map unit

"fms"). The mélange typically consists of intensely fractured to crushed shale that encases blocks of harder sandstone and greenstone, some of which are up to several hundred feet in length, with lesser blocks of serpentinite and chert. The area of more massive sandstone that occurs at the upper end of the spillway on the left abutment includes some interbedded shale.

Much of the dam footprint is presumably directly underlain by the sheared shale matrix of the Franciscan mélange, as indicated on numerous boring logs from studies conducted since construction. Areas of hard rock outcropping that were mapped by Marliave (Marliave, 1948) in the area of the dam foundation, prior to excavation/construction, are depicted on Figure 4-5. Undoubtedly, other areas of hard rock were exposed in the finished foundation excavation after removal of surficial soils; unfortunately, no as-constructed map documenting geologic conditions of the excavated foundation after completion of construction was uncovered in the DSOD project files. Localized areas of hard rock within the foundation can also be very roughly defined based on information presented on several boring logs.

As noted previously, several landslides occurred in the area of the left abutment both prior to and during construction, mainly as a result of the weaker and more sheared condition of the shale that characterizes portions of the left side foundation and spillway excavation downstream of the crest. One of these included a large slide estimated at about 250,000 yd^3 that occurred on the upstream left abutment in July 1952, during stripping activities for construction of Zone 1. This slide was approximately 300 feet wide and 400 feet long, and extended down slope in a southeastern direction from the area of the spillway approach channel; a comparison of the preconstruction and as-built topography indicates that excavations of up to about 65 feet were required in some areas of the slide to remove the debris and attain a suitable foundation. The estimated limits of this slide are shown on Figure 4-5.

Construction records do not provide detailed information on the rock conditions encountered at the base of the outlet pipe, although it is stated that an 800-foot long segment of the outlet conduit, from Station 5+70 to Station 13+70, was founded on rock. The outlet pipe foundation was reported to be very hard rock between Station 6+60 and Station 7+30 and blasting of the right abutment rock at streambed level in the vicinity of Station 6+60 was also reported. The inspection report of August 6, 1952 states that 350 feet of outlet pipe remained to be completed at that time: the foundation had not yet been cleaned for the first 100 feet of this remaining segment, from Station 7+74 to Station 8+74; the foundation for the next 100-foot section from Station 8+74 to Station 9+74 had been cleaned and approved and was noted to be soft blue shale through which protruded hard rock outcrops; and, for the last 150 feet, the steel liner was in place and ready for the concrete pour but there is no mention of rock conditions under this portion of the liner in the inspection report. The shale-founded section of the outlet pipe, from Station 8+74 to Station 9+74, roughly corresponds to the area where piezometric levels measured along the outlet pipe dropped significantly, as shown in Figure 2-6. RLVA (1999a and 1999b) completed a thorough evaluation of the outlet pipe and noted that the backfill around the pipe could be a major issue regarding the performance of the pipe but that there was scant mention of this material in the as-built drawings or construction records. Information collected by RLVA showed the backfill was similar to the pipe foundation materials or the lower core materials. This suggests a possible correlation between the total heads that were measured along the outlet and the lithology of the pipe foundation (i.e., areas of hard, more open-fractured

sandstone, if hydraulically connected to the reservoir, might more readily transmit water pressures from the reservoir than softer, crushed and more impermeable shale).

In-situ permeability (packer) tests were performed in four borings drilled during the 1999 outlet investigation (RLVA, 1999a and 199b) and subsequent Phase B instrumentation project (Frame and Volpe, 2001). Packer tests were also performed in a number of the borings drilled for design of the new outlet tunnel (Geomatrix, 2006b). The four borings drilled by the District in 1999 and 2001 were located along the right abutment, at the crest (LDP-18), on the right side of the upstream embankment slope near the groin (LDP-19), and on the right side of the downstream slope near the groin (LDP-20 and LDP-21). Calculated permeability values for these tests, as presented in the above-referenced data reports, ranged from 0 (i.e., no flow) to 4.7 x 10^{-4} cm/sec. Lower permeability values were commonly in the range of 10^{-6} cm/sec. Our review of these data (including the field test data sheets) led us to conclude that 10^{-6} cm/sec or less probably represents a typical permeability coefficient for the sheared shale mélange matrix comprising significant portions of the foundation (a laboratory permeability test on a sample of sheared shale produced a permeability coefficient of 10^{-9} cm/sec). For the most part, the higher calculated permeability coefficients (up to about 10^{-4} cm/sec) occurred within masses of harder and shallower rock; e.g., above a depth of 62 feet in LDP-20, where total drill fluid losses occurred while drilling through blocks of fractured sandstone, greenstone and serpentinite. Similarly, total drill fluid losses occurred while drilling into sandstone portions of the foundation in Wahler borings LD-4, LD-17 and LD-18, which were located directly under the embankment near the maximum section of the dam. Conversely, none of the 1999 and 2001 borings that were drilled through the deeper channel section of the embankment and into an underlying shale foundation were noted as having experienced drill fluid loss. This suggests that the harder rock blocks within the foundation (e.g., sandstone, greenstone, etc.) are more likely to be open fractured, with an attendant higher hydraulic conductivity, than the sheared mélange matrix (crushed shale) surrounding the blocks.

Numerous shears, localized faults and fractures of various orientations occur throughout the foundation. Many of these are oriented northwest to west-northwest, consistent with the overall local regional trend of the fault- and shear-bounded blocks of rock that comprise this region of the New Almaden block. Mapping by Gilpin Geosciences shows a broad, approximately 100-foot wide zone of west-northwest shearing crossing Los Gatos Creek at the downstream toe of the dam (Treadwell and Rollo, 2002). Several north-south oriented shears, approximately parallel to the course of Los Gatos Creek, have been previously mapped and were also noted during site reconnaissance mapping for this study, mostly along the cut slopes above the spillway walls.

Several slope failures occurred during foundation excavation, particularly along the left side, and the dam axis was shifted downstream on the left side and upstream on the right side to take advantage of better rock conditions. Much of this construction slope instability was probably the result of local over-steepening of the weak sheared shale that characterizes the Franciscan mélange matrix.

Several shear wave velocity surveys were conducted during previous studies. These include cross-hole surveys that were extended through the embankment and into the foundation by Wahler in 1975 (3 sets) and later in 1981 (one set), and two downhole surveys in the right

abutment ridge by Geomatrix along the new outlet tunnel alignment in 2006 (in Borings B-6 and B-11, at the upstream and downstream ends of the new tunnel, respectively). In addition, as discussed in Section 2.5, TGP completed OYO shear wave velocity measurements in three mud rotary borings and downhole shear wave velocity measurements using the "seismic" cone in three CPT soundings. The shear wave velocities recorded in the rock foundation are discussed In Section 6.3 while the measurements made in the embankment materials are addressed in Section 5.5.5.

4.3 EVALUATION OF POTENTIAL FOR OCCURRENCE OF SURFICIAL SOILS REMAINING IN-PLACE WITHIN DAM FOUNDATION

We closely examined a number of maps and reports that document the conditions in the foundation area that existed prior to, during, and after construction of the dam, for the purpose of determining whether potentially liquefaction-prone soil deposits were left in-place overlying the bedrock in the dam foundation. The data sources reviewed for this analysis included:

1. the pre-construction and as-constructed topographic maps of the foundation area;
2. the pre-construction geologic mapping and report of the dam site area (Marliave, 1948), along with subsequent memoranda describing foundation conditions as encountered during construction by Marliave and others;
3. pertinent exploration data from the various subsequent investigations of the dam, particularly explorations that penetrated the foundation under the dam including the 1975-1981 borings by Wahler (Wahler, 1982), the ESA exploration for design of the new intake structure (ESA, 1987), and later Phase A and B instrumentation borings drilled in 1999 and 2001 (RLVA, 1999a and 1999b; Frame and Volpe, 2001), and the 2011 supplemental investigations (Terra / GeoPentech, 2001b); and
4. detailed geologic mapping of the dam site area by Treadwell and Rollo (2002).

We also reviewed the District's Foundation Analysis Report of SSE-2 Dams (Nelson, 2010a). That report includes figures that depict the District's estimate of pre-construction soil thickness (colluvium, alluvium and landslide deposits) at Lenihan Dam (Nelson 2010a, Figure 2), their estimated depths of foundation excavation (ibid, Figure 6), and their estimated distribution and thickness of in-place surficial soils remaining within the dam foundation (Nelson 2010a, Figure 10). In our comparison of the pre-construction and as-built topographic surfaces (using digitized maps provided by the District), we found that the District's estimated depths of excavation as shown on Figure 6 of their report are in good agreement with the amount of excavation indicated by those maps. As noted on Figure 6 of the District's 2010 Foundation Analysis Report, the pre-construction and as-built maps indicate areas of anomalously positive excavation values (i.e. fill, not excavation), where the as-built surface is shown to be higher than the pre-construction surface over areas of the upstream and downstream right abutment slopes. Based on their estimated depths of excavation, subtracted from their assumed thicknesses of pre-construction soils, the District identified several discrete areas of the upstream foundation area that might contain significant thicknesses of in-place soils remaining in the foundation.

Figure 4-5, presented herein, shows a compilation of pertinent data that we used to make our assessment of the foundation conditions under the dam. Borings that encountered bedrock are

depicted along with the elevation of top of rock as encountered at each boring. Additionally, Figure 4-5 shows surface exposures of bedrock within, and adjacent to, the dam foundation as mapped by Marliave in 1948 and by Treadwell and Rollo in 2002, and includes notes that relate local geologic data to the District's estimated in-place soils for those areas. Our independent interpretation of foundation conditions at each of these areas found the following:

1. The areas of anomalously positive excavation values (and attendant estimated thicknesses of in-place soils of up to 18 feet) on the right abutment are most likely the result of a localized but pervasive as-constructed survey error over the upstream and downstream right abutment slopes. This is indicated by exploration data at borings LDP-19 and LDP-20 (Figure 4-5), which show the rock foundation directly under the embankment, but at elevations 18 feet to 27 feet higher than indicated on the as-built contour map. Similarly, geologic sections A-A and C-C from ESA's 1987 report indicate that their borings LO-1, LO-2 and LO-3, located on the upstream right abutment just above the original intake and the lowermost upstream embankment, were drilled into a rock slope without the overlying surficial soils that are suggested in that area on Figure 10 of the District's report (Nelson, 2010a).
2. The central area of estimated 10-foot-thick in-place soils, approximately 250 feet upstream of the axis, shown on the District's Figure 10 are within an area mapped by Marliave as containing several outcrops of massive sandstone. Consequently, we conclude that this area was probably overlain by minimal thicknesses of soil rather than the approximately 20 feet of pre-construction soils estimated for this area on the District's Figure 2 (see note on Figure 4-5 herein).
3. The upstream left abutment areas shown on the District's Figure 10 as being underlain by 14 to 20 feet of in-place soils along the upstream toe are within an area where the embankment abuts an upstream bedrock ridge spur that is shown to be underlain by areas with surface exposures of Franciscan Complex sandstone as mapped by Treadwell and Rollo in 2002 (see Figure 4-5). Given the mapped rock surface exposures in this area, we conclude that this foundation area was probably blanketed by only thin colluvial soils rather than the 35 feet of pre-construction colluvium estimated for that area on the District's Figure 2.
4. A portion of the mid-left abutment area, on the left end of the upstream embankment, is shown on the District's Figure 10 as being underlain by up to 18 feet of possible in-place landslide material (the District's Figure 2 shows an estimated thickness of 45 feet of pre-construction landslide material within this area). In the various construction inspection memoranda reviewed by TGP, we did not note any reports of slide debris being left in-place within the foundation and believe it is appropriate to think that most, if not all, slide materials were removed from the foundation area.

The results of our analysis indicate it is unlikely that there are any significant areas of thick, in-place soils remaining in the foundation between the embankment and the underlying Franciscan Complex bedrock. This is consistent with Marliave's concluding statement, from his 1948 geologic report, that bedrock is at, or within a few feet of, the surface within the narrow, V-shaped canyon underlying the dam site (Marliave, 1948). In summary:

1. Most of the previous exploration borings that have extended into the foundation indicate that the as-built elevation contours accurately depict the embankment foundation surface, except

for areas of the right abutment where we believe a survey error mis-characterized the level of the foundation (and the amount of excavation required to reach that level).

2. All of the borings drilled into the foundation under the dam show Franciscan Complex bedrock in direct contact with the overlying embankment.
3. DSOD construction memoranda indicate close inspection of the foundation preparation, and describe a common sequence of foundation excavation, clean-up and approval that immediately preceded fill placement. These records also document adherence to the design criteria of founding the entire embankment on Franciscan Complex.
4. The areas of estimated in-place soils depicted under the upstream portion of the embankment on the District's Figure 10 (Nelson, 2010a) are likely the result of the above-mentioned survey error for portions of the right abutment, and an over-estimation of the pre-construction soil thickness in the central and left side areas of the upstream foundation.

Given the information described above, it is our opinion that, for all practical purposes, the compacted dam embankment is founded directly on bedrock and that no alluvium or colluvium soils are present beneath the dam.

5.1 GENERAL

The material property characterization was developed using data from previous investigations, supplemented by the data from the subsurface investigation and laboratory testing program completed by TGP (Terra / GeoPentech, 2011b). The scopes of the previous investigations are described in Section 2.4 and the scope of TGP's investigations is summarized in Section 2.5. The following subsections describe the zoning of the dam, the general sources of the embankment materials and the general nature and variation of the materials within each zone; document the result of our review and assessment of previous testing performed on the embankment materials; and summarize the index properties and engineering properties of the embankment materials based on all data from the current and previous investigations.

5.2 DAM ZONING, SOURCES OF MATERIALS, AND MATERIAL VARIABILITY

As noted in Section 2.2, Lenihan Dam was constructed as an earthfill embankment consisting of various zones. Figure 5-1 shows a generalized configuration of the dam through the maximum section (section B-B' on Figure 2-2A) including the idealized limits of each zone based on construction records. These zones consist of the following:

- Zone 1 – Upstream Shell,
- Zone 2U – Upper Core,
- Zone 2L – Lower Core,
- Zone 3 – Drain, and
- Zone 4 – Downstream Shell.

The predominant soil classifications for each of the zones are also listed on Figure 5-1. The fillet of Zone 2 fill material shown on Figure 2-5 and discussed in Section 2.3.1 was placed to achieve the design geometry of the embankment zones while accommodating the delayed construction of Zone 3 and Zone 4 and is not shown on the generalized cross section.

As shown in Table 5-2, the upstream shell and upper core materials are generally classified as gravelly clayey sand (SC) to sandy clays (CL) (for the upstream shell) and gravelly clayey sands (SC) to clayey gravel (GC) (for the upper core). The materials forming the lower core are generally classified as highly plastic sandy clays (CH) to highly plastic silty sands-sandy silts (SM-MH). Materials for the core and upstream shell of the dam were obtained from borrow sources upstream of the dam. Materials for the upstream shell and the upper core were derived from excavation of Franciscan Complex just upstream of the upstream toe. The lower core was derived from clayey alluvial/colluvial fan deposits that occurred at the mouth of Limekiln Canyon just south of the boat ramp on the upstream right abutment.

The downstream shell consists mainly of gravelly clayey sands (SC) to clayey gravels (GC). The downstream shell was primarily derived from the spillway excavation. There is no classification information available on the drain materials. However, construction records indicate that limited amounts of materials for the drain were obtained from on-site borrow areas but that most of the materials were procured from off-site commercial quarries.

CPT data provide a good indication of the variability (in particular relative variability) of material properties with depth and at different plan locations. Four CPTs were performed by RLVA to collect in-situ data on the embankment materials (RLVA, 1999b). Four CPTs were also performed by TGP as part of the current investigations (Terra / GeoPentech, 2011b). The tip resistance and friction ratio data from these CPTs are plotted on Figures 5-2 and 5-3. In Figure 5-2, the data from six CPTs have been projected to the maximum section B-B' at Station 15+95. Figure 5-3 shows data from four CPTs located along the dam axis.

Inspection of the CPT data shown on Figures 5-2 and 5-3 shows that the friction ratios for all zones are typical of cohesive materials. The CPT data for CPT-1, CPT-2, CPT-3, and CPT-4 (RLVA, 1999b) are observed to be smoother than those from LD-CPT-101, LD-CPT-102, LD-CPT-103, and LD-CPT-104 (Terra / GeoPentech, 2011b). This is due to the fact that the CPT data reported by RLVA are average values over 0.25-meter intervals whereas the CPT data from TGP included data obtained at 0.05-meter intervals. However, the CPT "signatures" within a given zone of the dam at different locations are seen to be reasonably consistent, as expected for an engineered compacted fill. The variability of both the physical / index properties and the engineering properties of the various zones are discussed further in the following subsections.

5.3 REVIEW AND ASSESSMENT OF PREVIOUS TESTING

All existing data considered appropriate for material characterization, including field and laboratory test results, were reviewed. In particular, previous investigations performed by Wahler (1982), Geomatrix (1996), Harza (1997), RLVA (1999a and 1999b), and Frame and Volpe (2001) all contained information regarding the properties of the embankment materials. We examined the pertinent aspects of these investigations and evaluated whether or not the data from these investigations could be reliably used for deriving the material properties for the preliminary engineering analyses.

Table 5-1 is a summary of our review of the existing information regarding material properties. The types of tests and/or material properties available from each of the five investigations listed above have been divided among the following categories: classification properties, in-situ properties (properties based on in-situ test results), effective stress strength (effective stress strength parameters), undrained strength (undrained stress-strain-strength parameters), cyclic properties, shear wave velocity, and other properties. For each investigation and each category, we indicate whether or not the data was used in the material property characterization and the reasons why, under the headings "Application" and "Reasoning", respectively.

The material properties described in the following sections use the data and information from the previous investigations listed above that were judged to be adequately complete, appropriate, and reliable. The term "complete" refers to studies where testing encompassed all key zones of the dam and all pertinent data were reported. The term "appropriate" refers to testing methods and details considered to be adequately consistent with the current preferred approach. The term "reliable" refers to data and results judged to be reliable after careful review of the data and the discussions contained in reports.

As shown on Table 5-1, the results of cyclic property tests reported by Wahler (1982) and Harza (1997) were considered but not used in our material property characterization for the following reasons. The modulus degradation with cycles derived from these tests may be of interest.

However, the tests were for triaxial loading conditions rather than direct simple shear loading conditions. In addition, the tests by Wahler were stress-controlled, making interpretation difficult. The tests by Harza were strain-controlled but the specimens were consolidated to pre-testing effective confining pressures that were considerably greater than the in-situ stresses and there is a lack of information on the depth and in-situ effective stresses for the samples, again making interpretation difficult.

5.4 CLASSIFICATION AND INDEX PROPERTIES OF EMBANKMENT MATERIALS

The following sections provide a summary and discussion of the embankment material classification and index properties obtained from the current and previous investigations. Each zone of the embankment is addressed except Zone 3 – Drain because no samples were collected or tested for that zone.

Soil is classified using the Unified Soil Classification System (USCS) based on the gradation of particles that make up the soil (i.e., the amount by weight of gravel-, sand-, and silt- or clay-size particles) and the plasticity characteristics (Liquid Limit and Plasticity Index) of the material passing the No. 40 sieve.

The classification and index properties of each zone are summarized in Table 5-2 in terms of generalized USCS classification, in-situ conditions (i.e., dry unit weight, moisture content, and compaction), gradation characteristics (i.e., percent each by weight of gravel-, sand-, silt-, and clay-size particles), and Atterberg limits (i.e., Liquid limit and Plasticity Index). Average index properties are listed as well as minimum and maximum values.

5.4.1 Zone 1 – Upstream Shell

The upstream shell of the dam is founded on bedrock and has an upstream slope between 5.25 and 5.5H:1V. Samples obtained from Zone 1 are classified as gravelly clayey sands (SC per USCS) to sandy clays (CL per USCS). No data were collected on the upstream shell during the 2011 investigations. In previous studies, the conditions of the upstream shell material were determined by unit weight and moisture content testing on intact samples. A total of 19 unit weight tests were performed on intact samples of Zone 1 material and produced an average dry unit weight of 119 pcf. Similarly, a total of 21 moisture content tests were performed on Zone 1 samples and showed an average moisture content of 15.0%. Maximum density has not been determined in the laboratory for Zone 1 materials. Previous studies, including RLVA 1999, have reported an estimated maximum dry unit weight of 125 pcf for the upstream shell (based on ASTM D-1557 modified to 20,000 ft-lb/ft^3 of compactive energy), which would correspond to an average relative compaction of 95%.

As shown on Figure 5-4, a wide range of gradations have been recorded on samples of the upstream shell. A total of 14 gradation tests were performed on samples from Zone 1 with average gravel, sand, and fines contents of 27%, 34%, and 39%, respectively. Additionally, hydrometer tests were performed on 8 samples of Zone 1 material showing an average clay content of 21%. It was noted in reviewing the gradation information that several samples had over 40% gravel content, including one with 43% gravel. Several other samples had less than 20% gravel, including one with no gravel. Similarly, the fines content observed ranged from a

high of 97% to a low of 19% by weight. The cumulative distribution of fines content is plotted on Figure 5-5; it is noted that, despite the wide range of fines contents observed for all samples, the 20th and 80th percentile values form a much narrower range, approximately 20% to 45% by weight. Simplified results of the 14 gradation tests performed have been plotted vs. elevation on the left side of Figure 5-6 for the Zone 1 material. As shown in this plot, changes in gradation occur gradually with depth with the exception of one sample at elevation 520 feet, which has 97% fines content and 44% clay content and closely resembles the classification of the Zone 2L – Lower Core material.

A total of 8 Atterberg limits tests were performed on Zone 1 samples. The results of these tests are grouped closely together as shown on the plasticity chart on Figure 5-7. Upstream shell materials had a liquid limit range of 30 to 39 with an average value of 33, and a plasticity index (PI) range of 6 to 24 with an average value of 15. The cumulative distribution of PI is shown on Figure 5-8; it is noted that the 50th percentile PI is also 15. Moisture content and Atterberg limits information was combined to calculate liquidity index (LI) for all eight samples tested. The results are presented on the Liquidity Chart on Figure 5-9. It is observed that the LI values for upstream shell samples ranged from -1.87 to 0.23 with an average value of -0.57. The cumulative distribution of LI values is plotted on Figure 5-10; it is noted that the 50th percentile LI is -0.47. These low values are as expected for soils compacted to 95% relative compaction. All index test and moisture content data are plotted vs. elevation on Figure 5-11 to show where the in-situ water content falls with respect to the plastic limit and liquid limit of the upstream shell. Review of this figure indicates that the in-situ moisture content consistently falls near or below the plastic limit of the materials.

5.4.2 Zone 2 – Core

The core of Lenihan Dam has been divided into two zones based on source material and classification information reviewed; the Zone 2U - Upper Core extends from the dam crest to elevation 590 feet, and the Zone 2L – Lower Core extends from elevation 590 feet to the bedrock foundation. The material characterization for both zones is addressed in the following sections.

5.4.2.1 Zone 2U – Upper Core

Samples obtained from Zone 2U are predominantly classified as gravelly clayey sands (SC per USCS) and clayey gravels (GC per USCS). Additionally, several samples have been classified as silty sands (SM per USCS) and sandy clays (CL per USCS). As noted in Section 5.2, Zone 1 and Zone 2U were derived from the same source material; therefore, the two zones are expected to have similar in-situ gradation and index properties.

In-situ property testing from current and previous studies included determination of unit weight and moisture content on intact samples. A total of 65 unit weight tests were performed on intact samples of Zone 2U material and produced an average dry unit weight of 119. 6 pcf. Similarly, a total of 80 in-situ moisture content tests were performed on Zone 2U samples and showed an average moisture content of 11.9%. Maximum density has not been determined in the laboratory for Zone 2U materials. Previous studies, including RLVA in 1999, have reported an estimated maximum dry unit weight of 125 pcf for the upstream shell which is similar to the upper core

and would correspond to an average relative compaction of 95% for the upper core (based on ASTM D-1557 modified to 20,000 ft-lb/ft^3 of compactive energy).

The middle plot on Figure 5-4 shows the full range of gradations for Zone 2U and Zone 2L materials on samples tested by others. A total of 40 gradation tests were performed on samples from Zone 2U with average gravel, sand, and fines contents of 33%, 35%, and 31%, respectively. Additionally, hydrometer tests were performed on 11 samples of Zone 2U material showing an average clay content of 17%. It was noted in reviewing the gradation information that eight samples had over 50% gravel content, including one with 58% gravel. Conversely, nine samples had less than 20% gravel, including one with 3% gravel. The values of fines content observed ranged from a high of 65% to a low of 16% by weight. The cumulative distribution of fines content is plotted on Figure 5-5; it is noted that despite the wide range of fines contents observed for all samples, the 20th and 80th percentile values form a much narrower range, approximately 21% to 45% by weight. Simplified results of the 40 gradation tests performed have been plotted vs. elevation on the top half of the middle plot of Figure 5-6 for the Zone 2U materials. As shown in this plot, changes in gradation are rather abrupt; significantly higher gravel content is observed in the top 30 feet (above elevation 643 feet), and higher fines content is observed in the lower 20 feet (between elevations 590 feet and 610 feet).

A total of 23 Atterberg limits tests were performed on Zone 2U samples collected during previous investigations. The results of these tests are grouped closely together as shown on the plasticity chart on Figure 5-7. Upper core materials have a liquid limit range of 30 to 48 with an average value of 37, and a plasticity index (PI) range from 14 to 29 with an average value of 17. The cumulative distribution of PI is shown on Figure 5-8; it is noted that the 50th percentile PI is also 17. Moisture content and Atterberg limits information was combined to calculate liquidity index (LI) for 23 samples tested; these results are presented on the Liquidity Chart on Figure 5-9. It can be seen that the LI values for the upper core samples range from -0.53 to 0.23 with an average value of -0.26. The cumulative distribution of LI values is plotted on Figure 5-10; it is noted that the 50th percentile LI is -0.23. All index test and moisture content data are plotted on Figure 5-11 vs. elevation to show where the in-situ water content falls with respect to the plastic limit and liquid limit of the upper core. This figure shows that the in-situ moisture content consistently falls near or below the plastic limit of the materials, as expected for an engineered compacted fill.

5.4.2.2 Zone 2L – Lower Core

Samples obtained from Zone 2L are predominantly classified as sandy highly plastic clays (CH per USCS) and silty sands-sandy highly plastic silts (SM/MH per USCS). Additionally, several samples have been classified as clayey sands (SC per USCS) and sandy clays (CL per USCS). In-situ property testing from current and previous studies included determination of unit weight and moisture content on intact samples. A total of 33 unit weight tests were performed on Zone 2L material and produced an average dry unit weight of 99.9 pcf. Similarly, a total of 40 in-situ moisture content tests were performed on Zone 2L samples and yielded an average moisture content of 24.1%. Maximum density was determined in the laboratory for Zone 2L materials during the RLVA 1999 study, showing a maximum dry unit weight of 98.2 pcf, which corresponds to an average relative compaction of 101% (based on ASTM D-1557 modified to 20,000 ft-lb/ft^3 of compactive energy).

The middle plot on Figure 5-4 shows the full range of gradations for Zone 2U and 2L materials on samples tested by others. A total of 23 gradation tests were performed on samples from Zone 2L with average gravel, sand, and fines contents of 6%, 15%, and 79%, respectively. In addition, hydrometer tests were performed on 18 samples of Zone 2L material and yielded an average clay content of 42%. The fines content observed ranged from a high of 97% to a low of 29% by weight. The cumulative distribution of fines content is plotted on Figure 5-5; it is noted that only 20% of the samples tested had less than 50% fines. Simplified results of the 23 gradation tests performed have been plotted vs. elevation on the bottom half of the middle plot on Figure 5-6 for the Zone 2L material. As shown in this plot, gradation characteristics for the lower core are fairly uniform with the exception of two samples near elevation 550 feet that more closely resemble upstream shell material.

A total of 18 Atterberg limits tests were performed on Zone 2L samples collected during current and previous investigations. The results of these tests predominantly fall to the right of the B-line as shown on the plasticity chart on Figure 5-7 and are consequently classified as clays of high plasticity. Lower core materials had a liquid limit that ranged from 43 to 70 with an average value of 62, and a plasticity index (PI) that ranged from 15 to 48 with an average value of 35. The cumulative distribution of PI is shown on Figure 5-8; it is noted that the 50th percentile PI is also 35. Moisture content and Atterberg limits information was combined to calculate liquidity index (LI) for 18 samples tested; these results are presented on the Liquidity Chart on Figure 5-9. It was observed that the LI values for lower core samples ranged from -0.79 to 0.12 with an average value of -0.14. The cumulative distribution of LI values is plotted on Figure 5-10; it is noted that the 50th percentile LI is -0.10. The same characteristic is indicated by the distribution of in-situ water contents and plastic and liquid limits vs. depth plotted on Figure 5-11. The in-situ moisture content of the lower core materials consistently falls near or below the plastic limit of the materials, as expected for an engineered compacted fill.

5.4.3 Zone 4 – Downstream Shell

The downstream shell of the dam is founded on bedrock and is inclined between 2.5 and 3:1 H:1V. Samples obtained from Zone 4 are predominantly classified as gravelly clayey sands (SC per USCS) to clayey gravels (GC per USCS). Additionally, several samples have been classified as poorly-graded sands (SP per USCS) sandy clays (CL per USCS) and silty gravels (GM per USCS). In-situ property testing from current and previous studies included determination of unit weight and moisture content on intact samples and samples tested in test pits. A total of 47 unit weight tests were performed on samples of Zone 4 material and produced an average dry unit weight of 124.5 pcf. A total of 48 in-situ moisture content tests were performed on Zone 4 samples and showed an average moisture content of 11.9%. Maximum density was determined in the laboratory for Zone 4 materials during the RLVA 1999 study, showing a maximum dry unit weight of 140 pcf, which corresponds to an average relative compaction of 89% (based on ASTM D-1557 modified to 20,000 ft-lb/ft^3 of compactive energy).

The lower plot on Figure 5-4 shows the results of gradation analyses on samples of Zone 4 materials. It is noted that the 70th percentile of samples tested represents a significantly narrower range than the range of the entire set of samples tested. A total of 37 gradation tests were performed on samples from Zone 4 with average gravel, sand and fines contents of 32%, 38%

and 30%, respectively. Additionally, hydrometer tests were performed on 10 samples of Zone 4 material showing an average clay content of 11%. The cumulative distribution of fines content is plotted on Figure 5-5; it is noted that the distribution is very similar to those of the upper core and upstream shell materials. Simplified results of the 37 gradation tests performed have been plotted vs. elevation on the right of Figure 5-6 for the Zone 4 materials. As shown in this plot, changes in gradation are small and gradual with elevation.

A total of 23 Atterberg limits tests were performed on Zone 4 samples collected during current and previous investigations. The results of these tests are grouped closely together as shown on the plasticity chart on Figure 5-7. Downstream shell materials had a liquid limit that ranged from 22 to 46 with an average value of 33, and a plasticity index (PI) that ranged from 6 to 29 with an average value of 15. The cumulative distribution of PI is shown on Figure 5-8; it is noted that the distribution is nearly identical to that of the upstream shell. Moisture content and Atterberg limits information was combined to calculate liquidity index (LI) for 23 samples tested; these results are presented on the Liquidity Chart on Figure 5-9. The LI values for the downstream shell samples ranged from -1.09 to -0.01 with an average value of -0.42. The cumulative distribution of LI values is plotted on Figure 5-10; it is noted that the 50^{th} percentile is -0.38 and that the distribution is very similar to that of the upper core materials. All index test and moisture content data are plotted vs. elevation on Figure 5-11; the in-situ moisture content consistently falls near or below the plastic limit of the materials, again as expected for an engineered compacted fill.

5.5 ENGINEERING PROPERTIES OF EMBANKMENT MATERIALS

Seismic stability and non-linear deformation analyses require the following material properties: unit weight, effective stress friction angle, undrained strength, undrained stress-strain-strength relationship, and dynamic properties (i.e., shear-wave velocity, shear modulus reduction, and damping ratio curves). In addition, the permeability of the various materials is required as input to the seepage analyses that provide estimates of pore pressures that are necessary to calculate the initial effective stresses within the dam for input into the engineering analyses of seismic deformations. The following sub-sections describe how material properties were derived from the existing data for all zones except for the Zone 3 drain. The Zone 3 drain materials should be predominantly sand or sand and gravel mixes but no classification or engineering information is available from previous studies for these materials. For engineering analyses of seismic response and permanent displacements, we assigned the Zone 3 materials the same stiffness and strength as the Zone 4 materials.

Table 5-3 provides a summary of the properties selected for each of the zones in terms of actual values and/or Figure(s) where the appropriate relationships are displayed.

5.5.1 Unit Weight

The unit weight selected for each material corresponds to moist (or total) unit weight, γ_t, based on testing performed during current and previous studies. Figure 5-12 shows the cumulative distribution of unit weight for all samples tested. Based on the results shown on this figure, the 50^{th} percentile moist unit weight value was adopted for each material. Moist unit weights of 138 pcf, 132 pcf, 124 pcf, and 140 pcf were selected for Zone 1, Zone 2U, Zone 2L, and Zone 4,

respectively. In selecting the moist unit weight, no attempt was made to correct for small potential differences in the degree of saturation of the materials.

5.5.2 Effective Stress Friction Angle

An effective stress friction angle for each zone is needed for long term slope stability analyses. Forty-one (41) isotropically consolidated undrained triaxial compression test (ICU'C) were performed on Pitcher samples during previous studies. A secant effective stress friction angle was calculated at maximum obliquity for each test; i.e., the friction angle was determined as the angle of the line tangent to the failure envelope with zero cohesion intercept. The calculated values are plotted vs. effective normal stress on Figure 5-13. The average values for each zone are also plotted on Figure 5-13. Three ICU'C tests were performed on re-compacted samples of Zone 4 material by Wahler (1982); these results were considered in the evaluation, but were not used directly on the plot shown on Figure 5-13.

5.5.3 Undrained Strength

The undrained shear strength of idealized material in each zone is needed for evaluating seismically induced deformation of the embankment and for evaluating static short-term stability of the embankment slopes. As summarized in Table 5-1, previous investigators have measured the undrained strength of embankment materials using 34 isotropically consolidated undrained triaxial compression tests (ICU'C tests) with pore pressure measurements on intact Pitcher Barrel Samples. In addition, three (3) ICU'C tests were conducted on laboratory-fabricated (recompacted) samples of downstream shell materials. These previous data were supplemented during the current study by:

- seven ICU'C tests,
- four K_o consolidated undrained direct simple shear tests with pore pressure measurements (K_oU'DSS), and
- estimates of undrained shear strengths based on CPT data.

The undrained strength of the various embankment materials from triaxial compression tests are summarized below, and then compared to the undrained shear strengths measured in the K_oU'DSS tests and the CPT tests.

5.5.3.1 Strength from Triaxial Compression Tests

Figure 5-14 summarizes the undrained shear strength from ICU'TXC tests on upstream shell materials. Data are available from studies by Wahler (1982) and Harza (1997). The maximum undrained shear strength for each test, S_u, is plotted vs. the effective consolidation stress of the sample prior to shear, $\sigma'_{c(tested)}$ in the upper panel of the figure. The values of S_u were consistently found to increase with $\sigma'_{c(tested)}$ and are well-represented by the exponential curve fitted to the $Su/\sigma'_{c(tested)}$ data shown in the lower panel of the figure. We recommend that the undrained strengths for the upstream shell be defined using this relationship with a minimum strength of 2.0 kips/ft^2 because the material is a well-compacted fill.

Figure 5-15 summarizes the undrained shear strength from ICU'TXC tests on upper core materials. Data are available from studies by Wahler (1982), Harza (1997), and Terra / GeoPentech (2011b). The maximum undrained shear strength for each test, S_u, is plotted vs. the effective consolidation stress of the sample prior to shear, $\sigma'_{c(tested)}$ in the upper panel of the figure. The values of S_u were consistently found to increase with $\sigma'_{c(tested)}$ and are well-represented by the exponential curve fitted to the $Su/\sigma'_{c(tested)}$ data shown in the lower panel of the figure. We recommend that the undrained strengths for the upper core be defined using this relationship with a minimum strength of 2.0 kips/ft^2 because the material is a well-compacted fill.

Figure 5-16 summarizes the undrained shear strength from ICU'TXC tests on lower core materials. Data are available from studies by Wahler (1982), Harza (1997), and Terra / GeoPentech (2011b). The maximum undrained shear strength for each test, S_u, is plotted vs. the effective consolidation stress of the sample prior to shear, $\sigma'_{c(tested)}$ in the upper panel of the figure. The values of S_u were consistently found to increase with $\sigma'_{c(tested)}$ and are well-represented by the exponential curve fitted to the $Su/\sigma'_{c(tested)}$ data shown in the lower panel of the figure. We recommend that the undrained strengths for the lower core be defined using this relationship with a minimum strength of 2.0 kips/ft^2 because the material is a well-compacted fill.

Figure 5-17 summarizes the undrained shear strength from ICU'TXC tests on downstream shell materials. Data are available from studies by Wahler (1982), Harza (1997), Frame and Volpe (2001), and Terra / GeoPentech (2011c). The Wahler tests were on laboratory-compacted specimens and are shown for comparison only. The maximum undrained shear strength for each test, S_u, is plotted vs. the effective consolidation stress of the sample prior to shear, $\sigma'_{c(tested)}$ in the upper panel of the figure. Although there is more scatter in these test results than in the tests on materials from other embankment zones, the values of S_u were found to generally increase with $\sigma'_{c(tested)}$ and can be approximated by the exponential curve fitted to the $Su/\sigma'_{c(tested)}$ data shown in the lower panel of the figure. We recommend that undrained strengths for the downstream shell be defined using this relationship with a minimum strength of 2.0 kips/ft^2 because the material is a well-compacted fill.

5.5.3.2 Discussion of Strength Data from Triaxial Compression Tests

The undrained strength of a sample of compacted clay fill within an earth dam is influenced by the density of the fill when it was initially placed and compacted, the plasticity properties of the clay, the percentage of clay, the amount of sand and gravel in the material, and the magnitude of the effective stresses that the material has experienced when consolidated under the weight of the overlying embankment soils. Other factors being equal, we expect the undrained shear strength of a compacted clay fill to vary as follows:

Variable	Effect on Undrained Strength
Increasing compactive effort	Increase
Increasing Plasticity Index	Decrease
Increasing % fines	Decrease
Increasing % gravel	Increase
Increasing effective consolidation stress	Increase
Increasing sample disturbance	Decrease

The laboratory data from Lenihan Dam clearly show a decrease in shear strength with increasing Plasticity Index; the lower core, a clay of high plasticity with an average PI of 34, has an undrained strength that is approximately 40% lower than that of the upper core and upstream shell materials that are clays of low plasticity with an average PI of 17.

The gravel content of the downstream shell is considerably greater than that of the upstream shell and upper core and, as a result, the undrained strength would be expected to be higher for the downstream shell. On the other hand, the estimated relative compaction of the downstream shell and upstream shell materials are 89% and 95%, respectively, and as a result the undrained strength would be expected to be higher for the upstream shell than for the downstream shell. The laboratory data indicate that the undrained strength of the downstream shell is about 20% lower than that of the upstream shell and upper core. Apparently, the lower compactive effort has more of an impact on the laboratory-measured strength of the downstream shell than the greater gravel content. The cone data on the other hand show considerably higher cone tip resistance for the downstream shell than for the upstream shell and upper core. These larger strengths may reflect the effect of gravel content on cone tip resistance rather than an actual increase in undrained strength of the clay matrix.

The dominant effect of confining stress on undrained strength for all zones, as indicated by the plots of Su vs. $\sigma'_{c(tested)}$ discussed above, is somewhat surprising considering the high density and low liquidity index of the compacted clay soils. However, the consolidation test data indicate that the maximum past pressures of the Zone 1 and Zones 2U and 2L soils are approximately equal to the in-situ vertical effective stresses, and that the compressibilities for stress levels in the virgin compression range are typical of normally consolidated clays. Thus, the compacted clay soils at the depths of the samples tested are normally consolidated to lightly over-consolidated and, as a result, should have a gradually decreasing value of S_u/σ'_v with increasing values of σ'_v. The following data support these statements. One-dimensional consolidation tests were completed by TGP on specimens from four samples where ICU'TXC tests were also performed. The results of these four consolidation tests indicate that the maximum past consolidation pressure was approximately equal to the in-situ effective stress and that the compressibility of the soil samples at stress levels higher than the maximum past pressure was equal to the compressibility that would be expected for a normally consolidated clay. The virgin compression ratio, CR, defined as vertical strain per log cycle of vertical stress, varied from 0.12 to 0.15 for three tests on samples from the lower core and was equal to 0.08 for one sample from the upper core. RLVA (2009) completed three consolidation tests on samples from the lower

core and one consolidation test on a sample from the upstream shell. These tests also indicate the maximum past pressure was approximately equal to the in-situ vertical effective stress and that the compressibility in the virgin compression range was as expected for normally consolidated clays. The three tests on the lower core had values of CR that ranged from 0.07 to 0.14 and the one test from the upstream shell had a CR value of 0.14.

5.5.3.3 Strength from Direct Simple Shear Tests

The primary embankment loading conditions due to seismic shaking are reasonably represented by the conditions simulated in direct simple shear testing. Thus, for seismic deformation analyses, undrained shear strengths measured under direct simple shear (DSS) loading conditions are of interest.

As part of the current laboratory investigations, TGP selected companion specimens from four samples so that triaxial compression and direct simple shear tests could be performed and the measured undrained shear strengths compared. The results of these tests are summarized below.

Boring	Sample	Dam Zone	Depth ft	TX $S_{u(max)}$ ksf	DSS $S_{u(max)}$ ksf	DSS / TX
LD-B-101	PB-4	Lower Core	88	4.96	2.93	0.59
LD-B-101	PB-8	Lower Core	131	5.90	3.99	0.68
LD-B-101	PB-12	Lower Core	171	6.05	3.61	0.60
LD-B-103	PB-5	Upper Core	52	4.50	2.66	0.59

These data are very consistent and indicate that the direct simple shear strengths of the compacted clay soils at Lenihan Dam are typically 60% of the strengths measured in triaxial compression tests.

All the DSS tests described above were conducted using a static loading rate; as a result, some adjustment in static strength for the rate of loading effects needs to be made in order to estimate the seismic undrained shear strength values to be used in seismic deformation analyses. We recommend using the static DSS undrained shear strengths (estimated as 60% of the triaxial compression strengths) and then adjusting these strengths for rate of loading effects. These adjustments would probably be on the order of a 20 to 40 percent increase in strength. We will evaluate this recommendation further through a refined analysis of the performance of the dam during the Loma Prieta earthquake that will be completed as part of our final seismic stability analyses.

5.5.3.4 Calibration of CPT Strengths using Laboratory Data

CPT probes were completed adjacent to each of the mud rotary borings as part of the current field and laboratory investigation by TGP. We compared the measured undrained strengths from our triaxial tests to the undrained strengths estimated from the adjacent cone data. In order to provide representative values of the cone tip resistance for calculating undrained shear strength, we considered median and 16% values (mean – 1 standard deviation). The 16% values were

used in an attempt to overcome high values that may be associated with gravel content but are not representative of the undrained strength of the clay matrix. Table 5-4 summarizes the strength comparisons.

This comparison shows that there are relatively small differences between the median undrained strength values derived from the cone [CPT (50%) S_u] and the 16% values [CPT (16%) S_u] for the lower core which is a relatively homogeneous material with little to no gravel. The CPT-derived undrained strengths vary from about 0.7 to 1.3 times the undrained strengths measured in the laboratory triaxial tests on samples of lower core material.

On the other hand, the values of CPT (50%) S_u and CPT (16%) S_u for the downstream shell are quite different, and the difference probably reflects the strong influence of gravel. The undrained strengths estimated using the CPT data vary from 1.4 to 4.7 times the undrained strengths measured in the laboratory triaxial test. The values of CPT (50%) S_u and CPT (16%) S_u for the upper core appear to be mixed. It is evident from these comparisons that the use of the CPT to estimate undrained strength in the zones with gravel (upper core and downstream shell) can be misleading.

5.5.4 Stress-Strain-Strength Relationship for Static Loading

The stress-strain curves from the triaxial tests from current and previous investigations have been reviewed and summarized. For each stress-strain curve, the undrained secant modulus for a stress level that corresponds to 50% of the maximum shear strength of the sample, E_{u50}, was calculated and then normalized by dividing by the maximum undrained shear strength, S_u. The frequency distribution of the values of E_{u50}/S_u derived from the 41 triaxial compression tests are shown graphically on Figure 5-18. The average values for each of the four embankment zones are as follows:

Zone	E_{u50} / S_u
Upstream Shell	140
Upper Core	180
Lower Core	170
Downstream Shell	180

5.5.5 Dynamic Properties

Dynamic properties required for the engineering analyses consist of shear wave velocity, shear modulus reduction curves, and damping ratio curves. Wahler (1982) collected shear wave velocity data at the site. They conducted cross-hole, downhole, and surface refraction surveys at three locations. TGP measured shear wave velocity using OYO P-S logging in all three mud rotary borings, and also measured shear velocities using the seismic cone in the three CPT probes made along the dam crest. The shear wave velocity measurements are summarized in Figure 5-19 along with the recommended relationship between shear wave velocity and effective confining stress for Zones 1, 2U, 2L, and 4. The Wahler data for the lower core was not used

because the measurements do not agree with the measured values from the OYO and CPT surveys. This lack of agreement could be associated with errors in V_S measurements caused by the use of explosives or by possible misalignment of the boreholes used in the cross-hole survey.

The small strain shear modulus for each material type can be obtained from shear wave velocity and the known mass density of the material using the following relationship:

$$G_{max} = \rho \cdot V_S^2 \qquad \text{Eq. 5-1}$$

In this relationship, G_{max} is the small strain shear modulus, ρ is the mass density of the material, and V_s is the shear wave velocity.

Based on the observed clayey nature of the material for all zones of the dam, the shear modulus reduction and damping ratio curves were selected based on the work by Vucetic and Dobry (1991), corresponding to median plasticity index (PI) values of 15, 17, 35, and 15 for Zone 1, Zone 2U, Zone 2L, and Zone 4, respectively, as shown on Figure 5-20. These curves and the values of G_{max} will be used to develop stress-strain-strength relationships for seismic deformation analysis.

5.5.6 Permeability

The "Lenihan Dam Outlet Investigation, Vol. 1 – Final Engineering Report" (RLVA, 1999a) summarized all the data available on soil permeability of embankment materials that were available at the time; no permeability data have been added since then. Whaler (1982) conducted one triaxial permeability test on intact samples of the upstream shell, upper core, and lower core. They also measured permeability on a reconstituted sample of the downstream shell. RLVA (1999a) conducted triaxial permeability tests on samples of all zones of the embankment and also calculated values of permeability from the results of one-dimensional consolidation tests where measurements of coefficient of consolidation and soil stiffness were made. In addition, RLVA estimated soil permeability based on pore pressure dissipation tests in CPTs. The permeability values from these various tests are summarized in Table 5-5.

We noted that the data for the downstream shell and foundation are very limited and that the ratios of horizontal to vertical permeability were estimated by RLVA. Nevertheless, these values provide a starting point for the seepage analyses and will be adjusted, as appropriate, based on the results of the analyses.

The permeability of the foundation is indicated to be very low based on the one available test. However, as discussed in Section 4.2, data from borehole packer tests and from observed water loss in borings indicate that the very low permeabilities are representative of the sheared shale mélange within the Franciscan complex. However, the harder sandstone blocks contained within the mélange were found to have permeabilities on the order of 1×10^{-4} cm/sec.

No data are available on the permeability of the Zone 3 drain materials. However, from an engineering perspective, they are essentially free draining compared to the very low permeabilities of the other embankment zones provided the drain materials are continuous.

The continuity and effectiveness of the inclined drain is of concern. As discussed in Section 2.3.1, the inclined Zone 3 drain material was interrupted at elevation 510 feet because of

misalignment of the zone below elevation 510 feet that was corrected by adding a horizontal gravel layer as shown in Figure 2-4. We believe that the method used for "correcting" the problem may significantly limit the effectiveness of the drain material above elevation 510 feet because of the potential for the gravel layer to be "choked" by fines from Zone 2 materials washing into the layer since (a) Zone 2 and the gravel layer are not filter-compatible and (b) significant downward vertical gradients are expected to be induced by flow to the segment of horizontal drain within the inclined drain. Moreover, the construction records indicate that the quality and continuity of the Zone 3 drain materials may have been compromised because the placement of Zone 3 materials sometimes lagged behind the placement of Zones 2 and 4 materials and the Zone 3 layer had to be dug out after being covered by Zone 2 and/or Zone 4 material. In addition, the measured piezometric levels in the downstream shell shown on Figure 2-3 indicate that the downstream shell piezometers are not always dry as they should be if the inclined drain were functioning properly. Consequently, we believe that the Zone 3 inclined drain may not function as intended and will consider this further in our seepage analyses that will be included in a separate report on engineering analyses.

6.1 GENERAL

This section documents the earthquake ground motions from the controlling events on the Stanford-Monte Vista, Berrocal, and San Andreas faults that will be considered during the seismic stability evaluation of Lenihan Dam. These ground motions are developed in terms of response spectral values and candidate acceleration time histories to be used in developing time histories that are compatible with the specified response spectral values. The following subsections discuss the seismic sources considered, the development of V_{S30}, the attenuation relationships used, the resulting response spectra for the considered events, the candidate time histories, and the spectrally-matched time histories. The selection of candidate time histories considered the previous work on site-specific ground motions for Stevens Creek Dam (Terra/GeoPentech, 2011c) and the subsequent meeting and discussions between TGP and DSOD on the characterization of ground motions for that dam.

6.2 POTENTIAL SEISMIC SOURCES AND BACKGROUND INFORMATION

The significant seismogenic faults affecting seismic hazard at Lenihan Dam are discussed in Section 3.3.2 and shown on Figure 3-1. TM-3 (AMEC, 2009) indicates that the San Andreas, Berrocal, and Stanford-Monte Vista faults are the controlling seismic sources at the dam. The key parameters for these faults are listed in Table 6-1.

6.3 DAM CONSEQUENCE CLASSIFICATION, V_{S30}, Z1.0, AND Z2.0

Following the guidelines established by Fraser and Howard (2002), the statistical level of the design earthquake ground motion is based on factors including dam consequence and slip rate for each fault. We understand that the DSOD classification for Lenihan Dam is "high consequence" because of the populated community of Los Gatos downstream of the reservoir. Using the DSOD consequence-hazard matrix, the 84th percentile spectral accelerations are considered for all three faults studied.

As discussed in Section 4.2, Lenihan Dam was constructed on Franciscan Complex mélange bedrock, with an area of more massive sandstone occurring at the upper end of the spillway and under the left upstream side of the dam. The mélange typically consists of intensely fractured to crushed shale that encases blocks of harder sandstone and greenstone, some of which are up to several hundred feet in length, with lesser blocks of serpentinite and chert. The area of more massive sandstone that occurs at the upper end of the spillway on the left abutment includes some interbedded shale. Much of the dam footprint is directly underlain by the sheared shale matrix of the Franciscan mélange, with localized areas of hard rock, as discussed in Section 4.2.

The V_{S30} for the foundation of the dam was calculated based on OYO shear wave velocity data collected at two locations beneath the dam and one location within close proximity of the dam. During the TGP investigation, data was collected within the bedrock near the centerline of the embankment at LD-B-101 (approximately halfway between the abutments at Station 15+75), and at LD-B-103 (closer to the left abutment at Station 12+75). Previously, GeoVision (the same company that performed the OYO logging for the current study) completed OYO P-S borehole suspension logging for the Electric Power Research Institute (EPRI) near the dam spillway at the

left abutment, as shown on Figure 6-1. Figure 6-2 contains a cross section of the dam and foundation through the centerline of the embankment, with the three shear wave velocity profiles shown at their approximate locations; the location of the EPRI survey should be considered approximate because it is based on the recollection of Robert Steller of GeoVision who conducted the survey and provided the data (GeoVision, 2011). It is noted that LD-B-101 collected data within the bedrock at depths ranging from 192 feet to 246 feet below the ground surface, LD-B-103 collected data within the bedrock at depths ranging from 98.5 feet to 195 feet below ground surface, and the EPRI survey collected bedrock data from the surface to a depth of 84 feet. Figure 6-3 shows a summary of the shear wave velocity data from LD-B-101 plotted vs. depth below top of rock on the left side with the lithology from the boring log on the right side. Figure 6-4 shows the same summary for LD-B-103 where the shear wave velocity profile extends for the full 30 meters (m) below top of rock. The lithology for the EPRI survey was not available for review. Figures 6-3 and 6-4 indicate that the predominant rock encountered within the foundation during the TGP investigation is Franciscan Complex mélange consisting of crushed clay shale with thin interbeds of sandstone; this generally agrees with the geology mapped by Marliave in 1948, reported by Scott in 1976, reported by Wahler in 1982, and substantiated by RLVA (1999) and Frame and Volpe (2001). For these reasons, we believe the data collected is representative of the foundation conditions in general and is appropriate for developing the site-specific V_{S30}. The data tabulated in Tables 6-2A, 6-2B and 6-2C show the calculations made for the three sets of data at LD-B-101, LD-B-103 and EPRI Spillway, respectively. Table 6-3 summarizes these results: at LD-B-101 we have 17 meters of data yielding a V_{S17} of 1,160 m/sec, at LD-B-103 we have 30 meters of data yielding a V_{S30} of 1,390 m/sec and at the EPRI Spillway location we have 24 meters of data yielding a V_{S24} of 1,190 m/sec. In total 70 meters of data has been collected within the dam foundation and the results were combined to determine a site-specific V_{S30} of 1,260 m/sec, as shown on Tables 6-2A to 6-2C and Table 6-3..

Geomatrix (2006b) made downhole shear wave velocity measurements in two borings (B-11 and B-6) as part of their geotechnical investigation for the new outlet tunnel at Lenihan Dam. Boring B-11 located along Los Gatos Creek downstream of the toe of the dam extended 30 feet into greenstone/serpentine bedrock and had a measured shear wave velocity of 990 m/sec, which is relatively consistent with the 2011 measurements and the EPRI data discussed above. Boring B-6 was located on the upstream right abutment ridge, about 600 feet upstream of the crest of the dam, in the parking area to the west of the control building for the new outlet works. This boring was drilled to a depth of 130 feet into rock and encountered moderately to severely weathered, intensely fractured and sheared Franciscan Complex bedrock. The shear wave velocities measured in this boring ranged from 520 to 950 m/sec, the lower values being measured in the intensely fractured and sheared rock. The conditions at Boring B-6 do not appear to be similar to the rock conditions beneath the dam; i.e., the Franciscan complex has more closely spaced fractures and more severe weathering than observed at the dam site, perhaps because of the proximity of Boring B-6 to the mapped trace of the inactive Lexington Fault.

One of three attenuation relationships (Campbell and Bozorgnia, 2008) requires estimating the depths where the shear wave velocity is equal to 1 km/sec (Z1.0) and 2.5 km/sec (Z2.5). Since the measured shear wave velocities reach values greater than 1,000 m/sec in the first 1 to 2 meters of the top of rock, the Z1.0 depth is about zero. Nevertheless, we have conservatively

assumed a Z1.0 depth of 10 meters The Z2.5 depth is difficult to estimate precisely because the Franciscan complex extends to great depth at the site but this is not a problem because the calculated spectral accelerations are relatively insensitive to the estimated Z2.5 value. We assumed a Z2.5 depth of 500 meters and noted that the calculated Peak Ground Acceleration would only increase by 0.5 percent if the actual Z2.5 depth were 3,000 meters instead of 500 meters.

6.4 ATTENUATION RELATIONSHIPS AND DESIGN RESPONSE SPECTRA

Although five New Generation Attenuation (NGA) relationships are available, only four of them were used in the evaluation documented herein. The Idriss (2008) attenuation relationship was not considered because the value of V_{S30} for Lenihan Dam is outside the range of values for which the Idriss relationship can be applied. An arithmetic average of the four remaining NGA relationships (Abrahamson and Silva, 2008; Boore and Atkinson, 2008; Campbell and Bozorgnia, 2008 and Chiou and Youngs, 2008) was used to develop design response spectral values for the dam site.

In using the NGA relationships a number of parameters need to be specified. These parameters include the style of faulting, maximum magnitude, and distance to each fault listed in Table 6-1. Other required parameters associated with the site subsurface conditions include: (1) shear-wave velocity (V_{S30}) within the upper 30 m (100 ft) of the foundation rock (1,260 m/sec), (2) depth to V_S=1 km/sec or 3,300 ft/sec foundation material (10 m for the site), and (3) depth to V_S=2.5 km/sec (8,200 ft/sec) foundation material beneath the dam (0.5 km for the site). The development of these parameters is summarized in Section 6.3 above.

Table 6-1 also provides estimates of the median and 84th percentile peak horizontal ground acceleration (PGA), and median and 84th percentile Arias Intensity using the NGA relationships. It should be noted that the Arias Intensity values were obtained from the Watson-Lamprey and Abrahamson (2006) attenuation relationships.

Figure 6-5 shows the 84th percentile fault parallel (FP) response spectra for the three earthquake event scenarios shown in Table 6-1. As can be seen on this figure, the Stanford-Monte Vista event controls the shaking condition at the site for the lower magnitude earthquake scenario. Larger earthquake magnitude, such as the one occurring along the San Andreas Fault, controls the shaking condition at the site for periods larger than about 1 second.

Figure 6-6 shows the fault normal (FN) response spectra for the three earthquake event scenarios shown in Table 6-1. Fault rupture directivity effects used to develop the fault normal component response spectra were based on DSOD guidelines (Fraser and Howard, 2002). The forward directivity effects were estimated using the near source factor developed by Somerville et al. (1997), as modified by Abrahamson (2000). As in the case of the FP response spectra, the FN response spectra are dominated by the Stanford-Monte Vista event for a period less than about 1 second. The San Andreas event dominates the shaking condition at the site for periods larger than about 1 second.

Because of the disparity in the shaking between lower magnitude events (such as the Stanford-Monte Vista and the Berrocal events) and the larger magnitude event (such as the San Andreas event), we recommend that two response spectra be used in the seismic evaluation of the dam.

We recommend that the Stanford-Monte Vista response spectrum be used for the evaluation of lower magnitude events, and that the San Andreas spectrum be used for the evaluation of higher magnitude events. Figure 6-8 shows the FP and FN components of these recommended response spectra. The characteristics of these response spectra are also provided in tabular form on Tables 6-4A and 6-4B for the FP and FN components of the Stanford-Monte Vista event and on Tables 6-5A and 6-5B for the FP and FN components of the San Andreas event.

6.5 CANDIDATE ACCELERATION TIME HISTORIES AND SPECTRALLY-MATCHED TIME HISTORIES FOR STANFORD-MONTE VISTA EVENT

Based on the recommended response spectral values shown on Figure 6-7 and listed in Tables 6-4A through 6-5B, two sets of three seed acceleration-time histories were considered for potential use in developing spectrum-compatible acceleration time histories for the seismic response and deformation analyses.

The characteristics of the three selected seed time histories for the Stanford-Monte Vista event are summarized in Table 6-6A. These seed time histories were selected from the following earthquakes: the 1995 Kobe, the 1989 Loma Prieta, and the 1994 Northridge earthquakes. These same three earthquakes were selected for use in the analysis of the Stevens Creek Dam as well as other Santa Clara Valley District dams for lower magnitude local events and are also considered appropriate for this application. The acceleration, velocity, and displacement-time histories; the Arias Intensity; and the response spectra for each of the seed recordings are shown on Figures 6-8, 6-9, and 6-10, respectively. On the Arias Intensity plot, the 84th percentile Arias Intensity value corresponds to the calculated values using the Watson-Lamprey and Abrahamson (2006) relationship with input PGA and SA (T = 1s) from the recommended Fault Normal Stanford-Monte Vista response spectra. The lines representing the 84th percentile plus and minus one standard deviation are based on the uncertainty in the Watson-Lamprey and Abrahamson (2006) relationship. It should be noted that the selected time histories shown on these figures correspond to the FN component. Because the axis of the dam is sub-parallel to the San Andreas Fault and on the hanging wall of the Stanford-Monte Vista Fault (the two faults controlling the shaking condition at the site), only the FN component will be used in the seismic response and deformation analyses of the dam.

The selected candidate acceleration time histories were then adjusted using the software RSPMatch (Abrahamson, 1992; Al-Atik and Abrahamson, 2010) to match the target response spectra. RSPMatch adjusts the seed motion in the time domain by applying adjustment wavelets to better match the target response spectrum. Figure 6-11 shows the adjusted MDE time history based on the Kobe – Nishi-Akashi motion in terms of acceleration, velocity, displacement and Arias Intensity time histories and a comparison of the response spectral values with the MDE response spectral values. Figures 6-12 and 6-13 show the same information for the adjusted time history based on the Loma Prieta – LGPC and the Northridge – Sylmar OVMFF records, respectively. It should be noted that the Arias Intensity values of the three ground motions exceed the best estimate of Arias Intensity provided by the Watson-Lamprey and Abrahamson relationship with 84th percentile ground motion inputs.

6.6 CANDIDATE ACCELERATION TIME HISTORIES AND SPECTRALLY-MATCHED TIME HISTORIES FOR SAN ANDREAS EVENT

The selection of seed time histories for the San Andreas event was carried out more systematically due to the relatively small number of high quality ground motion records from stations that are very close to ruptures of very large magnitude earthquakes. The selection process began with a preliminary screening of all 3,551 records in the PEER Ground Motion Database. The records are plotted in Figure 6-14 with magnitude on the x-axis and closest distance in kilometers on the y-axis. From this pool, only records from events with Magnitude 7.0 or greater and within 40 km of the rupture were considered. This narrowed the field to 155 strong motion records as shown in the red rectangular area on Figure 6-14.

The second step in the screening process attempted to identify records with similar spectral accelerations to the target ground motion for the Fault Normal component of the San Andreas at key periods of interest. The first period of interest was peak ground acceleration (PGA) and all records with about half the PGA of the target ground motion (0.3g) were flagged for consideration. The second period of interest was the fundamental period of the dam, estimated as $T = 2.6*H/Vs$, with H equal to the height of the embankment and Vs equal to the average shear wave velocity of the embankment. Using this relationship, the fundamental period of the dam was estimated to be 0.5 seconds and the average spectral acceleration of the target spectrum between $0.8T$ and $1.2T$ was estimated to be 1.1g. All of the remaining records with a period of 0.7 seconds or more were included for consideration. These records are shown graphically in Figure 6-15 with average spectral acceleration in the fundamental period range on the x-axis and PGA on the y-axis. This second level of screening resulted in 30 records of interest as shown in the red rectangular area on Figure 6-15. An exception was made to include the Denali TAPS Pump Station #10 record which did not meet either criteria with regards to the spectral acceleration characteristics but is a record of a strike-slip event with magnitude 7.9 recorded 3.8 km from the rupture which is the most similar event with respect to magnitude and distance to that postulated for Lenihan Dam.

The final level of screening was based on the significant duration and Arias Intensity of the seed time histories. Significant duration, $D_{5\text{-}95}$, defined as the time in seconds between the 5^{th} and 95^{th} percentile Arias Intensity, of the San Andreas event was estimated using three procedures: Kempton and Stewart (2006) with no directivity effects, Kempton and Stewart (2006) with directivity effects, and Bommer et.al. (2009). Using these methods, the estimated $D_{5\text{-}95}$ for the M7.9 San Andreas earthquake ranged from 17 to 28 seconds. The Arias Intensity of the 84^{th} percentile ground motions of the San Andreas Fault was estimated to be 5.66 m/sec using Watson-Lamprey (2007. To compare these to the 30 records that were screened, the Arias Intensity and significant duration were calculated for each record. The results of this exercise are shown on Figure 6-16 with Arias Intensity plotted on the x-axis and significant duration plotted on the y-axis. As shown on Figure 6-16, eight records with similar Arias Intensity and significant duration similar to that of the San Andreas event, as well as the Denali TAPS record, were chosen for a final candidate selection. The two horizontal components for each record were rotated to Fault Normal and the resulting time histories and spectral accelerations were plotted for comparison. Figure 6-17 shows the Fault Normal spectral acceleration of each of the final nine records as compared to the target San Andreas spectrum. Based on visual analysis of these

records, three time histories for spectral matching were selected as follows: the 1990 Manjil earthquake, Abbar record; the 1999 Chi-Chi earthquake, TCU065 record; and the 1992 Landers earthquake, Lucerne record. These three records are highlighted on Figure 6-16. These same three earthquakes were also selected for use in the analysis of the Stevens Creek Dam for the San Andreas event and are also considered appropriate for this application. The acceleration, velocity, and displacement-time histories, the Arias Intensity; and the response spectra for each of the seed recordings are shown on Figures 6-18, 6-19, and 6-20, respectively.

The selected candidate acceleration time histories were then adjusted using the software RSPMatch (Abrahamson, 1992; Al-Atik and Abrahamson, 2010) to match the target response spectra. Figure 6-21 shows the adjusted MDE time history based on the Manjil – Abbar motion in terms of acceleration, velocity, displacement and Arias intensity time histories and a comparison of the response spectral values with the MDE response spectral values. Figures 6-22 and 6-23 show the same information for the adjusted time history based on the Chi Chi – TCU065 and the Landers – Lucerne records, respectively. It should be noted that the Arias Intensity values of the three ground motions exceed the best estimate of Arias Intensity provided by the Watson-Lamprey and Abrahamson relationship with 84th percentile ground motion inputs.

7.1 GENERAL

The purpose of this report is to provide a basis for the detailed analyses of the seismic stability of Lenihan Dam based on a thorough review and careful interpretation of the relevant data. As the title of the report indicates, the results of this work can be divided between site characterization, material properties, and ground motions. The key findings related to each of these topics are summarized below.

7.2 SITE CHARACTERIZATION

The key findings related to site characterization are as follows:

1. The dam is founded directly on bedrock – no alluvial or colluvial soils were left in place beneath the embankment.
2. The geometry of the valley where the dam was constructed is complex. The right side of the valley (looking downstream) has a relatively uniform side slope but the left side of the valley is characterized by a massive knob of bedrock that underlies the upstream portion of the dam.
3. With the exception of the internal drainage zones, all embankment materials are well-compacted soils with varying amounts of sand and gravel in a clay matrix.
4. Except for the drain materials, the embankment soils have very low permabilities.
5. There are no liquefiable materials within the dam or the dam foundation.

7.3 MATERIAL PROPERTIES

The generalized geometry and material classifications of Lenihan Dam at its maximum section are shown on Figure 5-1. The key findings related to material properties are as follows:

1. The source of materials for the construction of the upstream shell and upper core of the dam is the Franciscan Complex mélange from borrow areas located just upstream of the upstream toe of the dam. The physical/index properties and the engineering properties of these two zones are very similar.
2. The source of the materials used in the construction of the lower core is clayey alluvial/colluvial fan deposits from borrow areas at the mouth of Limekiln Canyon upstream of the dam on the right side of the valley. The lower core material is a clay of high plasticity; it contains little to no gravel and has a lower strength than the upper core and upstream shell.
3. The source of the materials for the construction of the downstream shell is Franciscan Complex sandstone and mélange excavated during construction of the spillway channel. The physical/index properties of the downstream shell are similar to those of the upstream shell and upper core except that the gravel content is higher than in those two other zones. The strength of the downstream shell materials is quite variable and appears to be, on average, lower than the strength of the upstream shell and upper core.
4. Table 5-3 summarizes the engineering properties of all embankment materials with the exception of the Zone 3 drain materials. The strength and stiffness of the Zone 4

(downstream shell) materials can be conservatively assigned to the Zone 3 materials for the seismic deformation analyses.

5. Table 5-5 summarizes the permeability of the various embankment zones and underlying bedrock for use in the seepage analyses.

7.4 GROUND MOTIONS

Site-specific input ground motions were developed for use in the seismic deformation analyses. Key elements in the development of these site specific ground motions are as follows:

1. Lenihan Dam is classified as a "high consequence" dam by DSOD, based on a DSOD Hazard Classification Total Class Weight of 30.
2. The two seismogenic faults controlling the seismic hazard at the dam are the Stanford-Monte Vista and San Andreas faults. The Stanford-Monte Vista event controls the shaking condition at the site for periods of 1 second or less for the lower magnitude earthquake scenario. The San Andreas event has a larger earthquake magnitude and controls the shaking condition at the site for periods larger than about 1 second.
3. The V_{S30} for the foundation of the dam was calculated based on OYO shear wave velocity data collected at two locations beneath the dam and one location within close proximity of the dam. A site-specific V_{S30} of 1,260 m/sec was determined based on these measurements and used in the development of the design response spectra for the Stanford-Monte Vista and San Andreas events.
4. Three seed time histories were selected for the Stanford-Monte Vista event and adjusted to match the target response spectra. It should be noted that the Arias Intensity values of the three selected ground motions exceed the best estimate of Arias Intensity provided by the Watson-Lamprey and Abrahamson relationship with 84th percentile ground motion inputs.
5. Seed time histories for the San Andreas event were selected through a multi-step screening of the PEER Ground Motion Database because of the relatively small number of high quality ground motion records from stations that are very close to ruptures of very large magnitude earthquakes. The selection process screened all 3,551 records in the Database and yielded eight records with values of Arias Intensity and significant duration similar to those of the San Andreas event. These eight records, as well as the Denali TAPS record, were chosen and evaluated, and three final seed time histories were selected. The final three selected seed time histories were then adjusted to match the target response spectra. As for the Stanford-Monte Vista event, the Arias Intensity values of the three ground motions exceed the best estimate of Arias Intensity provided by the Watson-Lamprey and Abrahamson relationship with 84th percentile ground motion inputs.

AMEC, 2009 (January), Technical Memorandum No. 3, Seismotectonic and Ground Motion Study, Seismic Stability Evaluation of DIP Phase 1 Dams.

Abrahamson, N.A., (1992). Non-Stationary Spectral Matching. Seismological Research Letters, 63(1).

Abrahamson, N.A., 2000, "Effects of rupture directivity on probabilistic seismic hazard analysis," Proc. 6th International Conference on Seismic Zonation, Palm Springs.

Abrahamson, N.A., and Silva, W.J., 2008 (February), "Summary of the Abrahamson & Silva NGA Ground Relations," *Earthquake Spectra*, Vol. 24, No. 1, pp. 67-98. EERI.

Al-Atik, L. and Abrahamson, N.A., (2010), "An Improved Method for Nonstationary Spectral Matching", Linda Al Atik and Norman Ambrahamson, Earthquake Spectra, Volume 26, No. 3, pages 601-617, August 2010

Bommer, J.J., Stafford, P.J., and Alarcon, J.E., 2009, "Empirical Equations for Prediction of the Significant, Bracketed, and Uniform Duration of Earthquake Ground Motions", Bulletin of the Seismological Society of America, Vol. 99, pp. 3217-3233.

Boore, D. M. and Atkinson, G.M., 2008 (February), "Ground-Motion Prediction Equations for the Average Horizontal Component of PGA, PGV, and 5%-Damped PSA at Spectral Period between 0.01s and 10.0 s," Earthquake Spectra, Vol. 24, No. 1, pp. 99-138. EERI.

Bryant, W.A., compiler, 2000, Fault no. 56, Monte Vista-Shannon fault zone, in Quaternary fault and fold database of the United States: U.S. Geological Survey website, http://earthquakes.usgs.gov/regional/qfaults.

California Department of Water Resources, 1948-1954, Geological and Engineering Construction Inspection Memoranda to Mr. H.W. Holmes, Lexington Dam, by E.C. Marliave, D.F. Dresselhaus, et al (on file at DSOD).

California Department of Water Resources, Division of Safety of Dams (DSOD), 1981 (July), Phase 1 Inspection Report for Lexington Dam.

California Department of Water Resources, Division of Safety of Dams (DSOD), 2006a (May), Memorandum of Geologic Review of Seismic Hazard, James J. Lenihan Dam, dated May 25, 2006.

California Department of Water Resources, Division of Safety of Dams (DSOD), 2006b (October), Geologic Review of Geotechnical Data Report and Lexington Fault Evaluation Memo, dated October 23, 2006.

California Department of Water Resources, Division of Safety of Dams (DSOD), 2006c (October), Memorandum of Design Review – Review of Performance During the Loma Prieta Earthquake, James J. Lenihan Dam, dated October 23, 2006.

California Department of Water Resources, Division of Safety of Dams (DSOD), 2007a (June), Memorandum of Design Review, James J. Lenihan Dam, dated June 29, 2007.

California Department of Water Resources, Division of Safety of Dams, 2007b (November), Geologic Inspection of Lexington Fault Exposure and Review of Lexington Fault Cove Exposure Memo, dated November 26, 2007.

California Department of Water Resources, Division of Safety of Dams (DSOD), 2009 (October), Updated Ground Motion Estimates, J. Lenihan Dam, dated October 15, 2009.

California Department of Water Resources, Division of Safety of Dams (DSOD), 2010a (June), DSOD Comments on DM-2 and Interim DM-4, Guadalupe, Almaden, and Calero Dams, dated June 10, 2010.

California Department of Water Resources, Division of Safety of Dams (DSOD), 2010b (November), Email message from Jeffrey D. Kuhl of DSOD to Steven Wu of Santa Clara Valley Water District , dated November 8, 2010.

Campbell, K.W., and Bozognia, Y. , 2008 (February), "NGA Ground Motion Model for the geometric Mean Horizontal Component of PGA, PGV, PGD and 5% Damped Linear Elastic Response Spectra for Periods Ranging from 0.01 to 10 s," Earthquake Spectra, Vol. 24, No. 1, pp. 139-172. EERI.

Chiou, B.S.J. and Youngs, 2008 (February), "An NGA Model for the Average Horizontal Component of Peak Ground Motion and Response Spectra," Earthquake Spectra, Vol. 24, No. 1, pp. 173-216. EERI.

Cotton and Associates, 1993, Pre-Design Investigation, Lexington Dam Freeboard Restoration Project, Santa Clara Valley Water District.

Earth Science Associates (ESA), 1987 (December), Lexington Reservoir Outlet Modifications, Final Geotechnical Investigation, prepared for Santa Clara Valley Water District.

Frame, P.A. and Volpe, R.L., 2001 (October), Santa Clara Valley Water District (SCVWD) Phase B Instrumentation Project Basic Data Report.

Fraser, W.A., and Howard, J.K., 2002 (October), "Guideline for Use of the Consequence-Hazard Matrix and Selection of Ground Motion Parameters," The Resource Agency, Dept. of Water Resources, Div. of Safety of Dams.

Geomatrix Consultants, 1992, Analysis of the Recorded Response of Lexington Dam During the Loma Prieta Earthquake.

Geomatrix Consultants, 1996 (April), Geologic/Geotechnical Study and Basis of Design report, Lexington Dam Freeboard Restoration Project.

Geomatrix Consultants, 2006a (July), Evaluation of Lexington Fault near Lenihan Dam, Memorandum to Mr. Nolting - Jacobs Associates, Lenihan Dam Outlet Modification Project, Memorandum, dated July 14, 2006.

Geomatrix Consultants, 2006b, Final Geologic and Geotechnical Data Report, Lenihan Dam Outlet Modification Project.

Geomatrix Consultants, 2007 (October), Field Review of Lexington Fault Exposure in "The Cove", Memorandum to Mr. Nolting, Jacobs Associates, in support of Lenihan Dam Outlet Modification Project, dated October 12, 2007.

GeoVision, 2011, Personal communication from Robert Steller.

Hancock, J., Watson-Lamprey, J., Abrahamson, N.A., Bommer, J., Markatis, A., McCoy, E., Mendis, R., 2006, An Improved Method of Matching Response Spectra of Recorded Earthquake Ground Motion Using Wavelets. Journal of Earthquake Engineering, Vol. 10, Special Issue 1, Pages 67-89.

Harza Engineering Company, 1997 (January), GEFDYN Verification of Lexington Dam, Draft Report, prepared for Tennessee Valley Authority.

Idriss, I. M., and Joseph I. Sun, J. I., 1992 (November), User's Manual for SHAKE-91. University of California, Davis, Center for Geotechnical Modeling, Department of Civil & Environmental Engineering.

Idriss, I. M., 2003, Personal communication.

Idriss, I.M., 2008 (February), "An NGA Empirical Model for Estimating the Average Horizontal Spectral Values Generated by Shallow Crustal Earthquakes," Earthquake Spectra, Vol. 24, No. 1, pp. 217-242. EERI.

Itasca, 2008, FLAC, version 6.0, Itasca Consulting Group Inc., Minneapolis.

Kempton, J.J. and Stewart, J.P., 2006, "Prediction Equations for Significant Duration of Earthquake Ground Motions Considering Site and Near-Source Effects", Earthquake Spectra, 22(4), pp. 985-1013.

Ladd, C.C. and DeGroot, D.J., 2003, Recommended Practice for Soft Ground Site Characterization, the Arthur Casagrande Lecture, Proceedings of the 12th Panamerican Conference on Soil Mechanics and Geotechnical Engineering, Boston MA, Vol.1, pp. 3-57.

William Lettis & Associates, Inc. (Lettis), 2008 (December), Final Technical Memorandum, Seismic Source Identification and Development of Earthquake Parameters for Deterministic Seismic Hazard Analysis, Eleven Santa Clara Valley Water District Dams, Santa Clara County, California.

Lewis, R.W. Jr., 1951, The Lexington Dam Site: unpublished report to Col. Van Court Warren, dated June 15, 1951.

Marliave, E.C., 1948, Geological Report on the Lexington Dam Site.

Marliave, E.C., 1951, Memorandum to Mr. H. W. Holmes, Lexington Dam No. 72-8, Inspected January 3 and 4, 1951.

McLaughlin, R.J., Oppenheimer, D., Helley, E.J., and Sebrier, M., 1992, The Lexington fault zone: a north-south link between the San Andreas fault and range front fault system, Los Gatos, California: Geologic Society of America Abstracts with Programs, v. 24, no. 5, p. 69.

McLaughlin, R.J., Clark, J.C., Brabb, E.E., and Helley, E.J., 2001, Geologic Maps and Structure Sections of the Southwestern Santa Clara Valley and Southern Santa Cruz Mountains, Santa Clara and Santa Cruz Counties, California, Sheet 1: Los Gatos Quadrangle.

McLaughlin et al, 2004, Geologic Map of the Loma Prieta Region, California, USGS Professional Paper 1550E.

Nelson, J.L., 2010a (January), Santa Clara Valley Water District (SCVWD) Foundation Analysis Report on Chesbro No.72-11, Lenihan No.72-8, Stevens Creek No. 72-7, and Uvas No. 72-12 Dams (SSE-2 Dams).

Nelson, J.L., 2010b (June), Santa Clara Valley Water District (SCVWD) 2010 Surveillance Report, March 2009 through April 2010, Lenihan Dam No.72-8.

Nelson, J.L. and Volpe, R.L., 2007 (July), Santa Clara Valley Water District (SCVWD) Second Summary Surveillance Report, December 2003 through July 2007, Lenihan Dam No. 72-8.

Robertson, P.K. and Campenella, R.G., 1990, Guidelines for Use, Interpretation and Application of CPT and CPTU, University of British Columbia, Soil Mechanics Series 105, Civil Engineering Department, Vancouver, B.C., V6T 1W5, Canada.

Robertson, P.K. and Wride, C.E., 1998, Evaluating Cyclic Liquefaction Potential Using the Cone Penetrometer Test, Canadian Geotechnical Journal, Vol. 35, No. 3, pp. 442-459.

Robertson, P.K., 2009, Interpretation of Cone Penetrometer Tests – a unified approach, Canadian Geotechnical Journal, Volume 46, Number 11, 1 November 2009, pp. 1337-1355.

Rogers. T.H., and Armstrong, C.F., 1971, Environmental geologic analysis of the Santa Cruz Mountains study area, Santa Clara County, California: California Division of Mines Open File Report 72-21, 75p.

Rogers, T.H. and Williams, J.W., 1974, Potential seismic hazards in Santa Clara County, California: California Division of Mines and Geology Special Report 107, 39 p., map scale 1:62,500.William Lettis & Associates (WLA), 2008, Seismic Source Identification and Development of Earthquake Parameters for Deterministic Seismic Hazard Analysis, Letter to Geomatrix Consultants, December 17, 2008.

Santa Clara Valley Water District (SCVWD), 1976, Reconnaissance of Landslide Conditions at Lexington Reservoir.

Santa Clara Valley Water District (SCVWD), 1996, Specifications and Contract Documents for the Construction of Lexington Dam Freeboard Restoration Project.

Scott, J., 1976, Lexington Reservoir, Landslide Investigation. Santa Clara Valley Water District, Santa Clara County, CA.

Terra / GeoPentech, 2010 (November 24), Technical Memorandum SSE2-TM-1LN, Initial Review of Available Data for Lenihan Dam.

Terra / GeoPentech, 2011a (April), Seismic Stability Evaluations of Chesbro, Lenihan, Stevens Creek, and Uvas Dams, Phase A: Stevens Creek and Lenihan Dams, Lenihan Dam, Work Plan for Site Investigations and Laboratory Testing (Report No. LN-1), prepared for Santa Clara Valley Water District.

Terra / GeoPentech, 2011b (June), Seismic Stability Evaluations of Chesbro, Lenihan, Stevens Creek, and Uvas Dams, Phase A: Stevens Creek and Lenihan Dams, Stevens Creek Dam, Site Characterization, Material Properties, and Ground Motions (Report No. SC-2), prepared for Santa Clara Valley Water District.

Terra / GeoPentech, 2011c (October), Seismic Stability Evaluations of Chesbro, Lenihan, Stevens Creek, and Uvas Dams, Phase A: Stevens Creek and Lenihan Dams, Lenihan Dam, Site Investigations and Laboratory Testing Data Report (Report No. LN-2), prepared for Santa Clara Valley Water District.

Treadwell and Rollo, 2002, Geotechnical Feasibility Report for Lenihan Dam New Tunnel Option.

URS Corporation, 2010 (October), Design Memorandum No.4, Task 3 – Site Specific Design Earthquake Motions, Seismic Stability Evaluation of Almaden, Calero, and Guadalupe Dams.

U.S. Geological Survey website, 2011, Rupture Length and Slip – The Northern California Earthquake April 18, 1906: http://quake.wr.usgs.gov/info/1906/offset.htm.

Volpe, R.L. and Associates (RLVA), 1990, Investigation of SCVWD Dams Affected by Loma Prieta Earthquake of October 17, 1989, Report to Santa Clara Valley Water District.

Volpe, R.L. and Associates (RLVA), 1997, Evaluation of Partial Collapse of Low Level Outlet Pipeline, James J. Lenihan Dam.

Volpe, R.L. and Associates (RLVA), 1998, Instrumentation Design and Review, Lenihan Dam.

Volpe, R.L. and Associates (RLVA), 1999a, Lenihan Dam Outlet Investigation, Vol. 1 – Final Engineering Report.

Volpe, R.L. and Associates (RLVA), 1999b, Lenihan Dam Outlet Investigation, Vol. 2 – Basic Data Report.

Vucetic, M. and Dobry, R., 1991, Effect of Soil Plasticity on Cyclic Response, Journal of Geotechnical Engineering Division, ASCE, Vol. 117, No. 1, pp.89-107.

Wahler Associates, 1982, Final Report on Seismic Safety Evaluation of Lexington Dam.

Wahler Associates, 1993, Investigation of Seepage on the Downstream Face of Lexington Dam.

Watson-Lamprey, J.A., 2007, "Selection and Scaling of Ground Motion Time Series", Ph.D. Dissertation, Department of Civil and Environmental Engineering, University of California, Berkeley.

Watson-Lamprey, J.A. and Abrahamson, N.A., 2006 (February), “Selection of Ground Motion Times Series and Limits on Scaling,” Soil Dynamics and Earthquake Engineering, vol. 26, pp. 477-482

Wells, R., editor, 2004, The Loma Prieta, California, Earthquake of October 17, 1989 - Geologic Setting and Crustal Structure, USGS Professional Paper 1550E.

Wills, C., Weldon, R., and Bryant, W., 2008, Appendix A: California Fault Parameters for the National Seismic Hazard Maps and Working Group on California Earthquake Probabilities 2007, USGS Open File Report 2007-1437A.

Woodward-Clyde Consultants, 1993, Nonlinear Dynamic Response Analysis of Lexington Dam.

TABLES

TABLE 5-1
REVIEW AND ASSESSMENT OF LABORATORY AND FIELD DATA FROM PREVIOUS INVESTIGATIONS

Study	Classification Properties	In-situ Properties	Effective Stress Strength	Undrained Strength	Cyclic Properties	Shear Wave Velocity	Other Properties
Wahler, 1982 Study conducted between 1975 and 1981, data compiled in 1982 report	Moisture content, density, specific gravity, sieve analysis, hydrometer and Atterberg limits Application: Data used Reasoning: Data was complete and considered reliable	In-place density tests and limited SPTs Application: Density data used Reasoning: SPT data not used because materials were clayey and hammer energy was not calibrated	9 ICU'C tests on pitcher samples for Zone 1, 2U and 2L, 3 ICU'C tests on re-compacted samples for Zone 4 Application: Data used, except re-compacted samples of Zone 4 Reasoning: Test results on re-compacted specimens may not be reliable	9 ICU'C tests on pitcher samples for Zone 1, 2U and 2L, 3 ICU'C tests on re-compacted samples for Zone 4 Application: Data used except for re-compacted specimens of Zone 4 Reasoning: Test results on re-compacted specimens may not be reliable	Stress controlled cyclic testing on pitcher samples and re-compacted samples Application: Data considered but not used Reasoning: Not relevant to current state of practice	Cross-hole, downhole and surface refraction surveys for all zones Application: Data considered Reasoning: Data was complete and considered	Resonant column, consolidation, permeability and maximum density Application: Density and permeability data used Reasoning: Shear wave data used in lieu of resonant column data for shear modulus
Geomatrix, 1996 Study conducted between 1995 and 1996	Moisture content, density, specific gravity, sieve analysis, and limits for Zone 2U Application: Data used Reasoning: Data was considered reliable but limited to Zone 2U	SPTs using modified California sampler Application: Data not used Reasoning: SPT data not used because a non-standard sampler was used, materials were clayey and energy was not calibrated	Unconfined compression (UC) tests on soil and rock samples Application: Data not used Reasoning: UC testing is not applicable for determining effective stress strength parameters	UU testing on disturbed rock samples obtained by modified California sampler Application: Data not used Reasoning: Sampling and testing considered inappropriate for assigning shear strength	No testing performed	No data collected	Maximum density on Zone 2U material Application: Density data used Reasoning: Data was considered reliable
Harza, 1997 Study conducted between 1996 and 1997	Moisture content, density, specific gravity and Atterberg limits Application: Data used Reasoning: Data was complete and considered reliable	No testing performed	16 ICU'C tests on four samples from each zone Application: Data used Reasoning: Data was complete and considered reliable	16 ICU'C tests on four samples from each zone Application: Data used Reasoning: Data was complete and considered reliable	Strain controlled cyclic testing on all zones Application: Data considered but not used Reasoning: Not relevant to current state of practice	No data collected	Consolidation tests on all zones Application: Data not used Reasoning: Testing was performed in non-standard way for determining maximum past pressure
RLVA, 1999 Study conducted between 1998 and 1999	Moisture content, density, specific gravity, sieve analysis, hydrometer and Atterberg limits Application: Data used Reasoning: Data was considered reliable but excluded Zone 4	CPT data on all four zones Application: Data used to assess variability of embankment materials Reasoning: Data was complete and considered reliable	No testing performed	Inferred data from CPT Application: Data used to assess variability of embankment materials Reasoning: Data was complete and considered reliable	No testing performed	No data collected	Consolidation, permeability and pore pressure dissipation testing performed Application: Data used Reasoning: Data was complete and reliable
SCVWD, 2001 Study conducted in 2001	Moisture content, density, specific gravity, sieve analysis, hydrometer and Atterberg limits for Zone 4 Application: Data used Reasoning: Data was considered reliable but limited to Zone 4	No testing performed	9 ICU'C tests on Zone 4 samples Application: Data used Reasoning: Data was considered reliable but limited to Zone 4	9 ICU'C tests on Zone 4 samples Application: Data used Reasoning: Data was considered reliable but limited to Zone 4	No testing performed	No data collected	Permeability testing performed on Zone 4 Samples Application: Data used Reasoning: Data was complete and reliable

Notes:
1. A solid red box around the "Application" section indicates that the data were used in the material property characterization; a dashed red box indicates the data were considered but not used.
2. In the "Reasoning" sections, "complete" is used to characterize studies where testing encompassed all zones and all pertinent data was reported; "considered reliable" is based on judgment.

TABLE 5-2
MATERIAL CLASSIFICATION SUMMARY

Zone[2]	Idealized Material Description	Generalized USCS Classification	In-Situ Conditions[3]			Gradation[3]				Atterberg Limits[3]	
			Dry Unit Weight, γd (pcf)	Moisture Content, W_c (%)	Compaction (%)[4]	Gravel (%)	Sand (%)	Fines (%)	Clay Fraction, -2μ (%)	Liquid Limit LL	Plasticity Index PI
1	Upstream Shell	SC, CL	119.3 (95.2 - 132.3)	15.0 (10.3 - 26.5)	95 (76 - 106)	27 (0 - 43)	34 (3 - 44)	39 (19 - 97)	21 (12 - 44)	33 (30 - 39)	15 (6 - 24)
2U	Upper Core (Above El. 590 ft)	SC, GC	119.6 (108.0 - 131.5)	11.9 (6.0 - 17.7)	95 (81 - 112)	33 (3 - 58)	35 (23 - 48)	31 (16 - 53)	17 (13 - 30)	37 (30 - 48)	17 (14 - 29)
2L	Lower Core (Below El. 590 ft)	CH, SM-MH	99.9 (89.7 - 111.2)	24.1 (17.8 – 37.1)	101 (91 - 113)	6 (0 - 29)	15 (3 - 43)	79 (29 - 97)	42 (16 - 53)	62 (43- 70)	35 (15- 48)
4	Downstream Shell	SC, GC	124.3 (100.6 - 143.3)	11.9 (6.2 - 19.9)	89 (72 - 102)	32 (13 - 56)	38 (16 - 60)	30 (15 - 63)	17 (11- 26)	33 (22 - 46)	15 (6 - 29)

Notes:

1. Data in this table are averages with minimum and maximum values in parentheses. No data is available for Drain Material (Zone 3).
2. See Figure 5-1.
3. In-situ conditions, gradation and Atterberg limits are summarized based on laboratory testing performed by Wahler (1981), Geomatrix (1996), Harza (1997), RLVA (1999), Frame and Volpe (2001), and Terra / GeoPentech (2011c).
4. Per D1557 modified, 20,000 ft-lbs.

TABLE 5-3
SUMMARY OF ENGINEERING PROPERTIES

Zone	Moist Unit Weight (pcf) γ_t	Effective Friction Angle [1] ϕ'	Triaxial Undrained Strength Parameter [2] S_u/σ_{vc}'	Stress-Strain Strength Relationship [3] E_{u50} / S_u	Dynamic Properties [4]		
					V_s		G/G_{max} and Damping Ratio
					K (ft/sec)	n	
1	138	37.5 °	$e^{[-0.22 \bullet \ln(\sigma_{vc}')+0.12]}$	140	1305	0.25	Figure 5-20
2U	132	35.5 °	$e^{[-0.20 \bullet \ln(\sigma_{vc}')-0.01]}$	180	1190	0.25	Figure 5-20
2L	124	25.5 °	$e^{[-0.27 \bullet \ln(\sigma_{vc}')-0.15]}$	170	680	0.25	Figure 5-20
4	140	35 °	$e^{[-0.21 \bullet \ln(\sigma_{vc}')-0.12]}$	180	1550	0.25	Figure 5-20

Notes:

[1] Effective Friction Angle, ϕ' (with no cohesion)

[2] σ_{vc}' in ksf; minimum S_u for all soils = 2.0 ksf; also see Figures 5-14 to 5-17

[3] Stress-Strain Strength Relationship

E_{u50} = Undrained Secant Modulus at 50% S_u

[4] Dynamic Properties, V_s (shear wave velocity), G/G_{max} (shear modulus) and Damping Ratio

$V_s = K \bullet (\sigma_{vc}'/p_a)^n$ where K is in ft/sec

TABLE 5-4
COMPARISON OF LABORATORY AND CPT UNDRAINED STRENGTHS

Boring No.	Sample No.	Dam Zone	Depth ft	TX $S_{u(max)}$ ksf	CPT (50%) S_u ksf	CPT (16%) S_u ksf	CPT S_u / TX $S_{u(max)}$	
							50%	16%
LD-B-101	PB-4	Lower Core	88	4.96	5.76	5.05	1.15	1.02
LD-B-101	PB-8	Lower Core	131	5.90	7.48	6.42	1.27	1.09
LD-B-101	PB-12	Lower Core	171	6.05	4.73	4.25	0.78	0.70
LD-B-103	PB-5	Upper Core	52	4.50	7.95	5.17	1.77	1.15
LD-B-103	PB-6	Upper Core	59	5.41	6.71	6.00	1.24	1.11
LD-B-102	PB-1	Downstream Shell	36	6.84	31.90	18.50	4.66	2.70
LD-B-102	PB-6	Downstream Shell	100	7.57	15.00	10.60	1.98	1.40

TABLE 5-5
RESULTS OF PERMEABILITY TESTS

Material	Measured Permeability, cm/sec			Estimated Permeability, cm/sec (RLVA, 1999a)	
	Triaxial Test	1-Dimensional Consolidation	Field CPT	Horizontal	Vertical
Upstream Shell	1.7×10^{-8} 3.3×10^{-8} 2.9×10^{-9}	2.0×10^{-9}	3.7×10^{-8} 7.3×10^{-7} 7.2×10^{-7} 7.9×10^{-8} 7.3×10^{-9}	5×10^{-8}	5×10^{-9}
Upper Core	1.7×10^{-8}	2.5×10^{-8}	2.4×10^{-8} 1.0×10^{-8} 1.1×10^{-8} 1.0×10^{-8}	1×10^{-8}	1.0×10^{-9}
Lower Core	6.6×10^{-9} 4.5×10^{-9} 5.3×10^{-9} 8.1×10^{-9} 4.4×10^{-9} 1.1×10^{-9}	5.0×10^{-8} 2.5×10^{-9}	1.2×10^{-8} 5.7×10^{-9} 2.4×10^{-8}	1×10^{-8}	5×10^{-9}
Downstream Shell	3.1×10^{-6}			1×10^{-7}	1×10^{-7}
Foundation	3.3×10^{-9}				

Data from RLVA (1999a)

TABLE 6-1
SUMMARY OF SEIMSIC SOURCES

Fault	Fault Parameters							Distance (km)			Average PGA (g)		Arias Intensity (m/sec)	
	Type	M_{max}	HW	Dip	Rup. Length	DWR	DTR	R_{map}	R_{JB}	R_{rup}	Median	84th Perc	Median	84th Perc
Berrocal	RV	6.8	Yes	60	28	13.9	12	2.3	0	2	0.58	1.00	1.88	4.72
Stanford-Monte Vista	RV	6.9	Yes	55	38	10.5	8.6	5.5	0.0	4.5	0.61	1.05	2.11	5.29
San Andreas	SS	7.9	-	-	470	-	-	2.1	2.1	2.1	0.43	0.73	2.15	5.66

Notes:

Fault Type: RV=Reverse; SS=Strike Slip

HW: Yes=On Hanging Wall; No=Not on Hanging Wall

Rup. Length = Rupture Length, km

DWR=Downdip Width of Rupture, km

DTR = Depth To Bottom of Rupture, km

Rmap = Map Distance

RJB = Boore-Joyner Distance

Rrup = Fault Rupture Distance

Arias Intensity computed using Watson-Lamprey and Abrahamson relationship (2006).

TABLE 6-2A
SHEAR WAVE VELOCITY FROM LD-B-101 DATA SET

DEPTH REPORTED (FT)	Shear Wave Velocity (ft/sec)	Depth Reported (m)	Shear Wave Velocity, v_{si} (m/sec)	Depth Below Top of Rock (m)	Top of Depth Interval (m)	Bottom of Depth Interval (m)	Interval Thickness, d_i (m)	d_i / v_{si}
193.6	2130	59.0	649	0.5	58.8	59.3	0.5	7.7E-04
195.2	2038	59.5	621	1.0	59.3	59.8	0.5	8.1E-04
196.9	2386	60.0	727	1.5	59.8	60.3	0.5	6.9E-04
198.5	3348	60.5	1020	2.0	60.3	60.8	0.5	4.9E-04
200.1	4464	61.0	1361	2.5	60.8	61.3	0.5	3.7E-04
201.8	5657	61.5	1724	3.0	61.3	61.8	0.5	2.9E-04
203.4	6628	62.0	2020	3.5	61.8	62.3	0.5	2.5E-04
205.1	7812	62.5	2381	4.0	62.3	62.8	0.5	2.1E-04
206.7	6190	63.0	1887	4.5	62.8	63.3	0.5	2.6E-04
208.3	5047	63.5	1538	5.0	63.3	63.8	0.5	3.3E-04
210.0	4494	64.0	1370	5.5	63.8	64.3	0.5	3.7E-04
211.6	5249	64.5	1600	6.0	64.3	64.8	0.5	3.1E-04
213.3	4261	65.0	1299	6.5	64.8	65.3	0.5	3.9E-04
214.9	3400	65.5	1036	7.0	65.3	65.8	0.5	4.8E-04
216.5	3281	66.0	1000	7.5	65.8	66.3	0.5	5.0E-04
218.2	4971	66.5	1515	8.0	66.3	66.8	0.5	3.3E-04
219.8	4790	67.0	1460	8.5	66.8	67.3	0.5	3.4E-04
221.5	3860	67.5	1176	9.0	67.3	67.8	0.5	4.2E-04
223.1	4001	68.0	1220	9.5	67.8	68.3	0.5	4.1E-04
224.7	4076	68.5	1242	10.0	68.3	68.8	0.5	4.0E-04
226.4	3793	69.0	1156	10.5	68.8	69.3	0.5	4.3E-04
228.0	5657	69.5	1724	11.0	69.3	69.8	0.5	2.9E-04
229.7	6249	70.0	1905	11.5	69.8	70.3	0.5	2.6E-04
231.3	4525	70.5	1379	12.0	70.3	70.8	0.5	3.6E-04
232.9	2646	71.0	806	12.5	70.8	71.3	0.5	6.2E-04
234.6	2929	71.5	893	13.0	71.3	71.8	0.5	5.6E-04
236.2	2780	72.0	847	13.5	71.8	72.3	0.5	5.9E-04
237.9	4790	72.5	1460	14.0	72.3	72.8	0.5	3.4E-04
239.5	4127	73.0	1258	14.5	72.8	73.3	0.5	4.0E-04
241.1	3472	73.5	1058	15.0	73.3	73.8	0.5	4.7E-04
242.8	3170	74.0	966	15.5	73.8	74.3	0.5	5.2E-04
244.4	3365	74.5	1026	16.0	74.3	74.8	0.5	4.9E-04
246.1	3382	75.0	1031	16.5	74.8	75.5	0.7	7.3E-04
						Total	**16.7**	**1.4E-02**

$$V_{S17} = \Sigma\, d_i / (\Sigma\, d_i / v_{si}) = 1160 \text{ m/sec}$$

TABLE 6-2B
SHEAR WAVE VELOCITY FROM LD-B-103 DATA SET

Depth Reported (ft)	Shear Wave Velocity (ft/sec)	Depth Reported (m)	Shear Wave Velocity, v_{si} (m/sec)	Depth Below Top of Rock (m)	Top of Depth Interval (m)	Bottom of Depth Interval (m)	Interval Thickness, d_i (m)	d_i / v_{si}
100.1	2310	30.5	704	0.5	30.3	30.8	0.5	7.1E-04
101.7	2386	31.0	727	1.0	30.8	31.3	0.5	6.9E-04
103.3	5514	31.5	1681	1.5	31.3	31.8	0.5	3.0E-04
105.0	5491	32.0	1674	2.0	31.8	32.3	0.5	3.0E-04
106.6	5965	32.5	1818	2.5	32.3	32.8	0.5	2.7E-04
108.3	6835	33.0	2083	3.0	32.8	33.3	0.5	2.4E-04
109.9	5445	33.5	1660	3.5	33.3	33.8	0.5	3.0E-04
111.5	7674	34.0	2339	4.0	33.8	34.3	0.5	2.1E-04
113.2	7542	34.5	2299	4.5	34.3	34.8	0.5	2.2E-04
114.8	5965	35.0	1818	5.0	34.8	35.3	0.5	2.7E-04
116.5	3400	35.5	1036	5.5	35.3	35.8	0.5	4.8E-04
118.1	3409	36.0	1039	6.0	35.8	36.3	0.5	4.8E-04
119.8	4404	36.5	1342	6.5	36.3	36.8	0.5	3.7E-04
121.4	4464	37.0	1361	7.0	36.8	37.3	0.5	3.7E-04
123.0	4755	37.5	1449	7.5	37.3	37.8	0.5	3.4E-04
124.7	4360	38.0	1329	8.0	37.8	38.3	0.5	3.8E-04
126.3	3656	38.5	1114	8.5	38.3	38.8	0.5	4.5E-04
128.0	3209	39.0	978	9.0	38.8	39.3	0.5	5.1E-04
129.6	3686	39.5	1124	9.5	39.3	39.8	0.5	4.5E-04
131.2	5028	40.0	1533	10.0	39.8	40.3	0.5	3.3E-04
132.9	5167	40.5	1575	10.5	40.3	40.8	0.5	3.2E-04
134.5	5067	41.0	1544	11.0	40.8	41.3	0.5	3.2E-04
136.2	3860	41.5	1176	11.5	41.3	41.8	0.5	4.2E-04
137.8	3374	42.0	1028	12.0	41.8	42.3	0.5	4.9E-04
139.4	3528	42.5	1075	12.5	42.3	42.8	0.5	4.6E-04
141.1	3965	43.0	1208	13.0	42.8	43.3	0.5	4.1E-04
142.7	4261	43.5	1299	13.5	43.3	43.8	0.5	3.9E-04
144.4	3929	44.0	1198	14.0	43.8	44.3	0.5	4.2E-04
146.0	3782	44.5	1153	14.5	44.3	44.8	0.5	4.3E-04
147.6	4755	45.0	1449	15.0	44.8	45.3	0.5	3.4E-04
149.3	4088	45.5	1246	15.5	45.3	45.8	0.5	4.0E-04
150.9	4179	46.0	1274	16.0	45.8	46.3	0.5	3.9E-04
152.6	6076	46.5	1852	16.5	46.3	46.8	0.5	2.7E-04
154.2	6800	47.0	2073	17.0	46.8	47.3	0.5	2.4E-04
155.8	7250	47.5	2210	17.5	47.3	47.8	0.5	2.3E-04
157.5	5731	48.0	1747	18.0	47.8	48.3	0.5	2.9E-04
159.1	6371	48.5	1942	18.5	48.3	48.8	0.5	2.6E-04
160.8	5514	49.0	1681	19.0	48.8	49.3	0.5	3.0E-04
162.4	5491	49.5	1674	19.5	49.3	49.8	0.5	3.0E-04
164.0	4289	50.0	1307	20.0	49.8	50.3	0.5	3.8E-04
165.7	4843	50.5	1476	20.5	50.3	50.8	0.5	3.4E-04
167.3	4179	51.0	1274	21.0	50.8	51.3	0.5	3.9E-04
169.0	4704	51.5	1434	21.5	51.3	51.8	0.5	3.5E-04
170.6	4807	52.0	1465	22.0	51.8	52.3	0.5	3.4E-04
172.2	4605	52.5	1404	22.5	52.3	52.8	0.5	3.6E-04
173.9	4621	53.0	1408	23.0	52.8	53.3	0.5	3.5E-04
175.5	4220	53.5	1286	23.5	53.3	53.8	0.5	3.9E-04
177.2	4140	54.0	1262	24.0	53.8	54.3	0.5	4.0E-04
178.8	3686	54.5	1124	24.5	54.3	54.8	0.5	4.4E-04
180.4	3760	55.0	1146	25.0	54.8	55.3	0.5	4.4E-04
182.1	5249	55.5	1600	25.5	55.3	55.8	0.5	3.1E-04
183.7	5249	56.0	1600	26.0	55.8	56.3	0.5	3.1E-04
185.4	5833	56.5	1778	26.5	56.3	56.8	0.5	2.8E-04
187.0	6628	57.0	2020	27.0	56.8	57.3	0.5	2.5E-04
188.6	5208	57.5	1587	27.5	57.3	57.8	0.5	3.2E-04
190.3	4738	58.0	1444	28.0	57.8	58.3	0.5	3.5E-04
191.9	5313	58.5	1619	28.5	58.3	58.8	0.5	3.1E-04
193.6	5756	59.0	1754	29.0	58.8	59.3	0.5	2.9E-04
195.2	5632	59.5	1717	29.5	59.3	60.0	0.7	4.4E-04
						Total	**29.7**	**2.1E-02**

$$V_{S30} = \Sigma\, d_i / (\Sigma\, d_i / v_{si}) = 1390 \text{ m/sec}$$

TABLE 6-2C
SHEAR WAVE VELOCITY FROM EPRI SPILLWAY DATA SET

Depth Reported (ft)	Shear Wave Velocity (ft/sec)	Depth Reported (m)	Shear Wave Velocity, v_{si} (m/sec)	Depth Below Top of Rock (m)	Top of Depth Interval (m)	Bottom of Depth Interval (m)	Interval Thickness, d_i (m)	d_i / v_{si}
9.8	2224	3.0	678	3.0	2.5	3.5	1.0	1.5E-03
13.1	4076	4.0	1242	4.0	3.5	4.5	1.0	8.1E-04
16.4	3081	5.0	939	5.0	4.5	5.5	1.0	1.1E-03
19.7	3953	6.0	1205	6.0	5.5	6.5	1.0	8.3E-04
23.0	3645	7.0	1111	7.0	6.5	7.5	1.0	9.0E-04
26.2	2942	8.0	897	8.0	7.5	8.5	1.0	1.1E-03
29.5	4101	9.0	1250	9.0	8.5	9.5	1.0	8.0E-04
32.8	3977	10.0	1212	10.0	9.5	10.5	1.0	8.3E-04
36.1	3953	11.0	1205	11.0	10.5	11.5	1.0	8.3E-04
39.4	3528	12.0	1075	12.0	11.5	12.5	1.0	9.3E-04
42.7	4317	13.0	1316	13.0	12.5	13.5	1.0	7.6E-04
45.9	3435	14.0	1047	14.0	13.5	14.5	1.0	9.6E-04
49.2	4897	15.0	1493	15.0	14.5	15.5	1.0	6.7E-04
52.5	3586	16.0	1093	16.0	15.5	16.5	1.0	9.2E-04
55.8	4374	17.0	1333	17.0	16.5	17.5	1.0	7.5E-04
59.1	4825	18.0	1471	18.0	17.5	18.5	1.0	6.8E-04
62.3	3666	19.0	1117	19.0	18.5	19.5	1.0	8.9E-04
65.6	3860	20.0	1176	20.0	19.5	20.5	1.0	8.5E-04
68.9	4755	21.0	1449	21.0	20.5	21.5	1.0	6.9E-04
72.2	5208	22.0	1587	22.0	21.5	22.5	1.0	6.3E-04
75.5	4317	23.0	1316	23.0	22.5	23.5	1.0	7.6E-04
78.7	4825	24.0	1471	24.0	23.5	24.5	1.0	6.8E-04
82.0	5514	25.0	1681	25.0	24.5	25.3	0.8	4.5E-04
83.7	4687	25.5	1429	25.5	25.3	26.0	0.8	5.2E-04
						Total	**23.5**	**2.0E-02**

$$V_{S24} = \Sigma\, d_i / (\Sigma\, d_i / v_{si}) = 1190 \text{ m/sec}$$

TABLE 6-3
SUMMARY OF V_{S30} DATA

Location	Σd_i	$\Sigma (d_i / v_{si})$	$\Sigma (d_i) / \Sigma (d_i / v_{si})$
LD-B-101	16.7	1.4E-02	1,160 m/sec
LD-B-103	29.7	2.1E-02	1,390 m/sec
EPRI Spillway	23.5	2.0E-02	1,190 m/sec
Foundation Total	**70.0**	**5.6E-02**	**1,260 m/sec**

V_{S30} = 1,260 m/sec

TABLE 6-4A
RECOMMENDED FAULT PARALLEL SPECTRAL ORDINATES
FOR STANFORD-MONTE VISTA EVENT

Spectral Damping=5%

No.	Period (s)	Frequency (Hz)	Sa (g)	Sv (cm/sec)	Sv (in/sec)	Sd (cm)	Sd (in)
1	0.01	100.00	1.052	1.643	0.647	0.003	0.001
2	0.02	50.00	1.082	3.382	1.331	0.011	0.004
3	0.03	33.33	1.213	5.682	2.237	0.027	0.011
4	0.05	20.00	1.570	12.263	4.828	0.098	0.038
5	0.075	13.33	2.045	23.955	9.431	0.286	0.113
6	0.10	10.00	2.383	37.218	14.653	0.592	0.233
7	0.15	6.67	2.662	62.376	24.558	1.489	0.586
8	0.20	5.00	2.566	80.162	31.560	2.552	1.005
9	0.30	3.33	1.997	93.569	36.838	4.468	1.759
10	0.40	2.50	1.633	102.023	40.166	6.495	2.557
11	0.50	2.00	1.316	102.747	40.452	8.176	3.219
12	0.75	1.33	0.876	102.629	40.405	12.250	4.823
13	1.00	1.00	0.659	102.933	40.525	16.382	6.450
14	1.50	0.67	0.395	92.446	36.396	22.070	8.689
15	2.00	0.50	0.254	79.480	31.291	25.299	9.960
16	3.00	0.33	0.125	58.632	23.083	27.995	11.022
17	4.00	0.25	0.077	48.014	18.903	30.567	12.034
18	5.00	0.20	0.057	44.277	17.432	35.235	13.872

Zero-Period Acceleration (PGA) = 1.05g

Notes:

Sa = Pseudo-Absolute Spectral Acceleration.

Sv = Pseudo-Relative Spectral Velocity.

Sd = Relative Spectral Displacement.

Significant figures in above table are provided for computation purposes only and do not necessarily reflect accuracies to those significant figures.

TABLE 6-4B
RECOMMENDED FAULT NORMAL SPECTRAL ORDINATES
FOR STANFORD-MONTE VISTA EVENT

Spectral Damping=5%

No.	Period (s)	Frequency (Hz)	Sa (g)	Sv (cm/sec)	Sv (in/sec)	Sd (cm)	Sd (in)
1	0.01	100.00	1.052	1.643	0.647	0.003	0.001
2	0.02	50.00	1.082	3.382	1.331	0.011	0.004
3	0.03	33.33	1.213	5.682	2.237	0.027	0.011
4	0.05	20.00	1.570	12.263	4.828	0.098	0.038
5	0.075	13.33	2.045	23.955	9.431	0.286	0.113
6	0.10	10.00	2.383	37.218	14.653	0.592	0.233
7	0.15	6.67	2.662	62.376	24.558	1.489	0.586
8	0.20	5.00	2.566	80.162	31.560	2.552	1.005
9	0.30	3.33	1.997	93.569	36.838	4.468	1.759
10	0.40	2.50	1.633	102.023	40.166	6.495	2.557
11	0.50	2.00	1.316	102.747	40.452	8.176	3.219
12	0.75	1.33	0.959	112.368	44.239	13.413	5.281
13	1.00	1.00	0.796	124.281	48.930	19.780	7.787
14	1.50	0.67	0.575	134.776	53.062	32.176	12.668
15	2.00	0.50	0.428	133.676	52.628	42.550	16.752
16	3.00	0.33	0.269	126.129	49.657	60.222	23.709
17	4.00	0.25	0.198	123.491	48.618	78.617	30.951
18	5.00	0.20	0.159	124.252	48.918	98.876	38.928

Zero-Period Acceleration (PGA) = 1.05g

Notes:

Sa = Pseudo-Absolute Spectral Acceleration.

Sv = Pseudo-Relative Spectral Velocity.

Sd = Relative Spectral Displacement.

Significant figures in above table are provided for computation purposes only and do not necessarily reflect accuracies to those significant figures.

TABLE 6-5A
RECOMMENDED FAULT PARALLEL SPECTRAL ORDINATES
FOR SAN ANDREAS EVENT

Spectral Damping=5%

No.	Period (s)	Frequency (Hz)	Sa (g)	Sv (cm/sec)	Sv (in/sec)	Sd (cm)	Sd (in)
1	0.01	100.00	0.733	1.145	0.451	0.002	0.001
2	0.02	50.00	0.752	2.350	0.925	0.007	0.003
3	0.03	33.33	0.830	3.889	1.531	0.019	0.007
4	0.05	20.00	1.046	8.169	3.216	0.065	0.026
5	0.075	13.33	1.349	15.798	6.220	0.189	0.074
6	0.10	10.00	1.557	24.326	9.577	0.387	0.152
7	0.15	6.67	1.760	41.233	16.233	0.984	0.388
8	0.20	5.00	1.729	54.004	21.261	1.719	0.677
9	0.30	3.33	1.447	67.803	26.694	3.237	1.275
10	0.40	2.50	1.227	76.649	30.177	4.880	1.921
11	0.50	2.00	1.039	81.136	31.943	6.457	2.542
12	0.75	1.33	0.780	91.357	35.967	10.905	4.293
13	1.00	1.00	0.633	98.936	38.951	15.746	6.199
14	1.50	0.67	0.454	106.336	41.864	25.386	9.994
15	2.00	0.50	0.340	106.230	41.823	33.814	13.313
16	3.00	0.33	0.230	107.662	42.387	51.405	20.238
17	4.00	0.25	0.167	104.263	41.049	66.376	26.132
18	5.00	0.20	0.135	105.187	41.412	83.705	32.955

Zero-Period Acceleration (PGA) = 0.73g

Notes:

Sa = Pseudo-Absolute Spectral Acceleration.

Sv = Pseudo-Relative Spectral Velocity.

Sd = Relative Spectral Displacement.

Significant figures in above table are provided for computation purposes only and do not necessarily reflect accuracies to those significant figures.

TABLE 6-5B
RECOMMENDED FAULT NORMAL SPECTRAL ORDINATES
FOR SAN ANDREAS EVENT

Spectral Damping=5%

No.	Period (s)	Frequency (Hz)	Sa (g)	Sv (cm/sec)	Sv (in/sec)	Sd (cm)	Sd (in)
1	0.01	100.00	0.733	1.145	0.451	0.002	0.001
2	0.02	50.00	0.752	2.350	0.925	0.007	0.003
3	0.03	33.33	0.830	3.889	1.531	0.019	0.007
4	0.05	20.00	1.046	8.169	3.216	0.065	0.026
5	0.075	13.33	1.349	15.798	6.220	0.189	0.074
6	0.10	10.00	1.557	24.326	9.577	0.387	0.152
7	0.15	6.67	1.760	41.233	16.233	0.984	0.388
8	0.20	5.00	1.729	54.004	21.261	1.719	0.677
9	0.30	3.33	1.447	67.803	26.694	3.237	1.275
10	0.40	2.50	1.227	76.649	30.177	4.880	1.921
11	0.50	2.00	1.039	81.136	31.943	6.457	2.542
12	0.75	1.33	0.864	101.210	39.847	12.081	4.756
13	1.00	1.00	0.780	121.762	47.938	19.379	7.630
14	1.50	0.67	0.663	155.343	61.159	37.085	14.601
15	2.00	0.50	0.564	176.161	69.355	56.074	22.076
16	3.00	0.33	0.485	227.312	89.493	108.533	42.730
17	4.00	0.25	0.419	261.846	103.089	166.697	65.629
18	5.00	0.20	0.362	282.594	111.257	224.881	88.536

Zero-Period Acceleration (PGA) = 0.73g

Notes:

Sa = Pseudo-Absolute Spectral Acceleration.

Sv = Pseudo-Relative Spectral Velocity.

Sd = Relative Spectral Displacement.

Significant figures in above table are provided for computation purposes only and do not necessarily reflect accuracies to those significant figures.

TABLE 6-6A
CHARACTERISTICS OF SELECTED EARTHQUAKE RECORDS
FOR STANFORD-MONTE VISTA EVENT

No.	Earthquake Event	Recording Station	Style of Faulting (1)	Magnitude (Mw)	Closest Distance (km)	NEHRP Site Class/Vs_{30}	Highest Usable Period (sec)	Event Date
1	Kobe	Nishi-Akashi	SS	6.9	7.1	C/609	8	1/16/1995
2	Loma Prieta	LGPC	RV/OBL	6.9	3.9	C/478	8	10/18/1989
3	Northridge	Sylmar-Olive View Med. FF	RV	6.7	5.3	C/440	8.3	1/17/1994

TABLE 6-6B
CHARACTERISTICS OF SELECTED EARTHQUAKE RECORDS
FOR SAN ANDREAS EVENT

No.	Earthquake Event	Recording Station	Style of Faulting (1)	Magnitude (Mw)	Closest Distance (km)	NEHRP Site Class/Vs_{30}	Highest Usable Period (sec)	Event Date
1	Manjil	Abbar	SS	7.4	12.6	C/724	7.7	11/03/1990
2	Chi-Chi	TCU065	RV/OBL	7.6	0.7	D/305	13.3	9/20/1999
3	Landers	Lucerne	SS	7.3	2.2	C/684	10.0	6/28/1992

Notes:

SS = Strike-Slip

IBL = Oblique

RV = Reverse of Thrust

FIGURES

Note: Base map printed from USGS 1:24,000 scale topographic maps by TOPO! ® © 2003 National Geographic.

TERRA / GeoPentech a Joint Venture	REGIONAL SITE LOCATION MAP LENIHAN DAM SEISMIC STABILITY EVALUATIONS (SSE2)	Figure 2-1

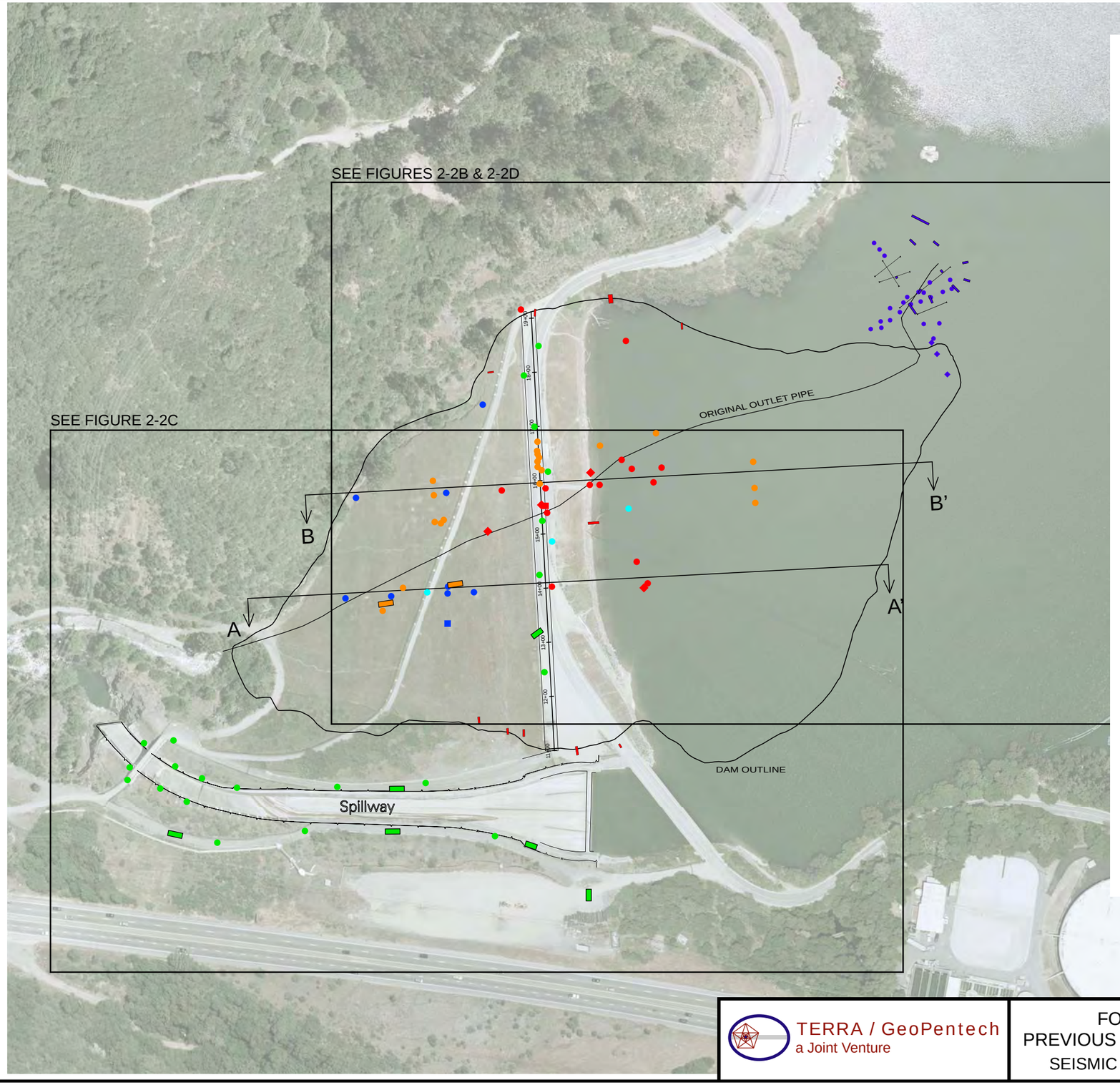

LEGEND

BORINGS / PIEZOMETERS / INCLINOMETERS AND CPTs

- WAHLER 1982 BORING
- ESA 1987 BORING
- ESA 1987 CPT
- GEOMATRIX 1996 BORING
- HARZA 1997 BORINGS
- VOLPE 1999 PIEZOMETER
- VOLPE 1999 INCLINOMETER
- VOLPE 1999 CPT
- DISTRICT 2001 PIEZOMETER
- DISTRICT 2001 INCLINOMETER

OTHER EXPLORATIONS

- WAHLER 1982 TEST PIT
- ESA 1987 TEST PIT
- ESA 1987 SEISMIC REFRACTION LINE
- VOLPE 1990 TRENCH
- GEOMATRIX 1996 TEST PIT

APPROXIMATE SCALE, FEET

200 0 200 400

NOTES:
1) SEE FIGURES 2-2B AND 2-2C FOR ADDITIONAL DETAILS.
2) INVESTIGATIONS FOR NEW OUTLET TUNNEL IN RIGHT ABUTMENT NOT SHOWN.
3) AERIAL PHOTOGRAPH DATED APRIL 2006 FROM USGS HIGH RESOLUTION STATE ORTHOIMAGERY

TERRA / GeoPentech
a Joint Venture

FOOTPRINT AND PLAN OF PREVIOUS EXPLORATIONS - LENIHAN DAM
SEISMIC STABILITY EVALUATIONS (SSE2)

Figure 2-2A

Rev. 0 11/18/2011 SSE2-R-3LN

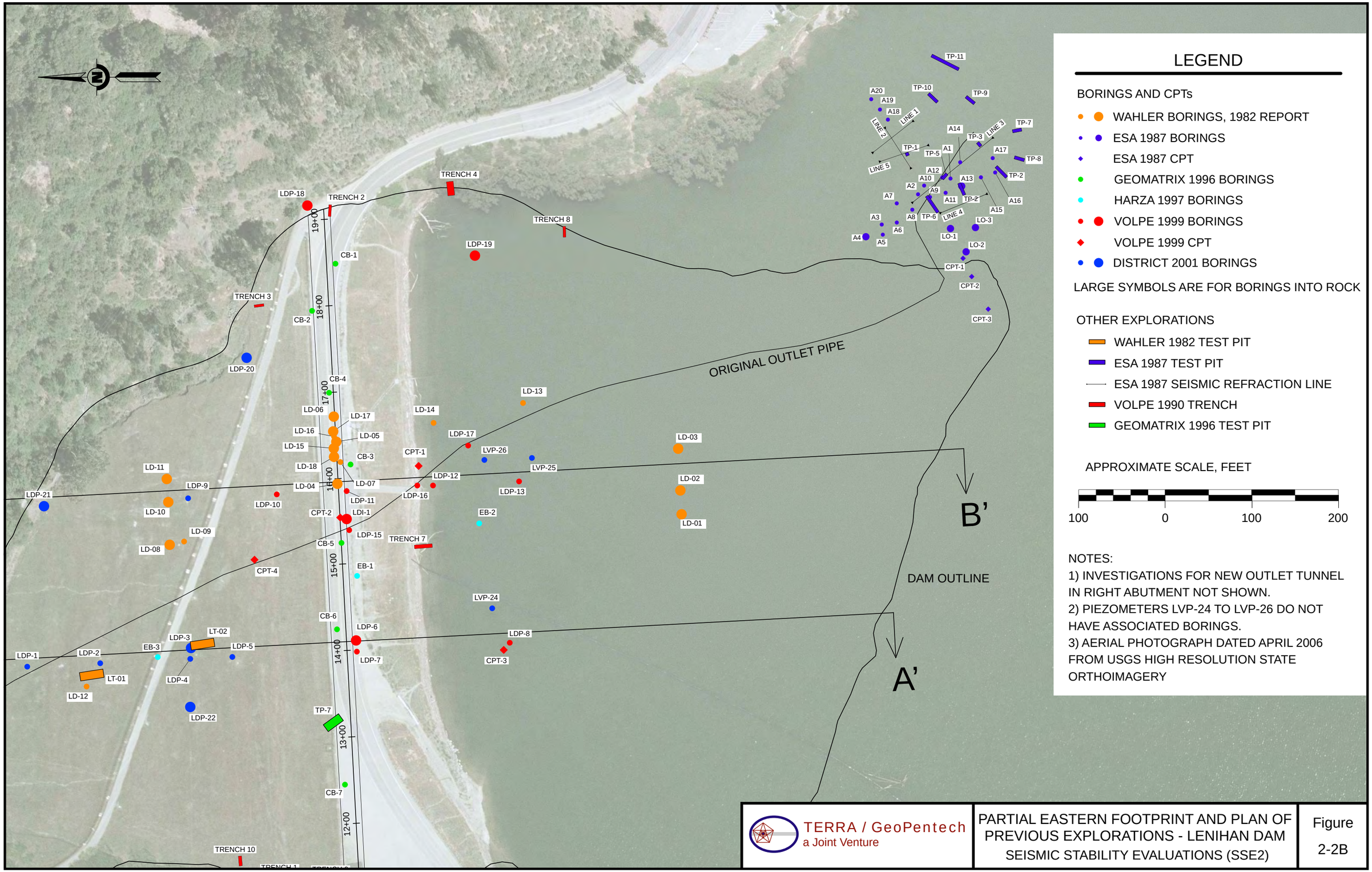

LEGEND

BORINGS AND CPTs

- WAHLER BORINGS, 1982 REPORT
- ESA 1987 BORINGS
- ESA 1987 CPT
- GEOMATRIX 1996 BORINGS
- HARZA 1997 BORINGS
- VOLPE 1999 BORINGS
- VOLPE 1999 CPT
- DISTRICT 2001 BORINGS

LARGE SYMBOLS ARE FOR BORINGS INTO ROCK

OTHER EXPLORATIONS

- WAHLER 1982 TEST PIT
- ESA 1987 TEST PIT
- ESA 1987 SEISMIC REFRACTION LINE
- VOLPE 1990 TRENCH
- GEOMATRIX 1996 TEST PIT

APPROXIMATE SCALE, FEET

100 0 100 200

NOTES:

1) INVESTIGATIONS FOR NEW OUTLET TUNNEL IN RIGHT ABUTMENT NOT SHOWN.
2) PIEZOMETERS LVP-24 TO LVP-26 DO NOT HAVE ASSOCIATED BORINGS.
3) AERIAL PHOTOGRAPH DATED APRIL 2006 FROM USGS HIGH RESOLUTION STATE ORTHOIMAGERY

TERRA / GeoPentech
a Joint Venture

PARTIAL EASTERN FOOTPRINT AND PLAN OF PREVIOUS EXPLORATIONS - LENIHAN DAM
SEISMIC STABILITY EVALUATIONS (SSE2)

Figure 2-2B

Rev. 0 11/18/2011 SSE2-R-3LN

LD-06 LD-17 LD-14 LD-16 LD-05 LD-15 LD-18 CB-3 LD-11 LDP-9 LD-04 LD-07 LDP-21 LD-10 LDP-10 LDP-11 LDI-1 CPT-2 LD-09 LD-08 LDP-15 CB-5 TRENCH 7 CPT-4 EB-1 CB-6 LDP-6 LDP-3 LT-02 LDP-5 EB-3 LDP-1 LDP-2 LDP-7 LT-01 LDP-4 LD-12 LDP-22 TP-7 CB-7 LDP-17 LVP-26 LVP-25 CPT-1 LDP-12 LDP-13 LDP-16 EB-2 LVP-24 LDP-8 CPT-3

16+00 15+00 14+00 13+00 12+00 11+00

B

A

ORIGINAL OUTLET PIPE

DAM OUTLINE

TRENCH 10 TRENCH 1 TRENCH 9 TRENCH 6 TRENCH 5

SB-11 SB-1 SB-14 SB-10 SB-9 SB-8 SB-7 TP-4 SB-6 SB-2 SB-13 SB-12 TP-5 SB-3 SB-4 TP-6 SB-5 TP-3 TP-1

Spillway

LEGEND

BORINGS AND CPTs

- WAHLER BORINGS, 1982 REPORT
- GEOMATRIX 1996 BORINGS
- HARZA 1997 BORINGS
- VOLPE 1999 BORINGS
- VOLPE 1999 CPT
- DISTRICT 2001 BORINGS

LARGE SYMBOLS ARE FOR BORINGS INTO ROCK

OTHER EXPLORATIONS

- WAHLER 1982 TEST PIT
- VOLPE 1990 TRENCH
- GEOMATRIX 1996 TEST PIT

APPROXIMATE SCALE, FEET

100 0 100 200

NOTES:
1) PIEZOMETERS LVP-24 TO LVP-26 DO NOT HAVE ASSOCIATED BORINGS.
2) AERIAL PHOTOGRAPH DATED APRIL 2006 FROM USGS HIGH RESOLUTION STATE ORTHOIMAGERY

Rev. 0 11/18/2011 SSE2-R-3LN

TERRA / GeoPentech
a Joint Venture

PARTIAL WESTERN FOOTPRINT AND PLAN OF PREVIOUS EXPLORATIONS - LENIHAN DAM
SEISMIC STABILITY EVALUATIONS (SSE2)

Figure 2-2C

LAP-1 & LAP-2
LAP-3 & LAP-4
LAP-5 & 6
LAP-7
LVP-1
LVP-2 & LVP-21
LVP-3
LVP-4 & LVP-23
LVP-5
LVP-6
LVP-7
LVP-8
LVP-9 & LVP-22
LVP-10
LVP-11 & LVP-12
LVP-13 & LVP-14
LVP-15
LVP-17
LVP-18
LVP-19
LVP-20
LVP-24
LVP-25
LVP-26
CPT-1
CPT-2
CPT-3
CPT-4
LDI-1
LDI-2
OW-1 & OW-2
OW-3
19+00
18+00
17+00
16+00
15+00
14+00
13+00
12+00
ORIGINAL OUTLET PIPE
DAM OUTLINE
B’
A’

LEGEND

PIEZOMETERS / INCLINOMETERS AND CPTs

- WAHLER BORINGS, 1982 REPORT
- VOLPE 1999 PIEZOMETERS
- VOLPE 1999 INCLINOMETER
- VOLPE 1999 CPT
- DISTRICT 2001 PIEZOMETERS
- DISTRICT 2001 INCLINOMETER

LARGE SYMBOLS ARE FOR BORINGS INTO ROCK

APPROXIMATE SCALE, FEET

100 0 100 200

NOTES:
1) INVESTIGATIONS FOR NEW OUTLET TUNNEL IN RIGHT ABUTMENT NOT SHOWN.
2) AERIAL PHOTOGRAPH DATED APRIL 2006 FROM USGS HIGH RESOLUTION STATE ORTHOIMAGERY

TERRA / GeoPentech
a Joint Venture

PARTIAL EASTERN FOOTPRINT AND PLAN OF EXISTING INSTRUMENTATION - LENIHAN DAM
SEISMIC STABILITY EVALUATIONS (SSE2)

Figure 2-2D

Rev. 0 11/18/2011 SSE2-R-3LN

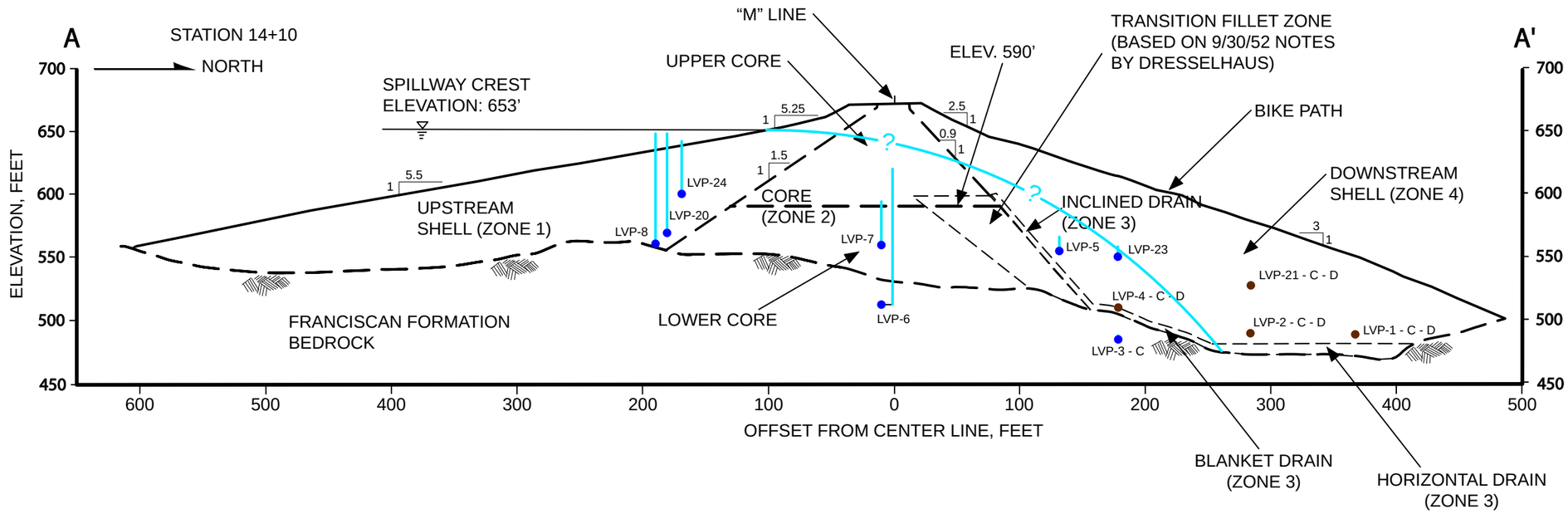

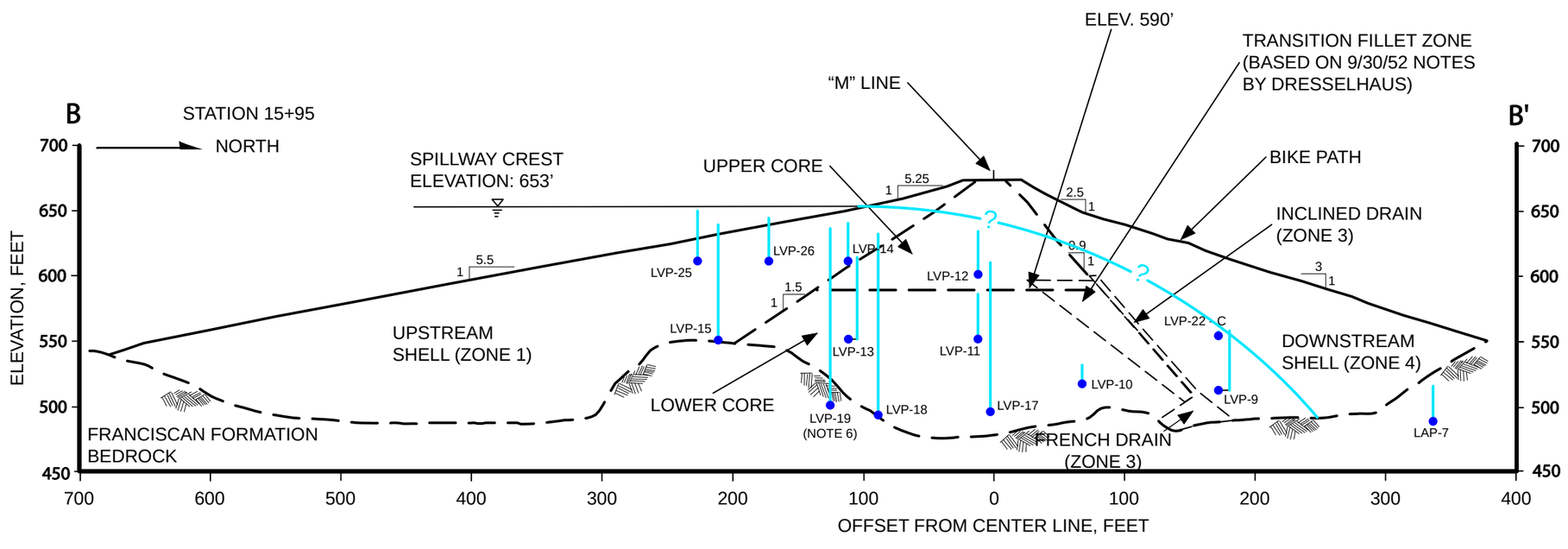

LEGEND

LVP-5 — LOCATION AND NUMBER OF PIEZOMETER TIP

NOTES

1) ELEVATION OF THE TOP OF BLUE BAR REPRESENTS MEASURED TOTAL HEAD AT FULL RESERVOIR LEVEL.

2) HEIGHT OF BLUE BAR REPRESENTS MEASURED PRESSURE HEAD.

3) C INDICATES TOTAL HEAD IS INDEPENDENT OF RESERVOIR LEVEL.

4) D INDICATES THE PIEZOMETER TIP IS DRY. A BROWN TIP IS SHOWN AT THESE LOCATIONS.

5) TOP FLOW LINE SHOWN IS APPROXIMATE, PARTICULARLY IN VICINITY OF CHIMNEY DRAIN, AND IS AT THE SAME LOCATION ON BOTH SECTIONS.

6) LVP-19 IS PROJECTED 30 FT WEST AND IS SCREENED IN EMBANKMENT

Rev. 0 11/18/2011 SSE2-R-3LN

TERRA / GeoPentech
a Joint Venture

CROSS SECTIONS AND MEASURED PIEZOMETRIC LEVELS - LENIHAN DAM
SEISMIC STABILITY EVALUATIONS (SSE2)

Figure 2-3

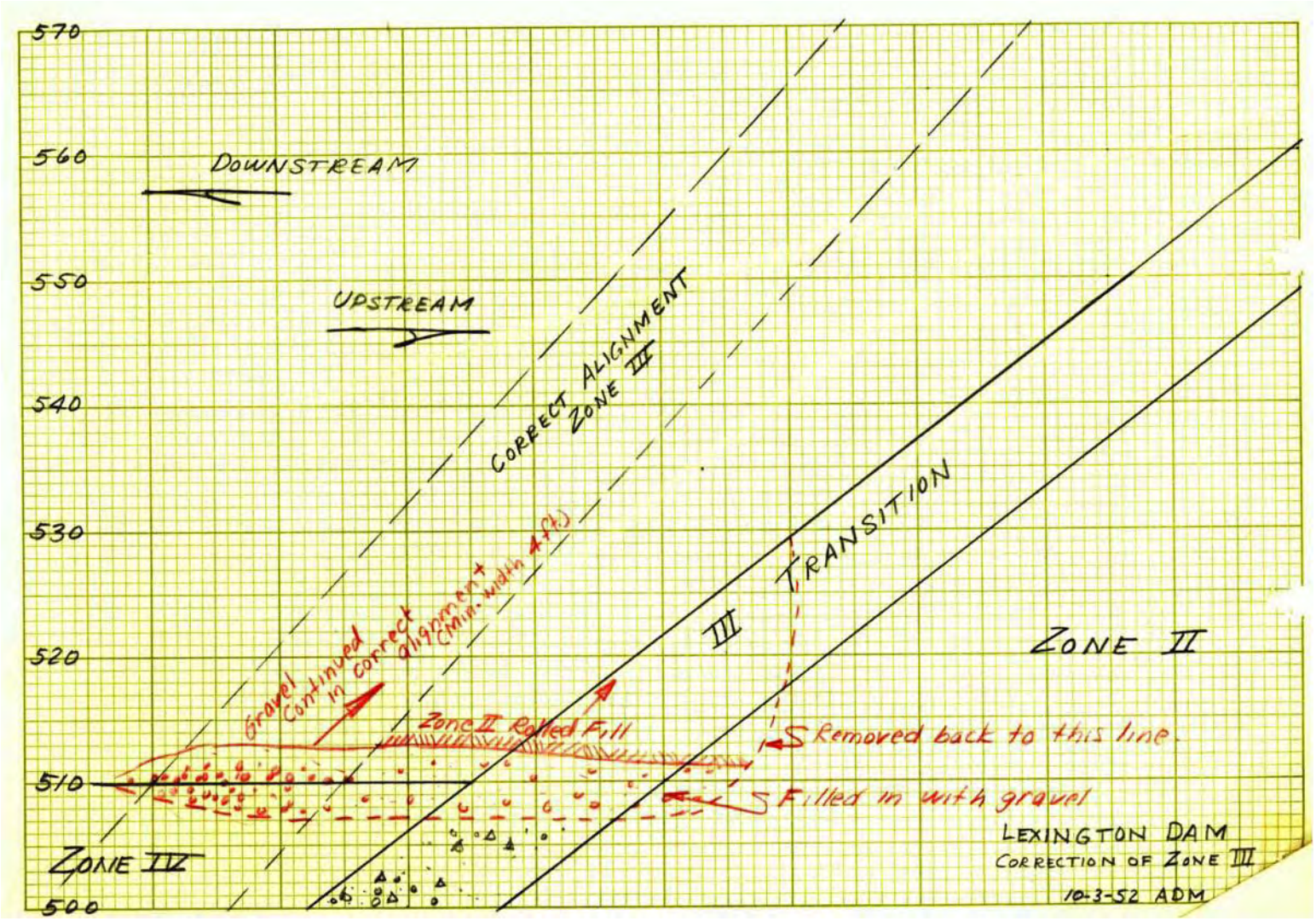

Note: Sketch by A.D. Morrison (DSOD) dated October 3, 1952, excerpted from DSOD Files.

TERRA / GeoPentech a Joint Venture	AS-BUILT SIZE OF INCLINED DRAIN LENIHAN DAM SEISMIC STABILITY EVALUATIONS (SSE2)	Figure 2-4

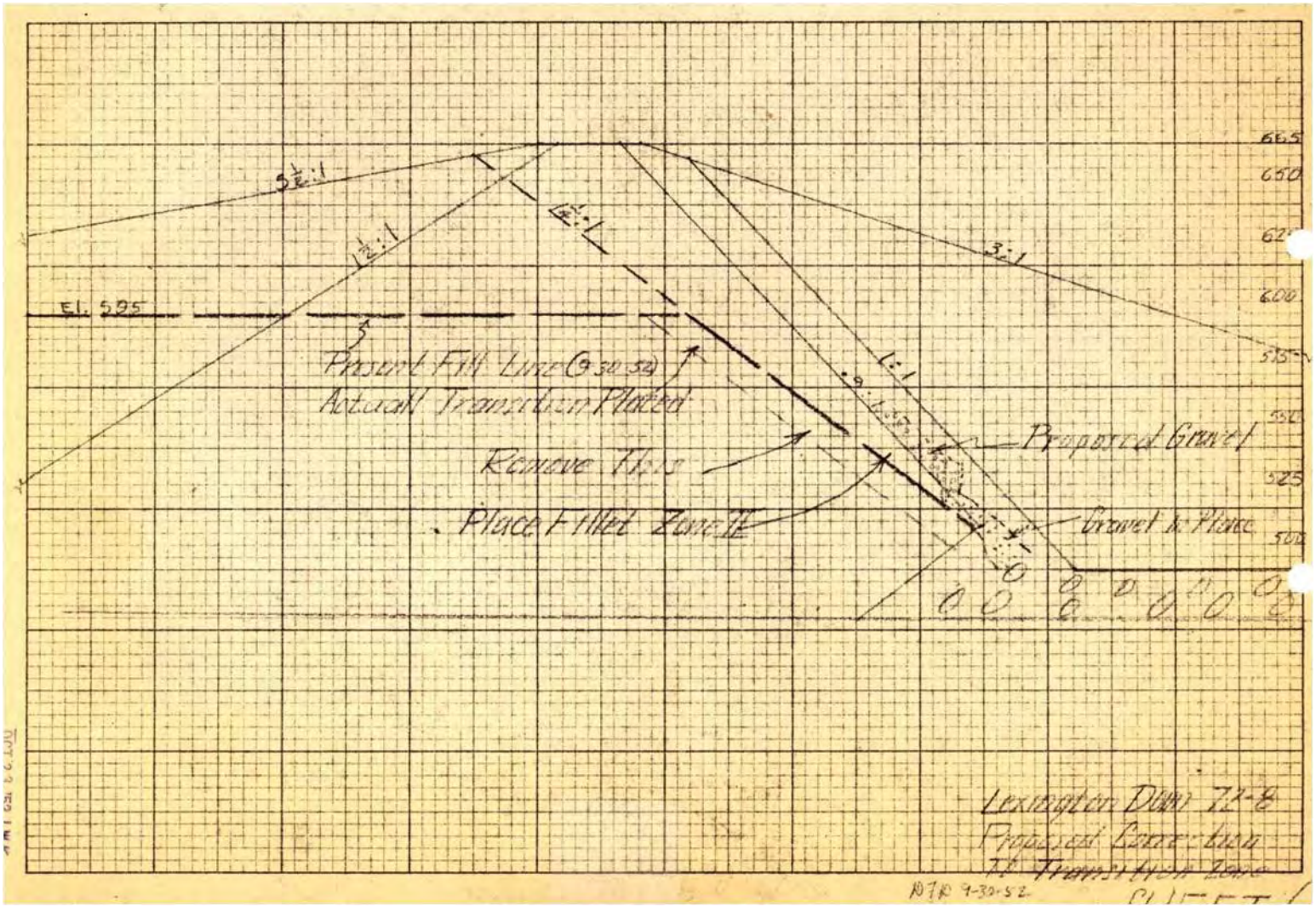

Note: Sketch by DSOD inspector D. Dresselhaus dated September 30, 1952, excerpted from DSOD Files.

TERRA / GeoPentech a Joint Venture	AS-BUILT FILLET OF ZONE 2 MATERIAL LENIHAN DAM SEISMIC STABILITY EVALUATIONS (SSE2)	Figure 2-5

LINE	PIEZOMETER NUMBER	STATION	EMBANKMENT ZONE
	Reservoir		
	LOP-14	3+20	UPSTREAM SHELL
	LOP-13	3+70	
	LOP-12	4+20	4+50
	LOP-10	5+20	
	LOP-06	5+70	
	LOP-21	5+70	
	LOP-17	6+00	
	LOP-09	6+30	
	LOP-16	7+00	
	LOP-19	7+14	CORE
	LOP-08	7+30	
	LOP-04	7+80	
	LOP-15	8+00	
	LOP-18	8+00	
	LOP-07	8+30	
	LOP-03	8+80	9+30
	LOP-02	9+80	
	LOP-01	10+80	DRAIN

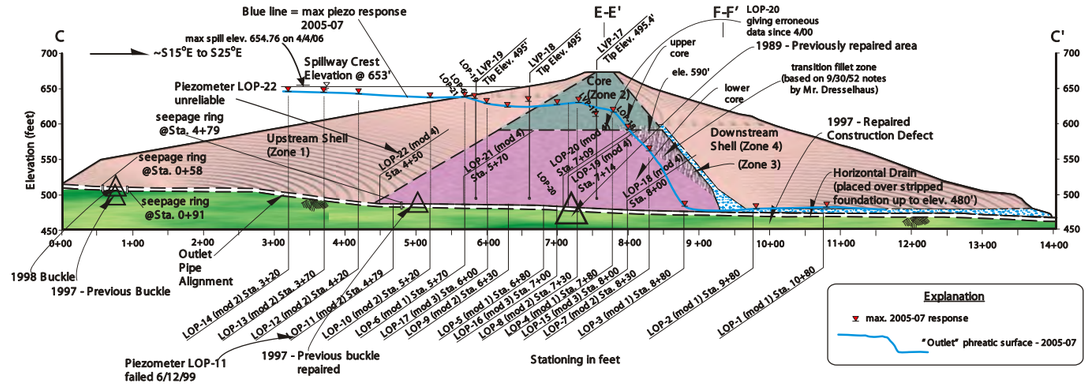

SECTION ALONG OUTLET PIPE

(EXCERPTED FROM SECOND SUMMARY SURVEILLANCE REPORT, SCVWD (2007))

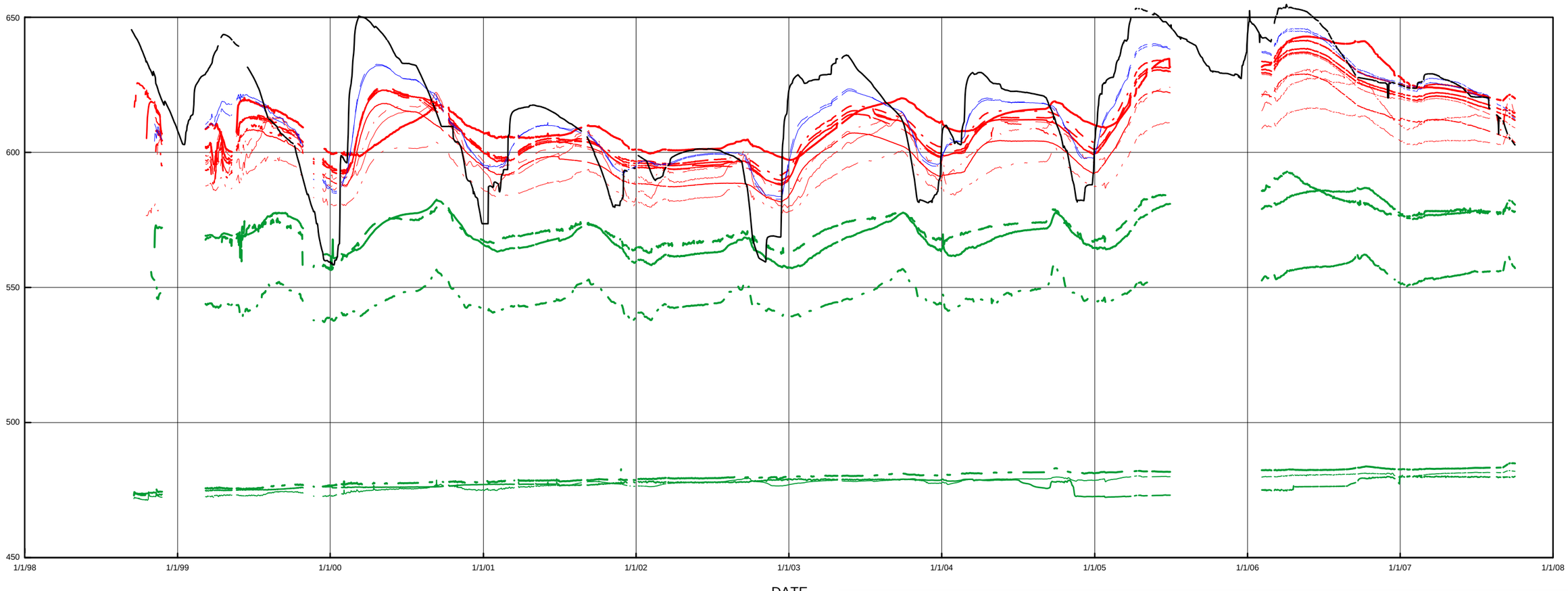

TERRA / GeoPentech
a Joint Venture

REVIEW OF PIEZOMETER DATA ALONG OUTLET PIPE - LENIHAN DAM
SEISMIC STABILITY EVALUATIONS (SSE2)

Figure 2-6

Rev. 0 11/18/2011 SSE2-R-3LN

LEGEND

2011 EXPLORATIONS

LD-B-103
LOCATION AND NUMBER OF BORING

LD-CPT-102
LOCATION AND NUMBER OF CPT PROBE

PREVIOUS EXPLORATIONS

BORINGS / PIEZOMETERS / INCLINOMETERS AND CPTs

- WAHLER 1982 BORING
- ESA 1987 BORING
- ESA 1987 CPT
- GEOMATRIX 1996 BORING
- HARZA 1997 BORINGS
- VOLPE 1999 PIEZOMETER
- VOLPE 1999 INCLINOMETER
- VOLPE 1999 CPT
- DISTRICT 2001 PIEZOMETER
- DISTRICT 2001 INCLINOMETER

NOTE: LARGE SYMBOLS ARE FOR PREVIOUS BORINGS THAT EXTENDED INTO ROCK.

OTHER EXPLORATIONS

- WAHLER 1982 TEST PIT
- ESA 1987 TEST PIT
- ESA 1987 SEISMIC REFRACTION LINE
- VOLPE 1990 TRENCH
- GEOMATRIX 1996 TEST PIT

19+00
18+00
17+00
16+00
15+00
14+00
13+00
12+00
11+00

LD-B-102
LD-CPT-102
LD-B-101
LD-CPT-101
LD-CPT-104
LD-CPT-104B
LD-B-103
LD-CPT-103

N
0' 100' 200'

Rev. 1 12/08/2011 SSE2-R-3LN

TERRA / GeoPentech
a Joint Venture

PLAN LOCATIONS OF FIELD EXPLORATIONS
LENIHAN DAM
SEISMIC STABILITY EVALUATIONS (SSE2)

Figure
2-7

NOTES:
1. MAPPED LOCATIONS OF CRACKS SHOWN IN RED
2. TRENCH NUMBERS SHOWN NEXT TO TRENCHES i.e. (4)

LEXINGTON DAM

CRACKING DUE TO THE LOMA PRIETA EARTHQUAKE OF 10/17/89

Mapped by S. Hoose & T. Gomes

Field work through 11/14/89.

0 50 100 150 200 250

GRAPHIC SCALE (FT)

SYMBOLS USED ON MAP
- Crack well located
- Approximately located crack
- Uncertainty about continuation of crack
- Crest Monument
- Utility Pole
- I Inclinometer Casing
- P Pneumatic Piezometer Terminal
- Utility Terminal w/ Pull Box
- W Water Line, location approximate
- T Buried Telephone Line, location approximate
- N9 NOTES Refer to Text
- MH MAN HOLE
- LD-12 LD-9=OW-1&2, LD-12=OW-3

NOTE: NOT ALL INSTRUMENTATION IS SHOWN

THIS AREA COMPILED FROM HIGH ALTITUDE PHOTOS DATED : 10/06/87.

Trench No.	Maximum Depth of Cracking (ft)	Width of Crack (if recorded) (inches)	Material Cracked (if recorded)
1	7.0	1/2	Contact of Colluvium & Bedrock
2	3.6	-	-
3	4.2	-	-
4	6.3	-	Colluvium & Greenstone
5	4.7	-	Bridge Fill
6	3.8	-	Loose Fill Over Bedrock
7	3.3	-	Embankment
8	5.4	3/4	Colluvium
9	4.0	3/8	Embankment
10	4.2	-	Colluvium

TERRA / GeoPentech
a Joint Venture

EFFECTS OF LOMA PRIETA EARTHQUAKE
LENIHAN DAM
SEISMIC STABILITY EVALUATIONS (SSE2)

Figure 2-8

Rev. 0 11/18/2011 SSE2-R-3LN

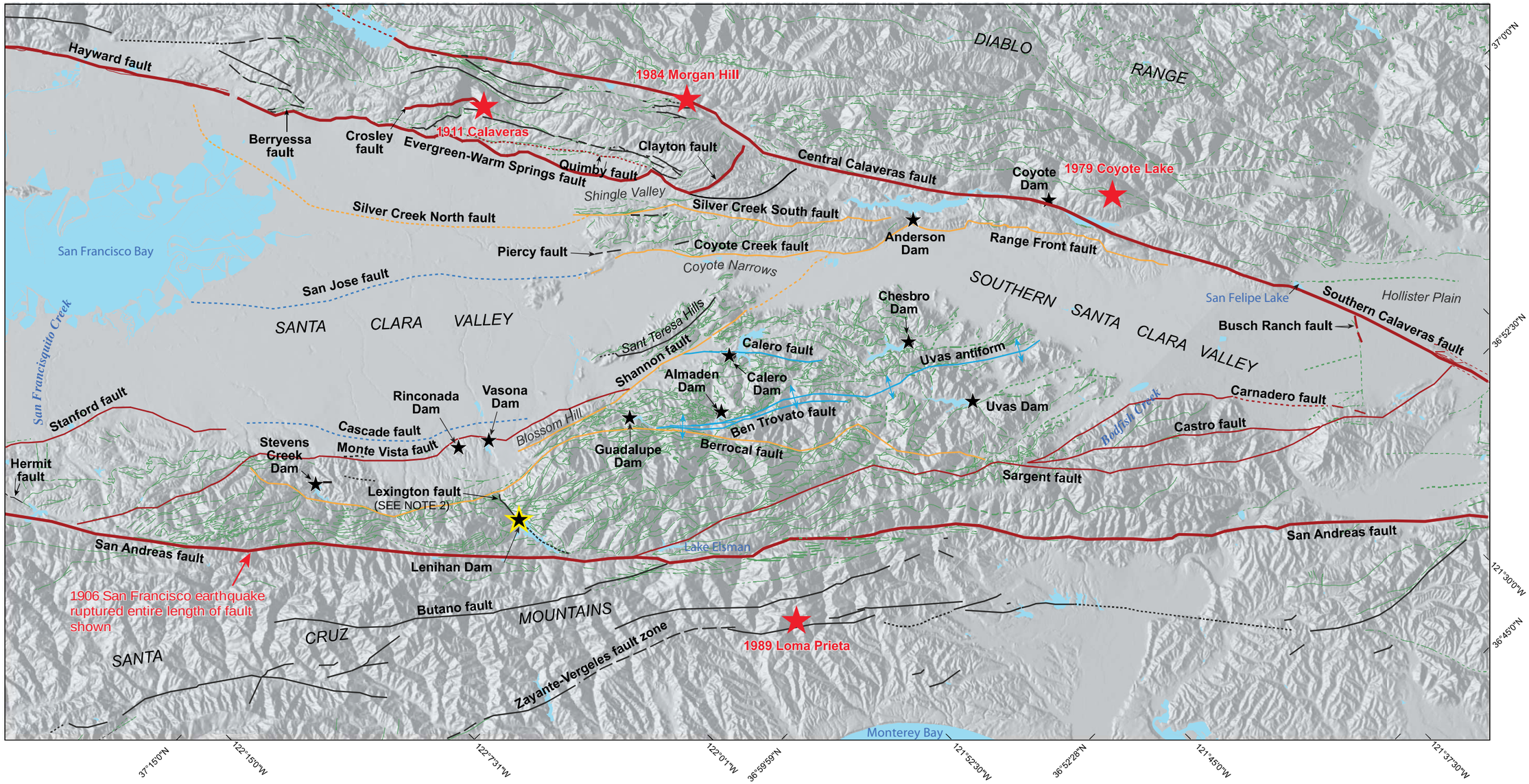

Explanation

- Active fault; dotted where concealed.
- Conditionally Active fault; dotted where concealed
- Other faults; dotted where concealed
- Jennings (1992) detailed faults
- Inactive Faults; dashed where inferred, dotted where concealed
- SCVWD Dams
- Historically significant earthquake

N

0 4 8 Miles

0 4 8 Kilometers

NOTES:
1) FIGURE EXCERPTED FROM FINAL TECHNICAL MEMORANDUM BY WILLIAM LETTIS & ASSOCIATES, INC. (LETTIS, 2008)
2) LEXINGTON FAULT RECENTLY ESTABLISHED AS INACTIVE BY DSOD (DSOD 2010b)

TERRA / GeoPentech
a Joint Venture

REGIONAL FAULT MAP
LENIHAN DAM
SEISMIC STABILITY EVALUATIONS (SSE2)

Figure
3-1

Rev. 0 11/21/2011 SSE2-R-3LN

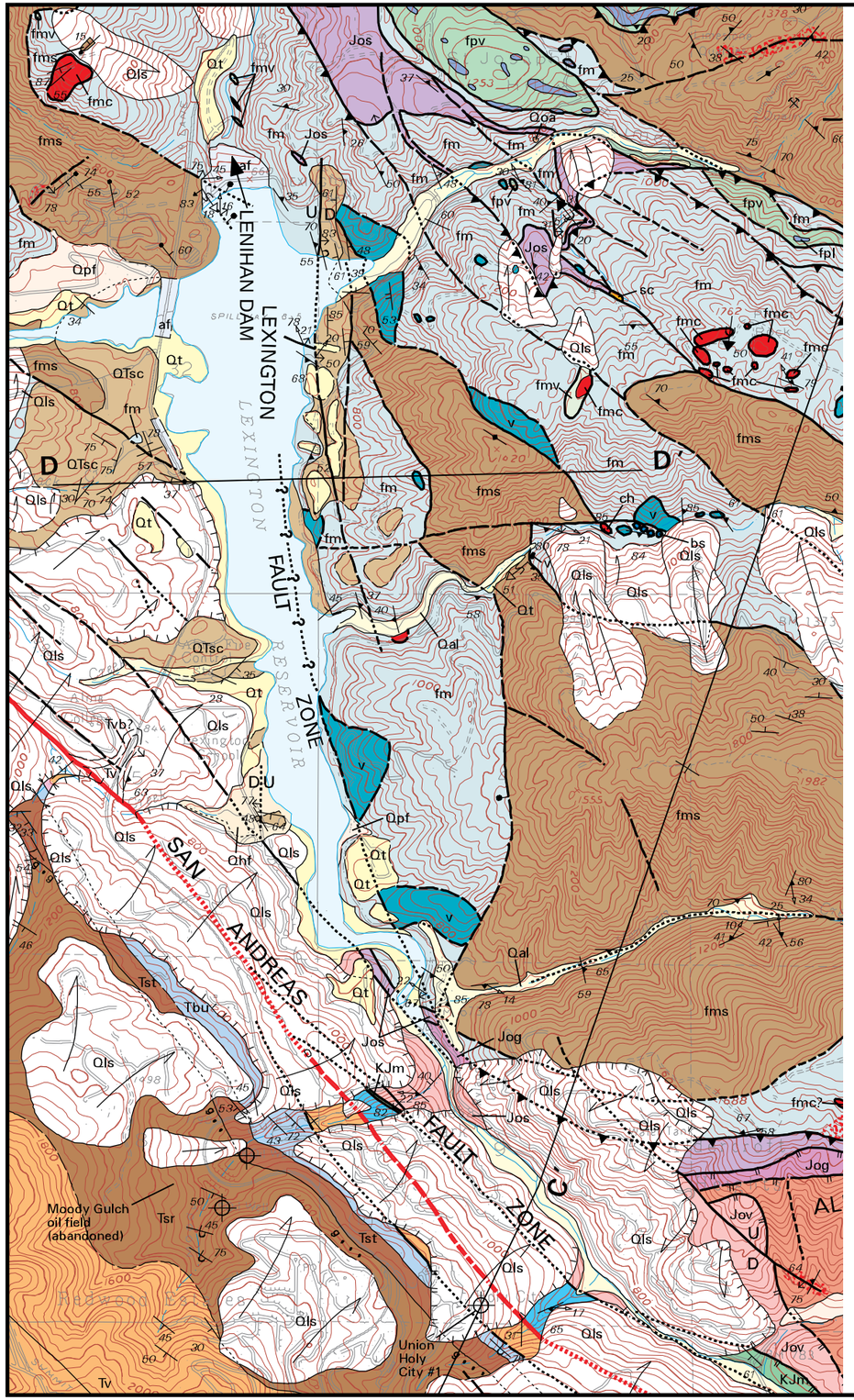

EXPLANATION

QUATERNARY TO LATE TERTIARY UNITS

- md — Mine dump (Holocene)
- gp — Gravel pit (Holocene)
- pp — Percolation pond (Holocene)
- af — Artificial fill (Holocene)
- Qal — Alluvium, undivided (Holocene and Pleistocene)
- Qls — Landslide deposits, undivided (Holocene and Pleistocene)
- Qt — Alluvial terrace deposits, undivided (Holocene and Pleistocene)
- Qhf — Alluvial fan deposits (Holocene)
- Qhb — Basin deposits (Holocene)
- Qhl — Levee deposits (Holocene)
- Qhfp — Floodplain deposits (Holocene)
- Qhc — Stream channel deposits (Holocene)
- Qa — Aromas Sand (Pleistocene) - Locally divided into:
- Qad — Dune deposits
- Qaf — Fluvial deposits
- Qof — Old floodplain deposits (Pleistocene?)
- Qmt — Marine terrace deposits (Pleistocene)
- Qoa — Old alluvium, undivided (Pleistocene)
- Qpf — Alluvial fan deposits (Pleistocene)
- QTf — Fluvial deposits, undivided (Pleistocene and Pliocene?)
- QTsc — Santa Clara Formation (Pleistocene and Pliocene)

TERTIARY AND OLDER ROCK UNITS Northeast of San Andreas fault New Almaden Block

- sc — Silica-carbonate rock (Miocene?)
- Tus — Unnamed sandstone (middle Miocene or younger)
- Tms — Monterey Shale (middle and lower Miocene)
- Tt — Temblor Sandstone (middle Miocene to Oligocene?) - Locally includes:
- Ttv — Volcanic and intrusive rocks (middle Miocene)
- Jos — Serpentinized ultramafic rocks (Jurassic)

Franciscan Complex (Cretaceous and Jurassic) - Consists of:

- fm — Melange of the Central belt (Upper Cretaceous) - Includes:
- bs — Blueschist blocks
- am — Amphibolite blocks
- ch — Chert blocks
- v — Basaltic volcanic rock blocks
- cg — Conglomerate block
- mdi — Metadiorite block

Permanente terrane (Cretaceous) - Divided into:

- fpl — Foraminiferal limestone (Upper and Lower Cretaceous)
- fpv — Volcanic rocks (Lower Cretacvveous)
- fpt — Siliceous radiolarian-bearing tuff

Marin Headlands terrane (Cretaceous and Jurassic) - Divided into:

- fms — Sandstone (Upper and (or) Lower Cretaceous)
- fmc — Radiolarian chert (Lower Cretaceous and Jurassic)
- fmv — Basaltic volcanic rocks (Lower Jurassic)

- Contact - Dashed where approximate, dotted where concealed, queried where uncertain
- Fault - Dashed where approximate, dotted where concealed, queried where uncertain. U and D denote upthrown and downthrown blocks. Arrows with (without) numbers denote fault dip (or dip direction). Bar and ball locally denote downthrown block. Horizontal arrows denote relative horizontal movement. Double barb denotes vertical fault
- Attenuation fault - Fault at low angle to bedding, interpreted as low-angle normal fault, double hachures on down-dropped (upper plate) side. Dashed where approximate, dotted where concealed, queried where uncertain
- Thrust fault - Barbs on upper plate. Dashed where approximate, dotted where concealed, queried where uncertain
- Principal trace of the San Andreas fault - Dashed where approximate, dotted where concealed

Strike and dip of bedding

- Inclined - Ball denotes that facing direction is known from sedimentary structures; no dip means dip unknown
- Vertical - Ball denotes that facing direction is known from sedimentary structures
- Horizontal
- Overturned - Ball denotes that facing direction is known from sedimentary structures
- Approximate - Based on photo interpretation or estimated dip in field
- In trench - Measured from exposures at geotechnical or construction trench site

N 15 MN

UTM GRID AND 2001 MAGNETIC NORTH

SCALE 1:24 000

1 1/2 0 1 MILE

1000 0 1000 2000 3000 4000 5000 6000 7000 FEET

1 .5 0 1 KILOMETER

CONTOUR INTERVAL 40 FEET

NATIONAL GEODETIC VERTICAL DATUM OF 1929

MAP LOCATION

FROM:
R.J. MCLAUGHLIN, J.C. CLARK, E.E. BRABB, E.J. HELLY, AND C.J. COLON - 2001

TERRA / GeoPentech
a Joint Venture

LOCAL REGION GEOLOGIC MAP
LENIHAN DAM
SEISMIC STABILITY EVALUATIONS (SSE2)

Figure 3-2

Rev. 0 11/21/2011 SSE2-R-3LN

NOTES

1. DATA PROVIDED BY SCVWD
2. CONTOUR INTERVAL 5FT
3. ELEVATIONS SHOWN REFLECT ADDITION OF 2.96 FT TO CONVERT ORIGINAL CONTOURS IN NGVD 1929 VERTICAL DATUM TO NAVD 88 VERTICAL DATUM
4. CONTOURS IN AREAS OF SUSPECTED SURVEY ERROR ARE SHOWN IN BROWN. SEE FIGURE 4-3 FOR CORRECTED CONTOURS.

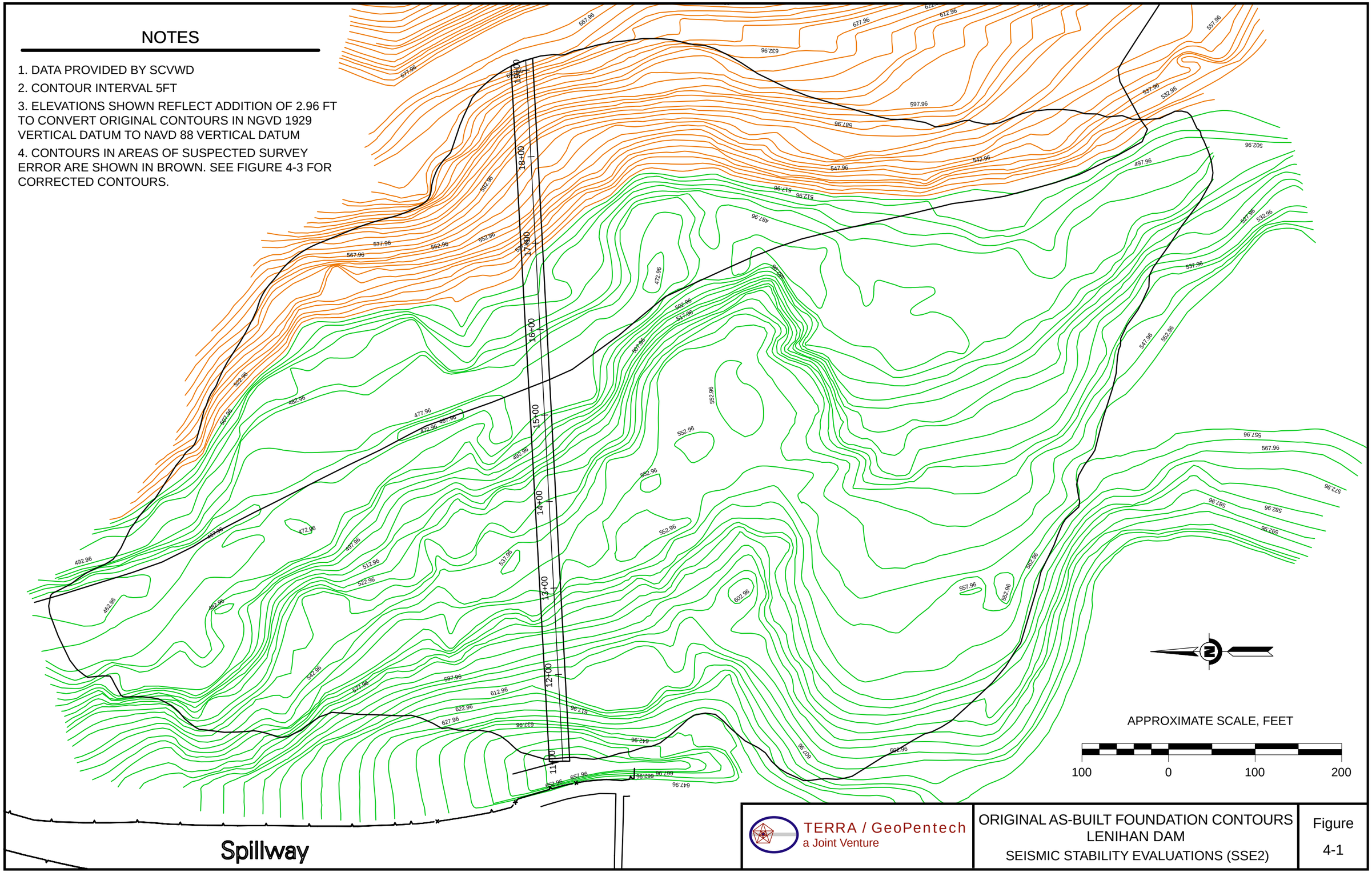

TERRA / GeoPentech
a Joint Venture

ORIGINAL AS-BUILT FOUNDATION CONTOURS
LENIHAN DAM
SEISMIC STABILITY EVALUATIONS (SSE2)

Figure
4-1

Rev. 1 12/08/2011 SSE2-R-3LN

0' 100' 200' 300' 400'

N

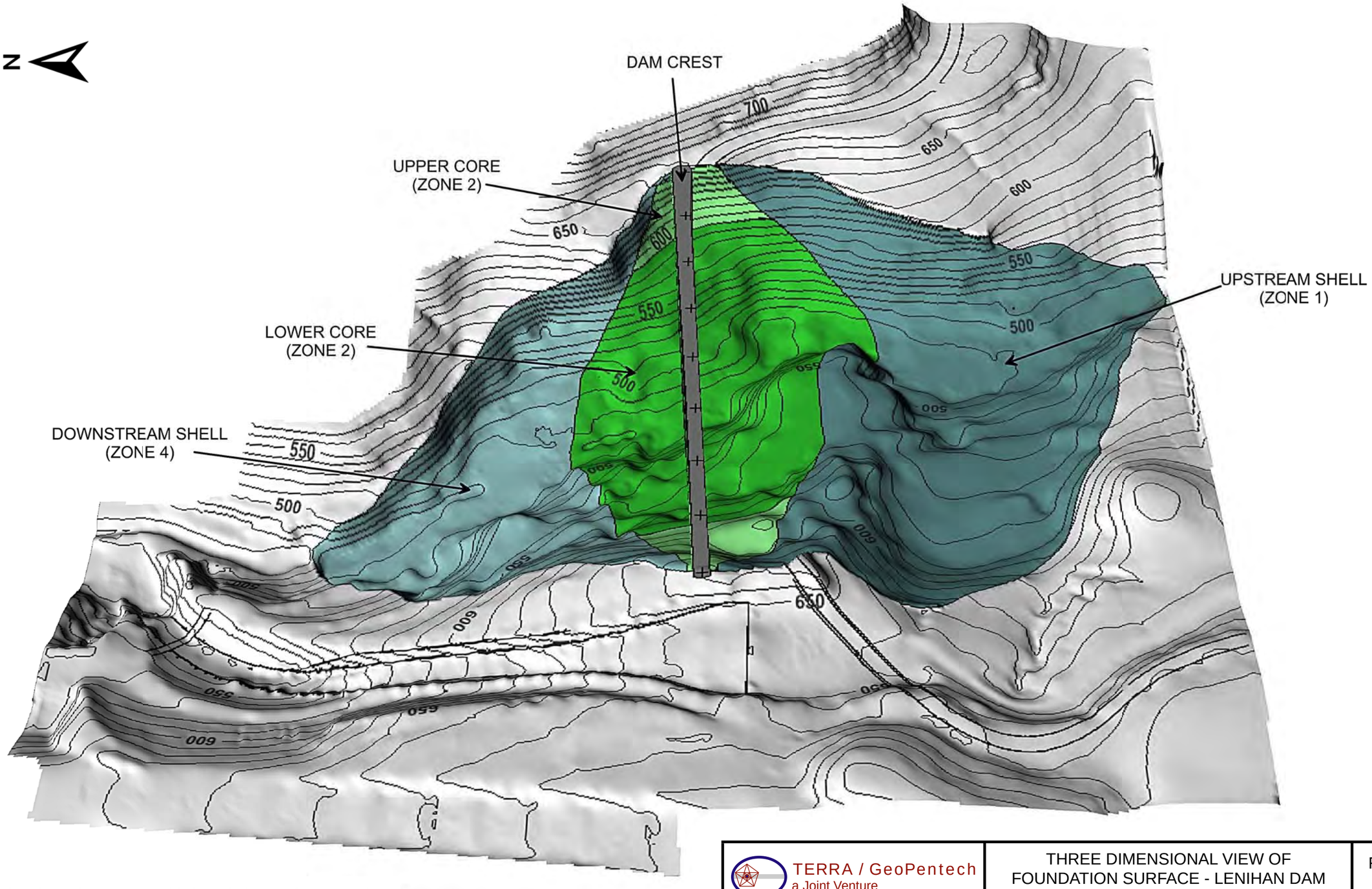

Note:
1. Contacts of various dam zones with foundation surface are shown.

TERRA / GeoPentech
a Joint Venture

THREE DIMENSIONAL VIEW OF
FOUNDATION SURFACE - LENIHAN DAM
SEISMIC STABILITY EVALUATIONS (SSE2)

Figure
4-2

Rev. 0 11/22/2011 SSE2-R-3LN

NOTES

1. DATA PROVIDED BY SCVWD
2. CONTOUR INTERVAL 5FT
3. ELEVATIONS SHOWN REFLECT ADDITION OF 2.96 FT TO CONVERT ORIGINAL CONTOURS IN NGVD 1929 VERTICAL DATUM TO NAVD 88 VERTICAL DATUM
4. AREAS OF SUSPECTED SURVEY ERROR ARE SHOWN IN BROWN; CONTOURS WERE MODIFIED IN THESE AREAS BASED ON ROCK ELEVATIONS FROM BORINGS AND ORIGINAL GROUND SURFACE ELEVATIONS

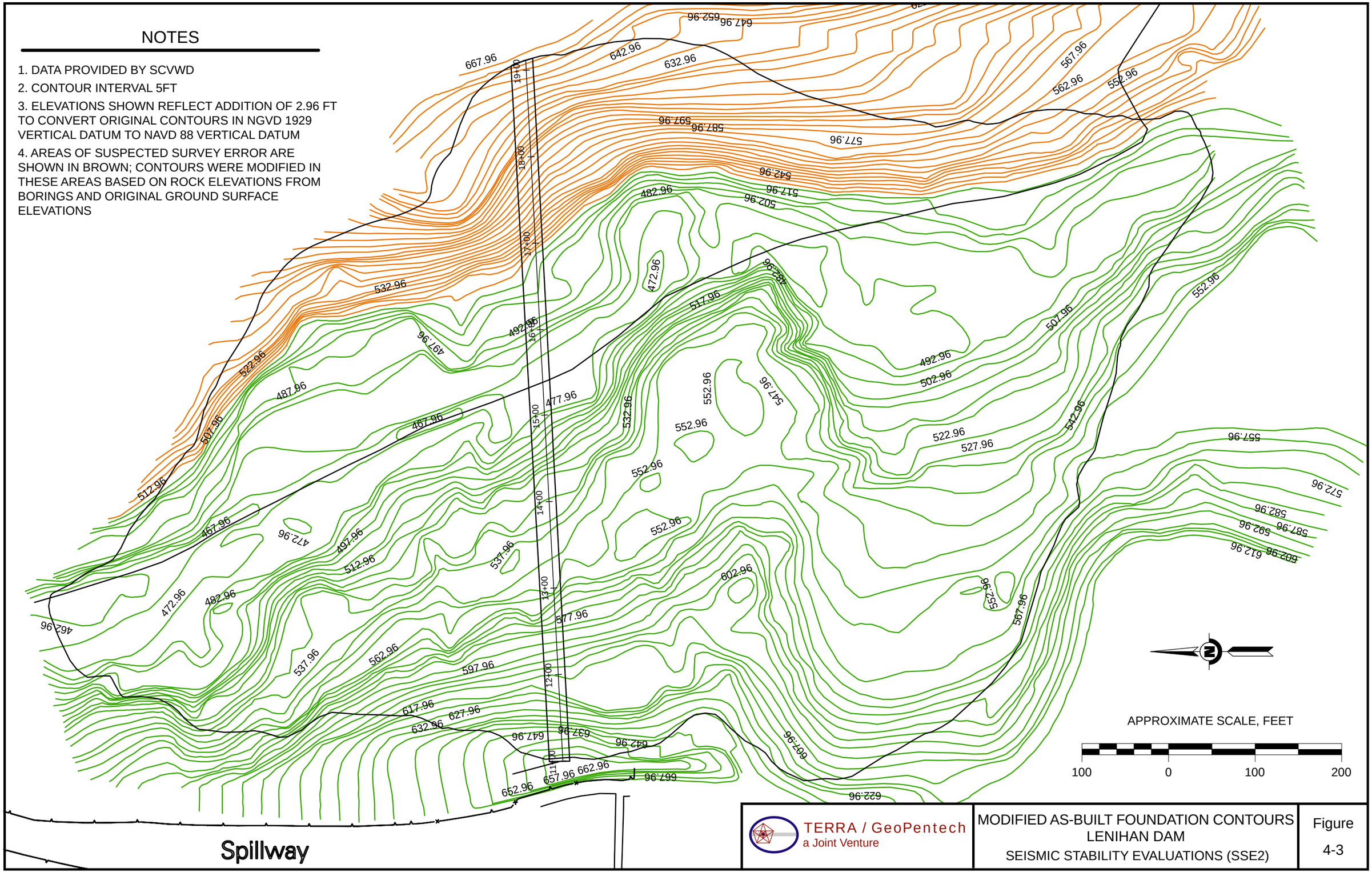

TERRA / GeoPentech
a Joint Venture

MODIFIED AS-BUILT FOUNDATION CONTOURS
LENIHAN DAM
SEISMIC STABILITY EVALUATIONS (SSE2)

Figure
4-3

Rev. 0 11/22/2011 SSE2-R-3LN

CROSS SECTION LOCATION MAP

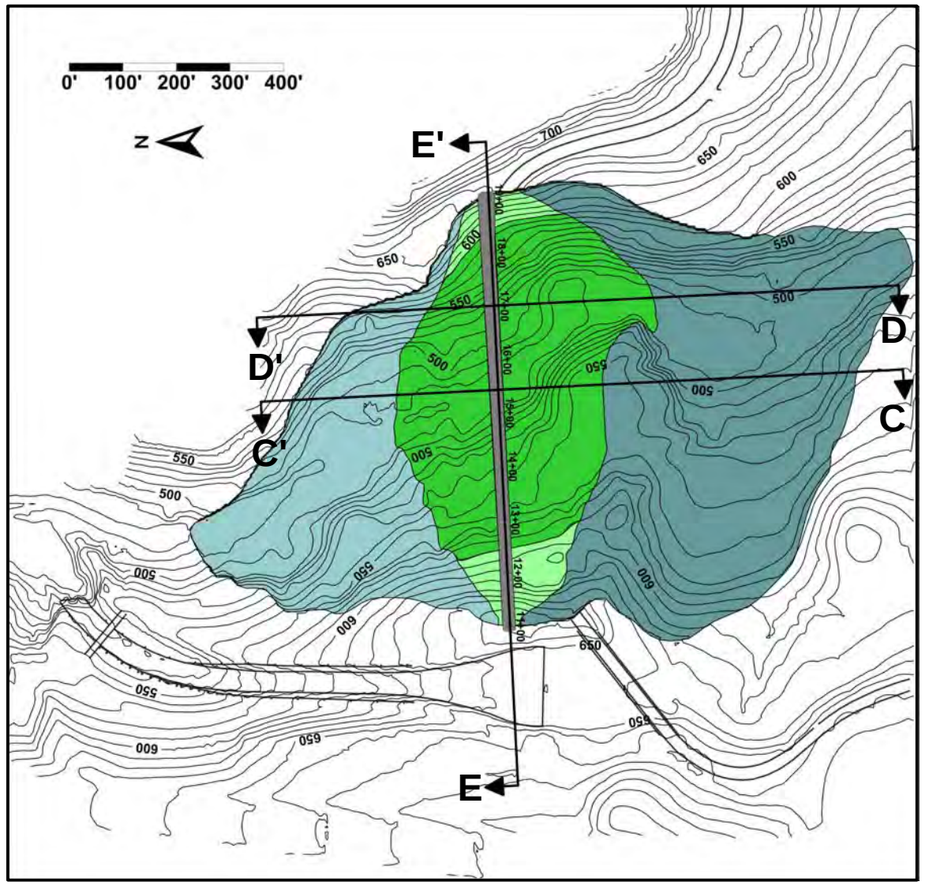

LEGEND

- Upstream Shell (Zone 1)
- Lower Core (Zone 2, Below El. 590)
- Upper Core (Zone 2, Above El. 590)
- Drain Zone (Zone 3)
- Downstream Shell (Zone 4)
- Franciscan Complex Bedrock

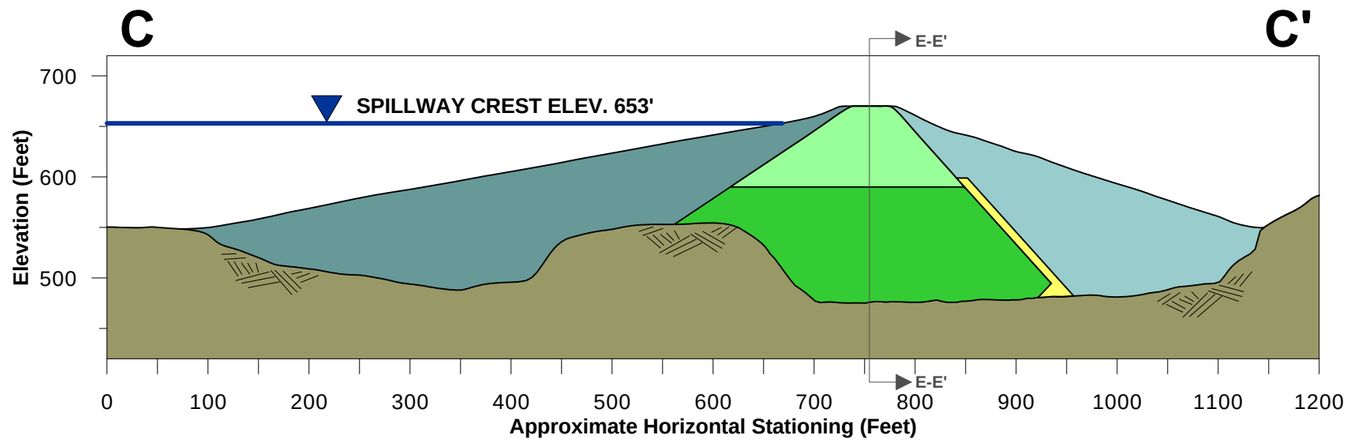

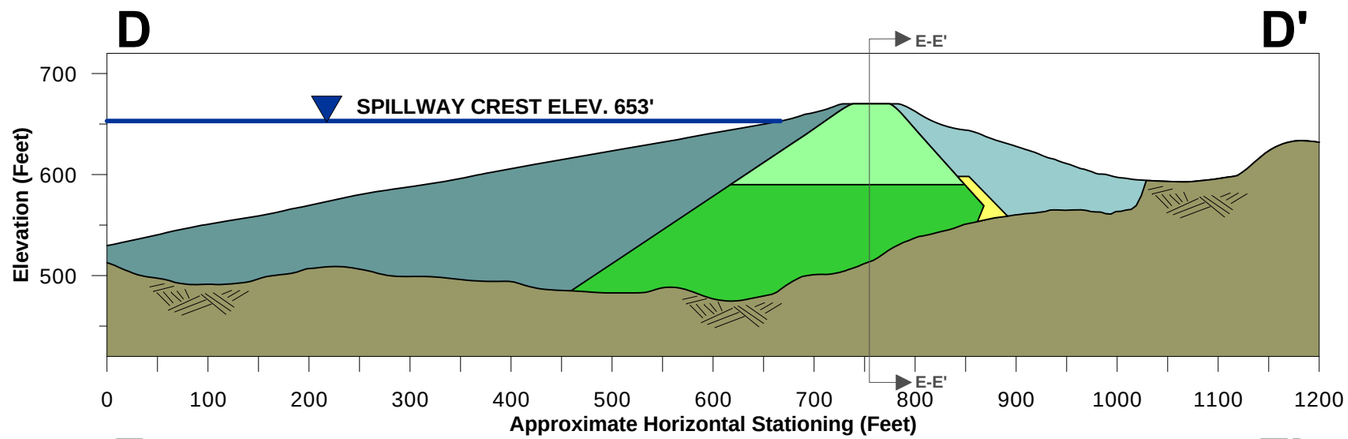

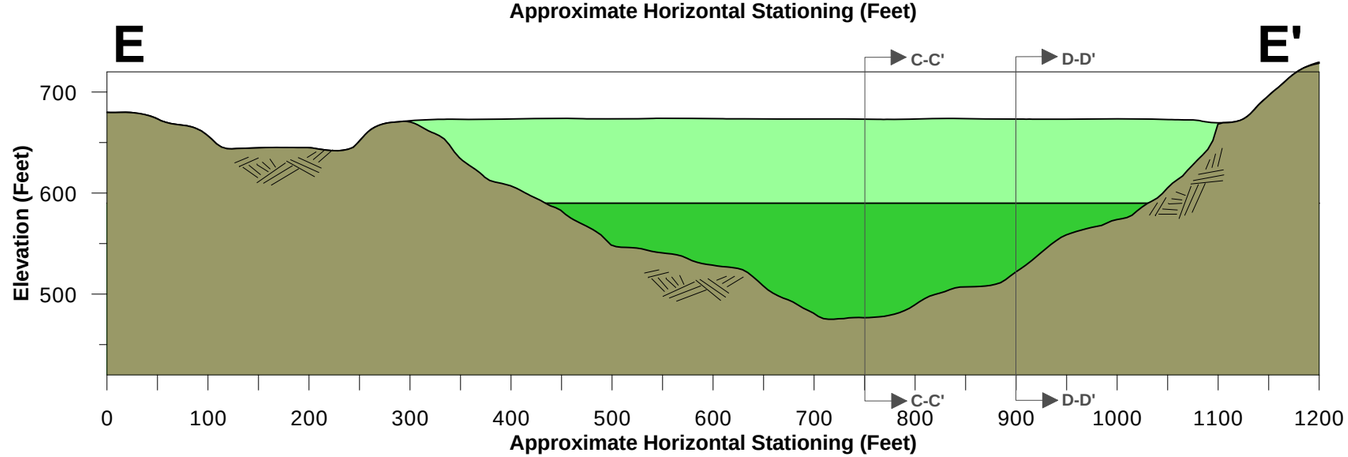

TERRA / GeoPentech
a Joint Venture

CROSS SECTIONS WITH FOUNDATION SURFACE - LENIHAN DAM
SEISMIC STABILITY EVALUATIONS (SSE2)

Figure 4-4

Rev. 0 11/22/2011 SSE2-R-3LN

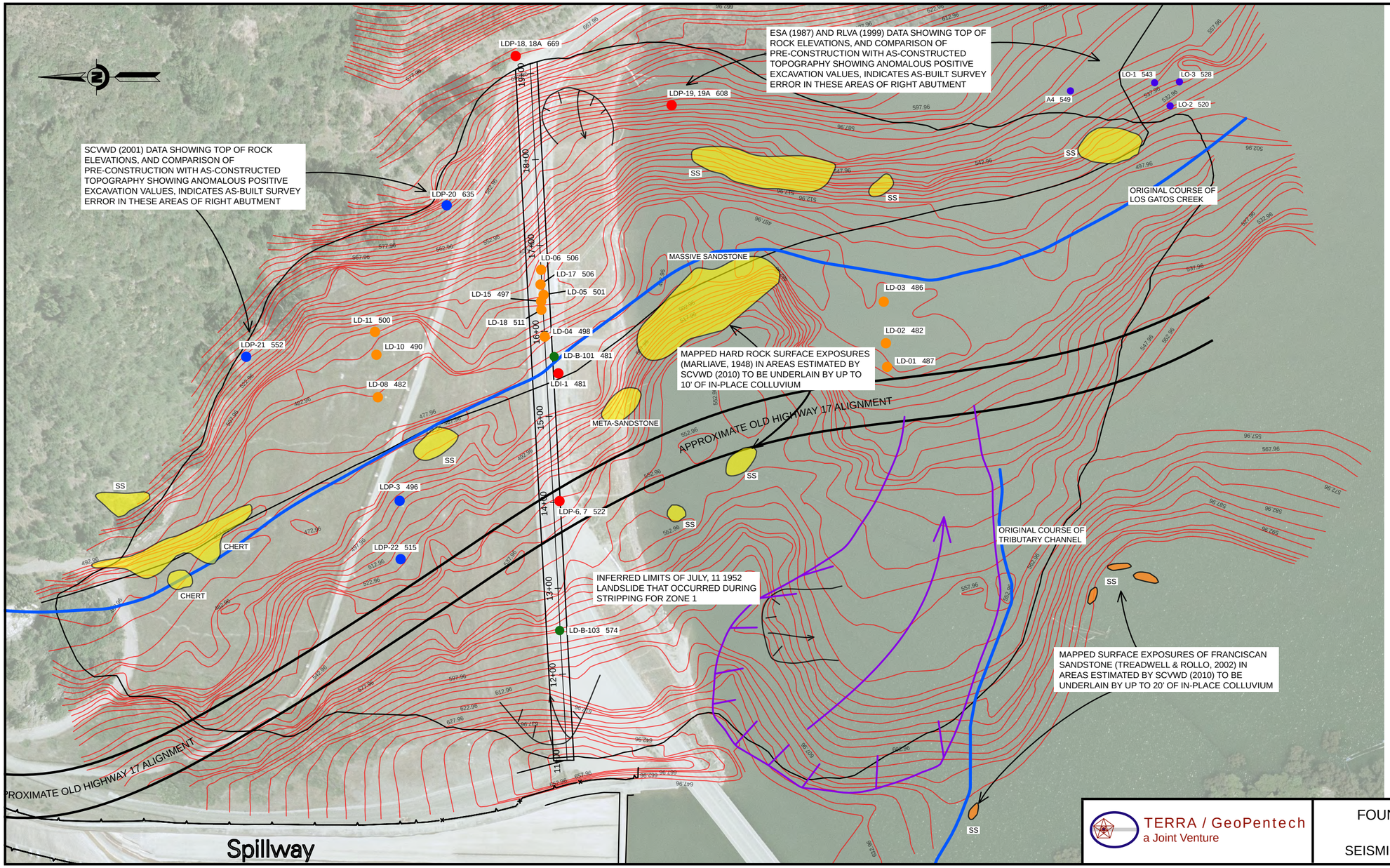

EXPLANATION

BORINGS FROM INVESTIGATIONS AND INSTRUMENTATION (WITH ELEVATION OF TOP OF ROCK INDICATED):

- WAHLER 1982 BORINGS
- ESA 1987 BORINGS
- VOLPE 1999 BORINGS
- DISTRICT 2001 BORINGS
- TGP 2011 BORINGS

HARD ROCK OUTCROP (MOSTLY FRANCISCAN SANDSTONE) MAPPED IN DAMSITE AREA PRIOR TO CONSTRUCTION (MARLIAVE, 1948)

LANDSLIDE MAPPED PRIOR TO CONSTRUCTION (MARLIAVE, 1948)

AS-BUILT FOUNDATION ELEVATION CONTOUR (FROM AS-CONSTRUCTED GENERAL PLAN-SCVWD 1955; CORRECTED TO 1988 NAVD

587.96

APPROXIMATE SCALE, FEET

100 0 100 200

NOTES:

1) ONLY THOSE BORINGS THAT WERE EXTENDED INTO THE FOUNDATION ARE DEPICTED.
2) BORING LOCATIONS FROM WAHLER 1982, RLVA 1999, SCVWD 2001 EXPLORATION PLANS, AND SCVWD 2010 SURVEILLANCE REPORT
3) REFER TO SECTION 4.0 FOR DISCUSSION OF INFERRED FOUNDATION CONDITIONS AND COMPARISON WITH SCVWD 2010 FOUNDATION ANALYSIS REPORT.

TERRA / GeoPentech
a Joint Venture

FOUNDATION EXPLORATION DATA
LENIHAN DAM
SEISMIC STABILITY EVALUATIONS (SSE2)

Figure 4-5

Rev. 0 11/21/2011 SSE2-R-3LN

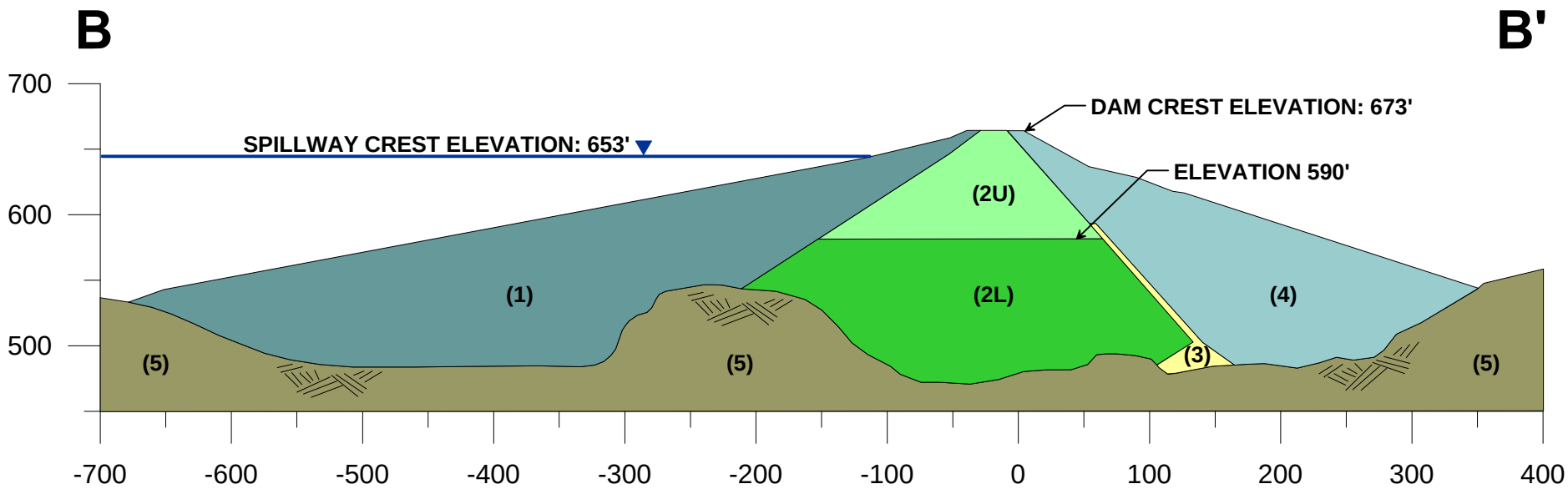

Zone	Color Code	Material Description	Predominant Soil Classification
1		Upstream Shell	Gravely Clayey Sands (SC) to Sandy Clays (CL)
2U		Upper Core (Above El. 590)	Gravely Clayey Sands (SC) to Clayey Gravels (GC)
2L		Lower Core (Below El. 590)	Sandy Highly Plastic Clays (CH) to Silty Sands-Sandy Highly Plastic Silts (SM-MH)
3		Drain Material	N/A
4		Downstream Shell	Gravely Clayey Sands (SC) to Clayey Gravels (GC)
5		Bedrock	Franciscan Complex

Note: See Figure 2-2A for location of section B-B'

TERRA / GeoPentech
a Joint Venture

MAXIMUM CROSS SECTION B-B'
LENIHAN DAM
SEISMIC STABILITY EVALUATIONS (SSE2)

Figure
5-1

Rev. 1 12/08/2011 SSE2-R-3LN

B

B'

SPILLWAY CRESTELEV. 653'

CPT-3
(Projected 180' East)

CPT-1
(Projected 20' West)

LD-CPT-101 and CPT-2
(Projected 20' East)

CPT-4
(Projected 80' East)

Actual Location of CPT-4
Shifted for convienence

LD-CPT-102
(Projected 20' East)

R_f (%) 10 5 0

q_c (tsf) 100 200

LEGEND

- CPT by Volpe
- CPT by TGP
- Upstream Shell (Zone 1)
- Lower Core (Zone 2, Below El. 590)
- Upper Core (Zone 2, Above El. 590)
- Drain Zone (Zone 3)
- Downstream Shell (Zone 4)
- Franciscan Complex Bedrock

Elevation (Feet)

690 660 630 600 570 540 510 480

-210 -180 -150 -120 -90 -60 -30 0 30 60 90 120 150 180

Approximate Horizontal Stationing (Feet)

Note: See Figure 2-3 for complete zoning and piezometric data.

TERRA / GeoPentech
a Joint Venture

CROSS SECTION B-B' WITH CPT DATA PLOTS
LENIHAN DAM
SEISMIC STABILITY EVALUATIONS (SSE2)

Figure
5-2

Rev. 1 12/08/2011 SSE2-R-3LN

E

E'

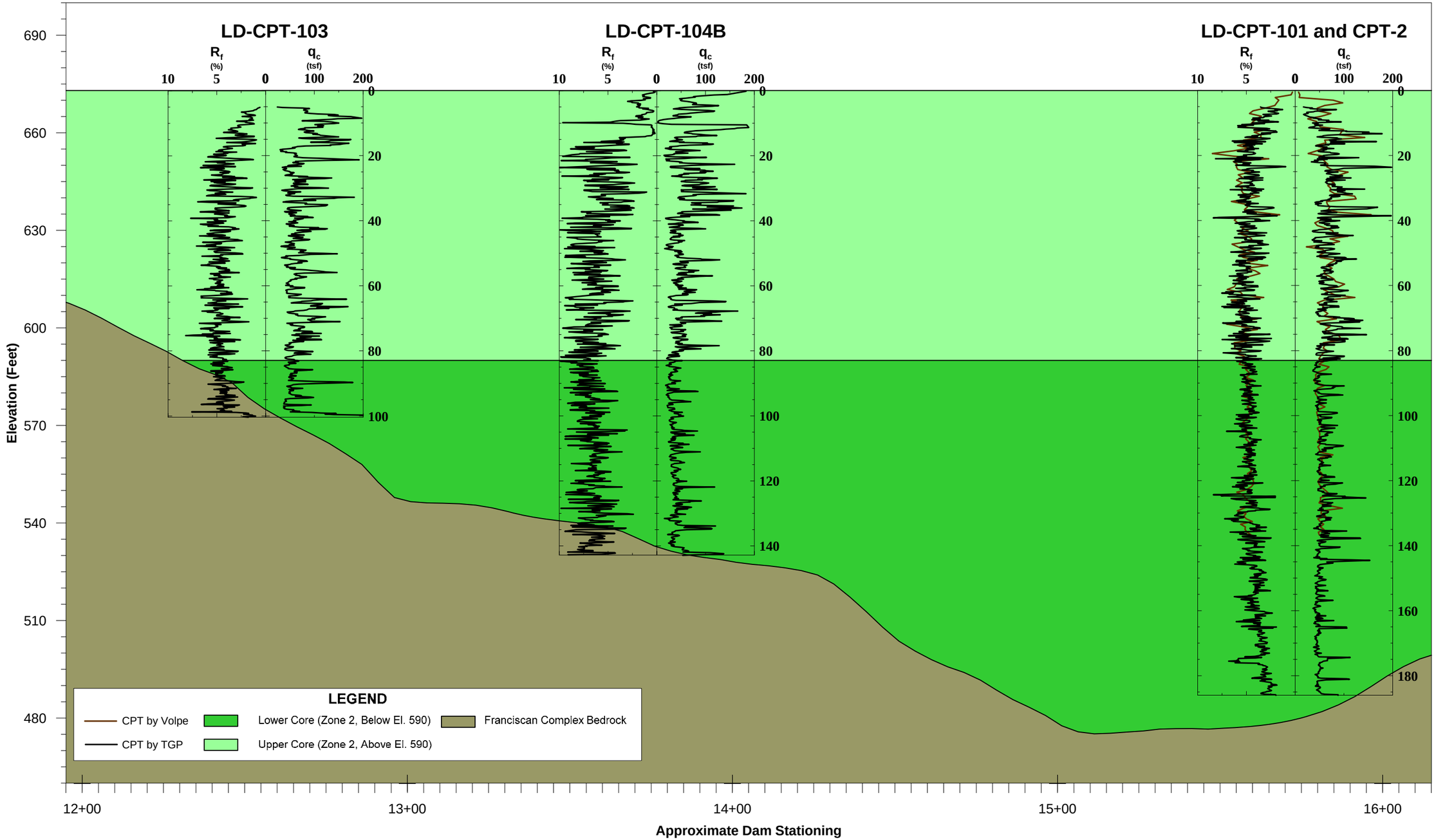

Note: See Figure 4-4 for location of section E-E'

TERRA / GeoPentech
a Joint Venture

CROSS SECTION E-E' WITH CPT DATA PLOTS
LENIHAN DAM
SEISMIC STABILITY EVALUATIONS (SSE2)

Figure
5-3

Rev. 1 12/08/2011 SSE2-R-3LN

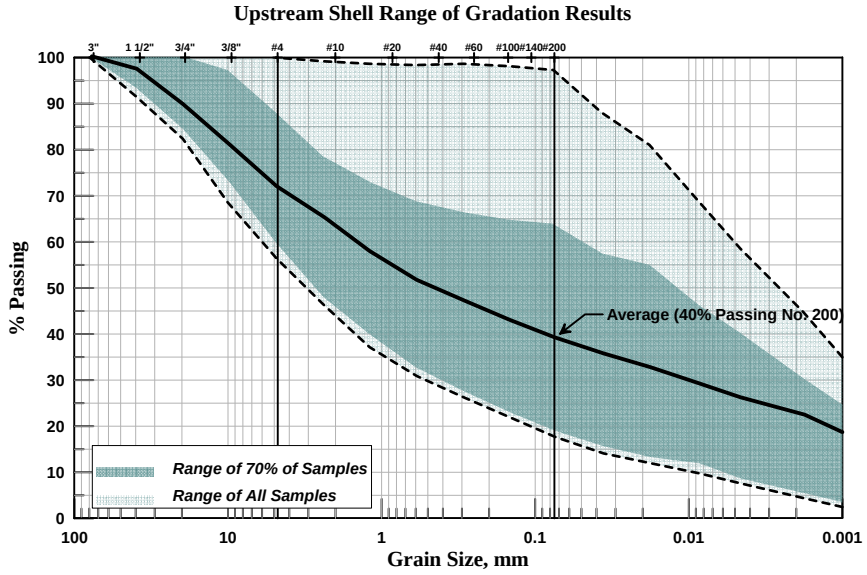

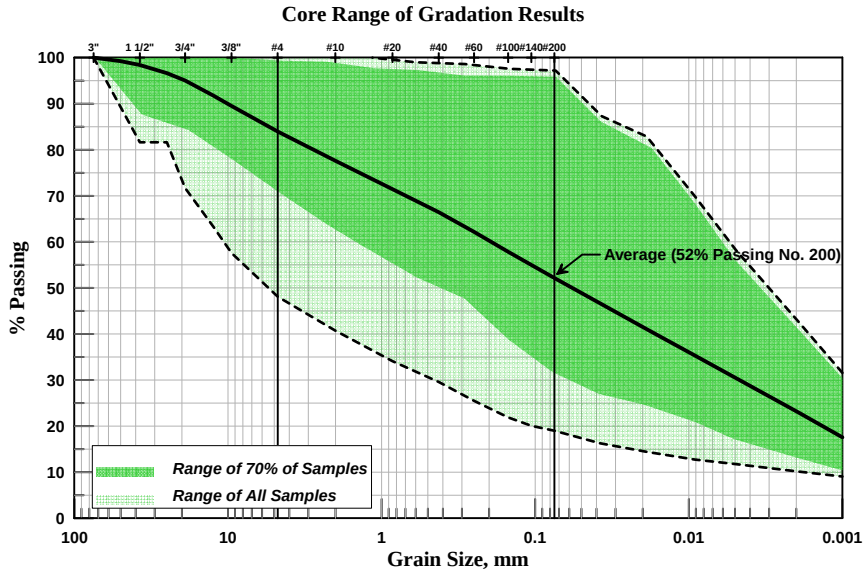

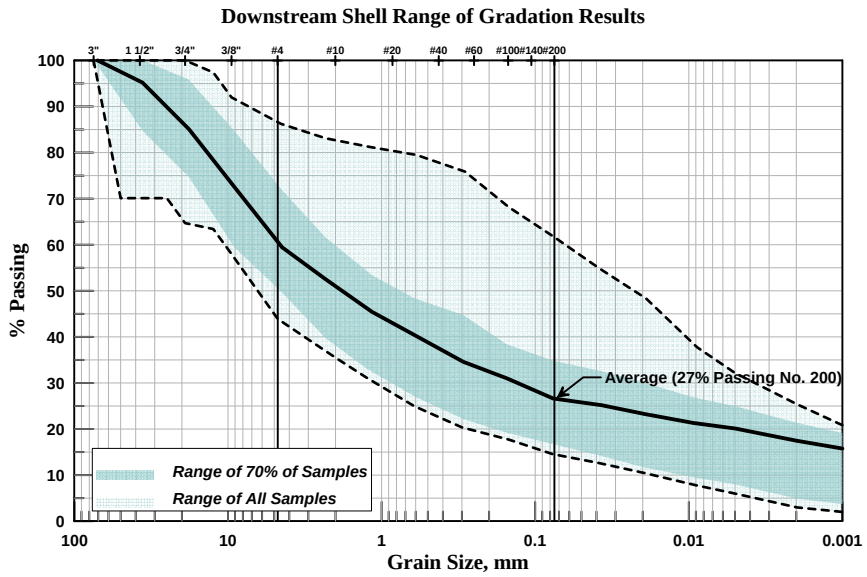

TERRA / GeoPentech
a Joint Venture

GRADATION RANGES
LENIHAN DAM
SEISMIC STABILITY EVALUATIONS (SSE2)

Figure
5-4

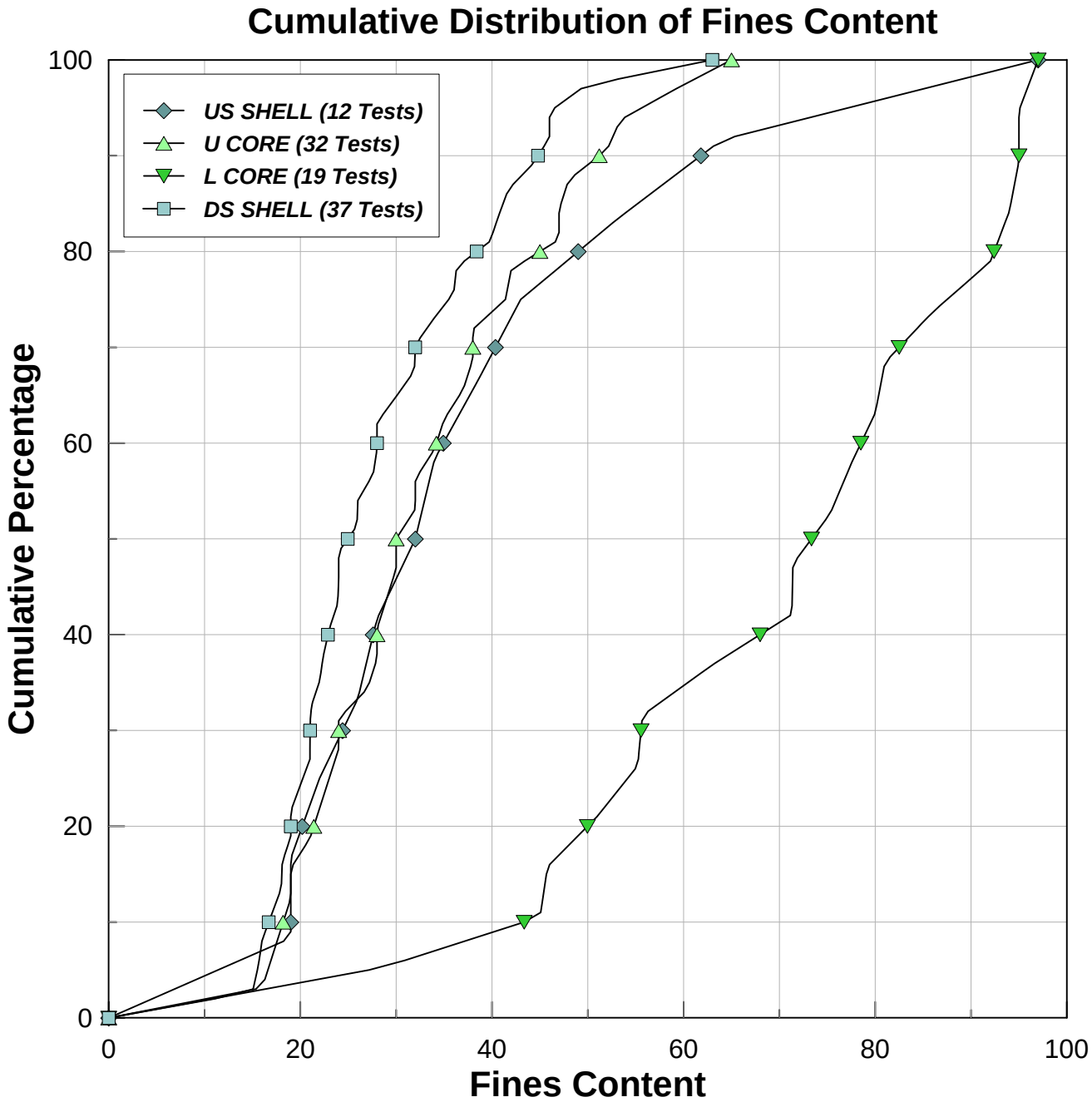

TERRA / GeoPentech
a Joint Venture

FINES CONTENT DISTRIBUTION
LENIHAN DAM
SEISMIC STABILITY EVALUATIONS (SSE2)

Figure
5-5

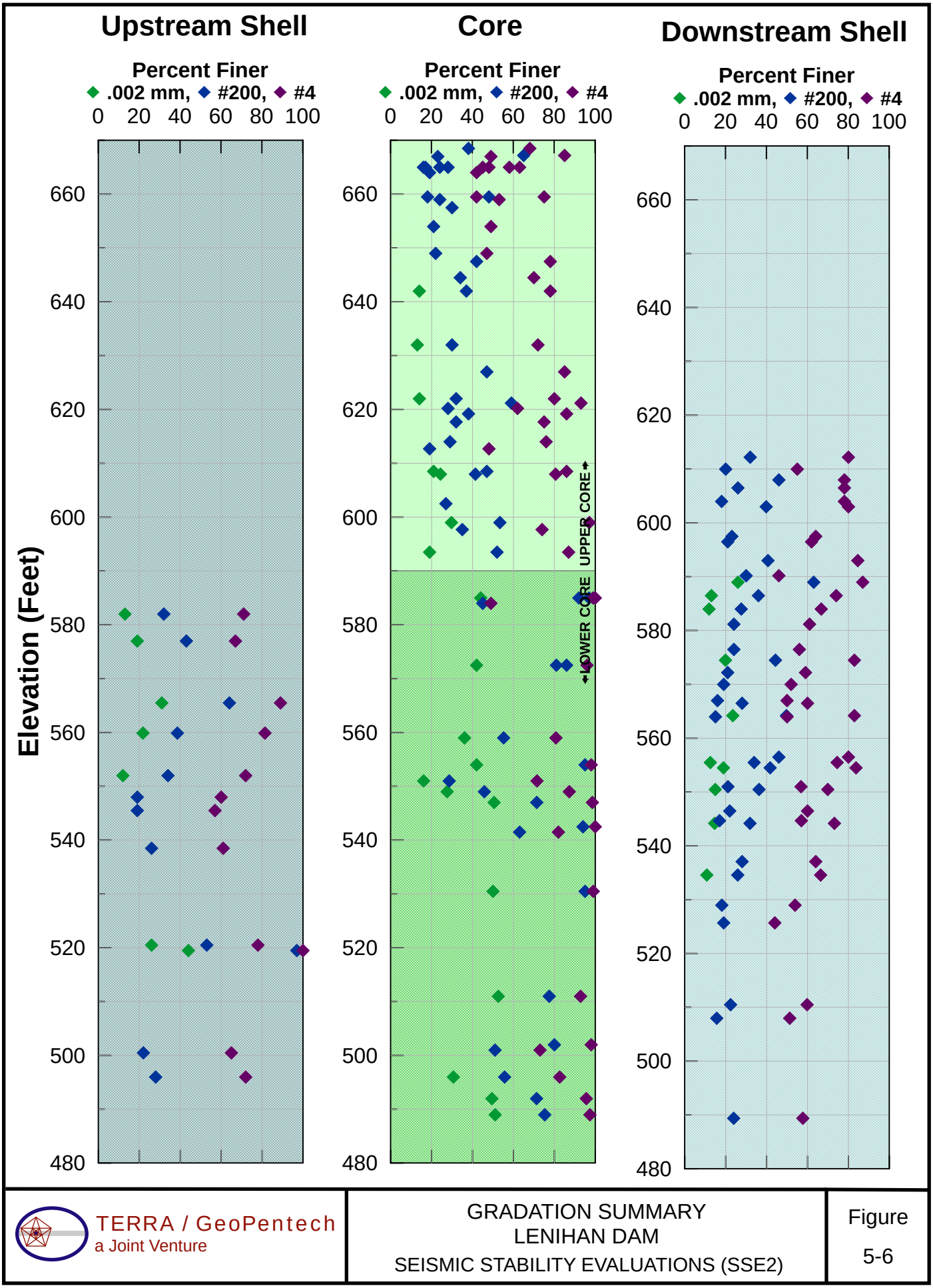

TERRA / GeoPentech
a Joint Venture

GRADATION SUMMARY
LENIHAN DAM
SEISMIC STABILITY EVALUATIONS (SSE2)

Figure
5-6

Rev. 0 11/21/2011 SSE2-R-3LN

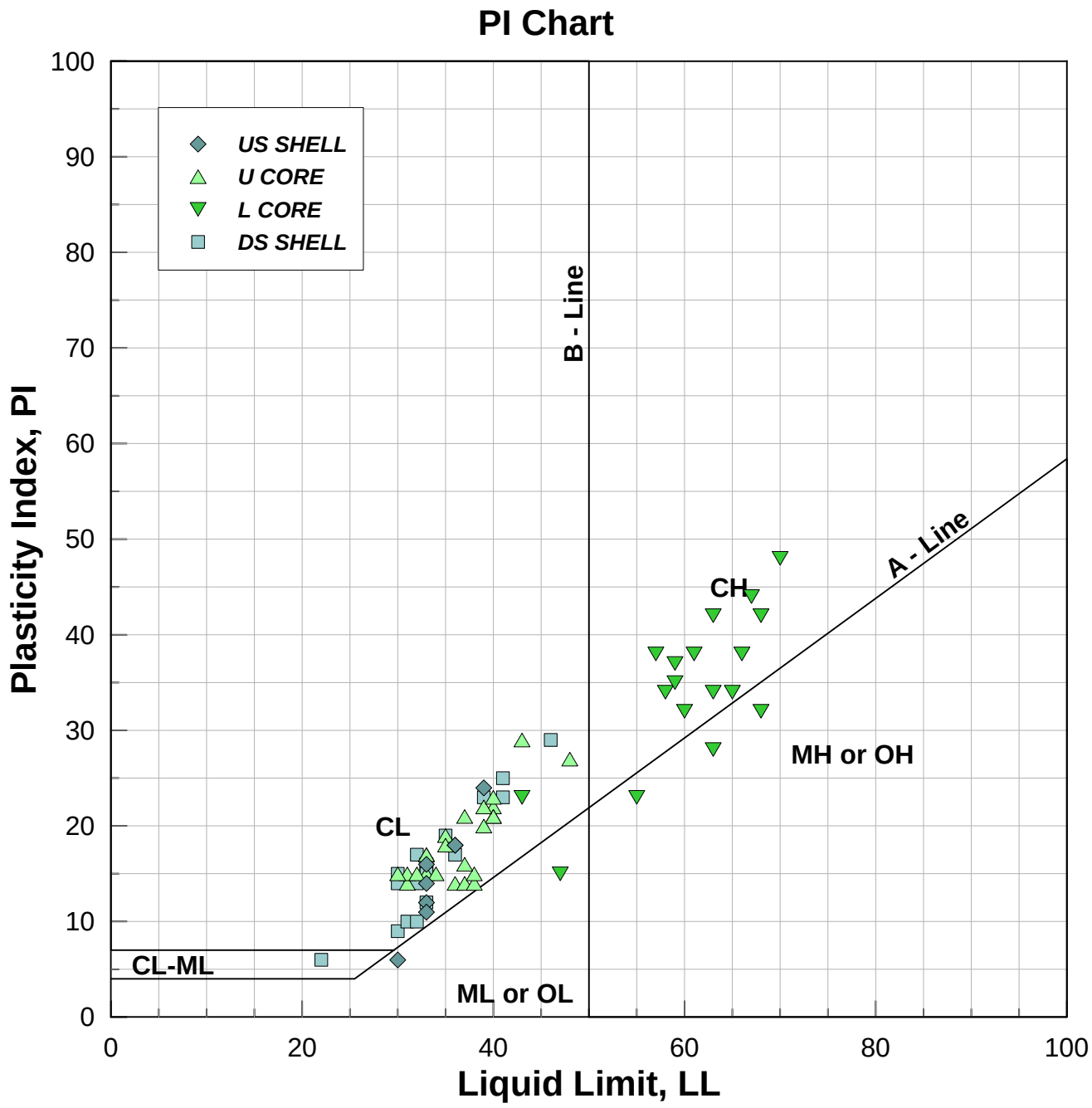

SUMMARY OF ATTERBERG LIMITS TEST RESULTS

Zone	Material	Material Description	No. Tests	Range of LL	Median LL	Range of PI	Median PI
1	Upstream Shell	SC-CL	8	30 to 39	33	6 to 24	15
2U	Upper Core	SC-GC-SM-CL	23	30 to 48	37	14 to 29	17
2L	Lower Core	CH-CL-MH-SM-CL	18	43 to 70	62	15 to 48	35
4	Downstream Shell	SC-GC-SP-CL-GM	23	22 to 46	33	6 to 29	15

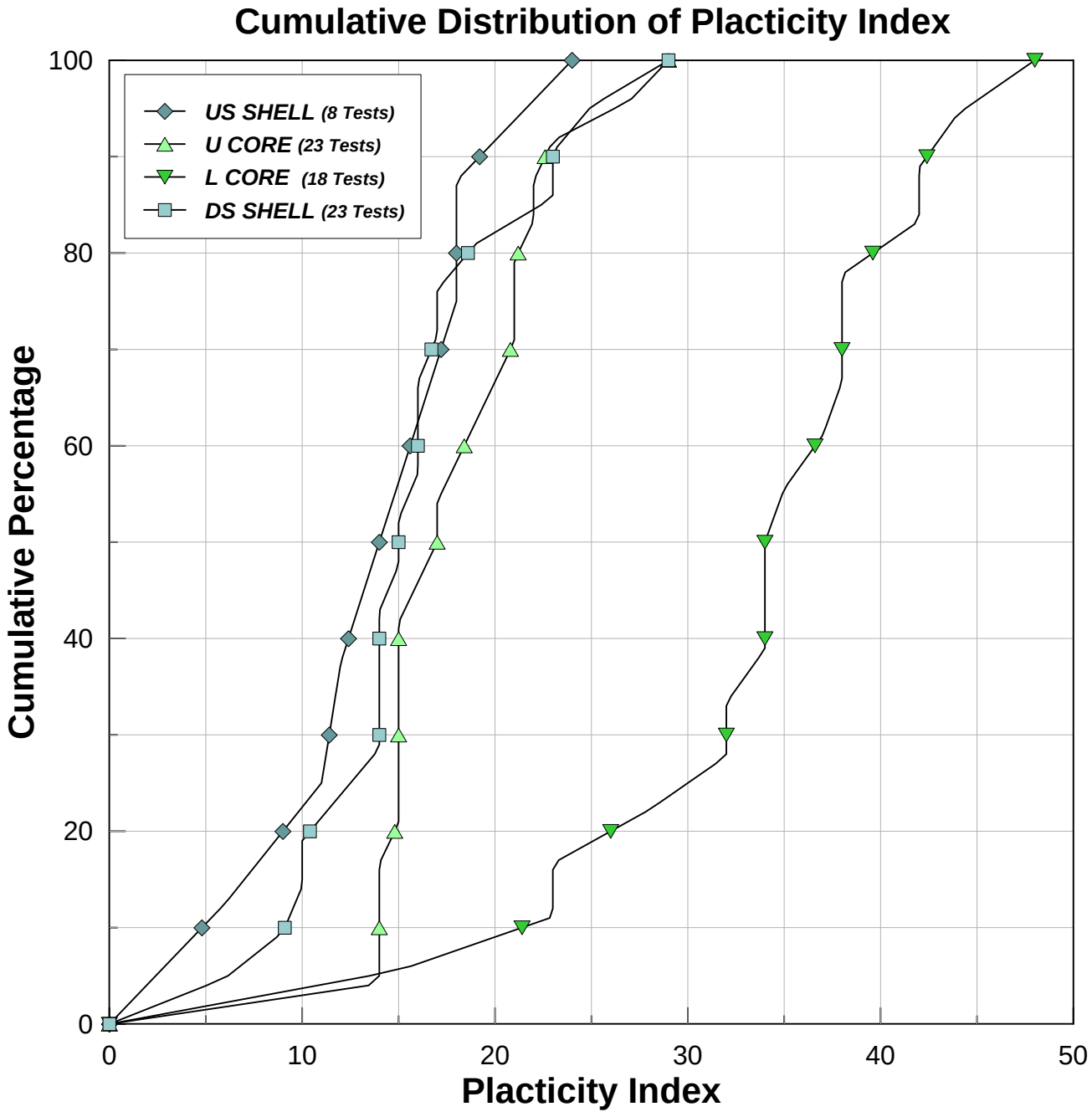

TERRA / GeoPentech
a Joint Venture

PLASTICITY INDEX DISTRIBUTION
LENIHAN DAM
SEISMIC STABILITY EVALUATIONS (SSE2)

Figure
5-8

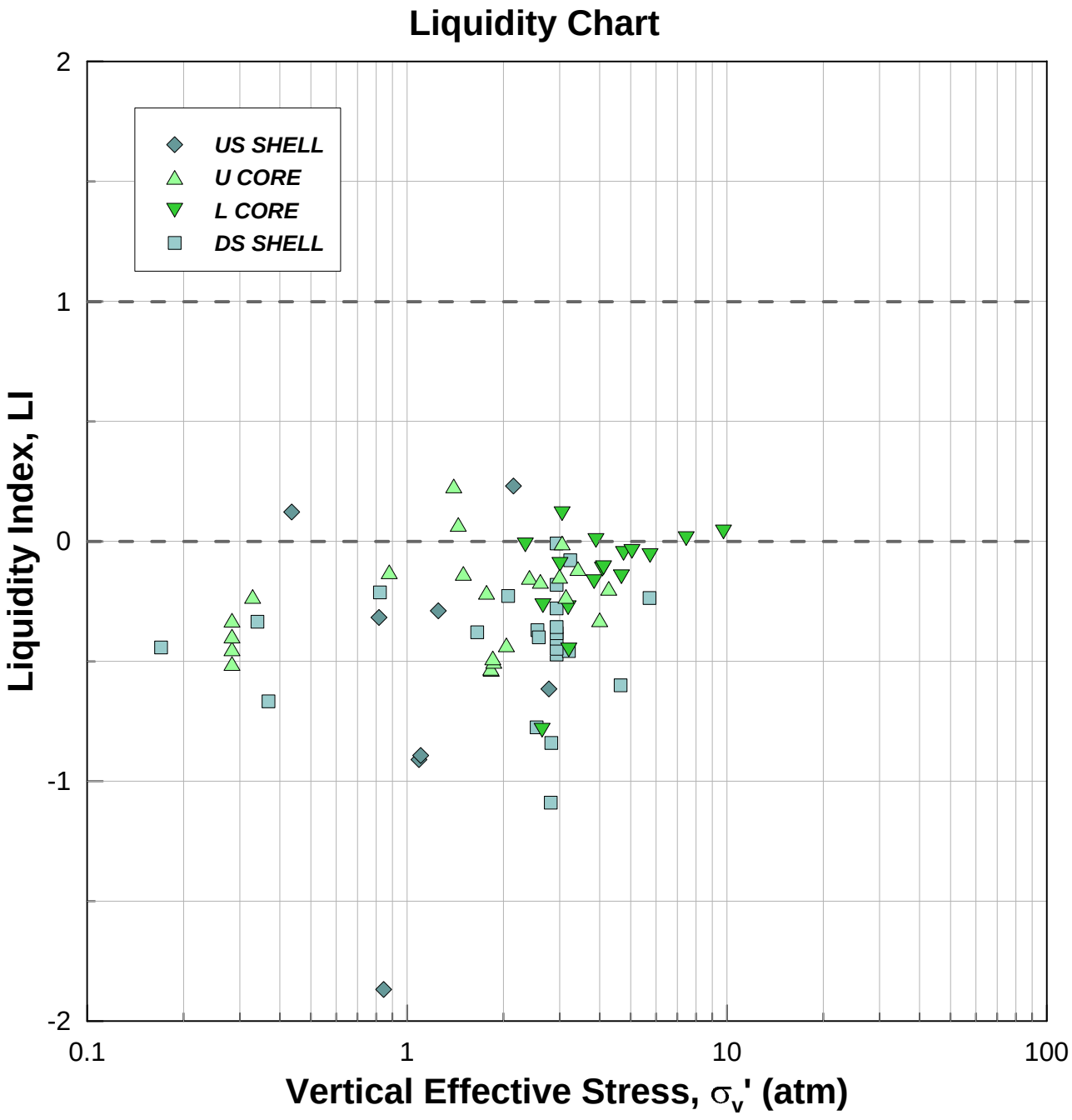

SUMMARY OF LIQUIDITY INDEX TEST RESULTS

Zone	Material	Material Description	No. Tests	Range of LI	Median LI
1	Upstream Shell	SC-CL	8	-1.87 to 0.23	-0.47
2U	Upper Core	SC-GC-SM-CL	23	-0.53 to 0.23	-0.23
2L	Lower Core	CH-CL-MH-SM-CL	17	-0.79 to 0.12	-0.10
4	Downstream Shell	SC-GC-SP-CL-GM	23	-1.09 to -0.01	-0.38

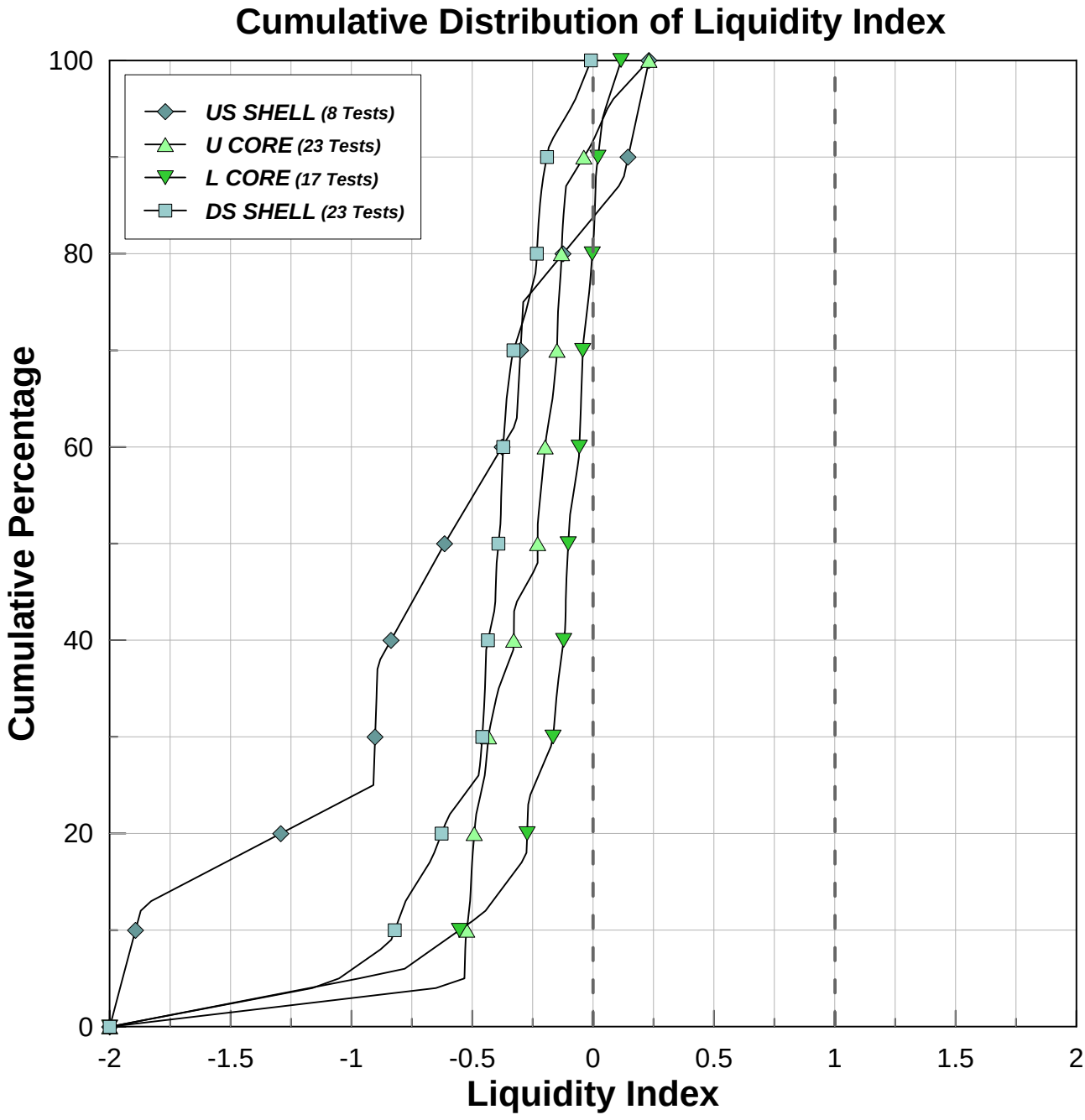

TERRA / GeoPentech
a Joint Venture

LIQUIDITY INDEX DISTRIBUTION
LENIHAN DAM
SEISMIC STABILITY EVALUATIONS (SSE2)

Figure
5-10

Rev. 0 11/21/2011 SSE2-R-3LN

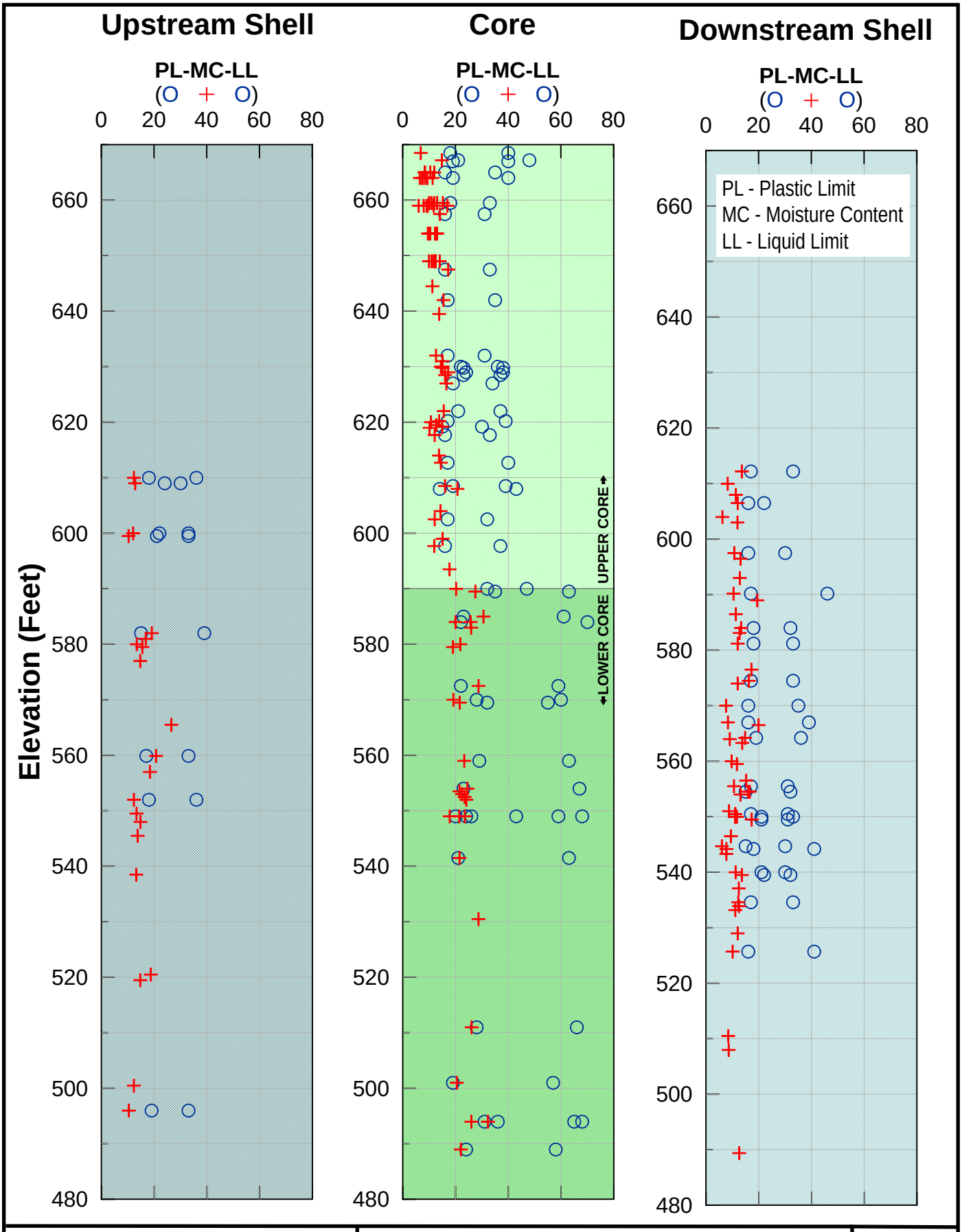

Rev. 1 12/08/2011 SSE2-R-3LN

TERRA / GeoPentech
a Joint Venture

WATER CONTENT AND ATTERBERG LIMITS
LENIHAN DAM
SEISMIC STABILITY EVALUATIONS (SSE2)

Figure
5-11

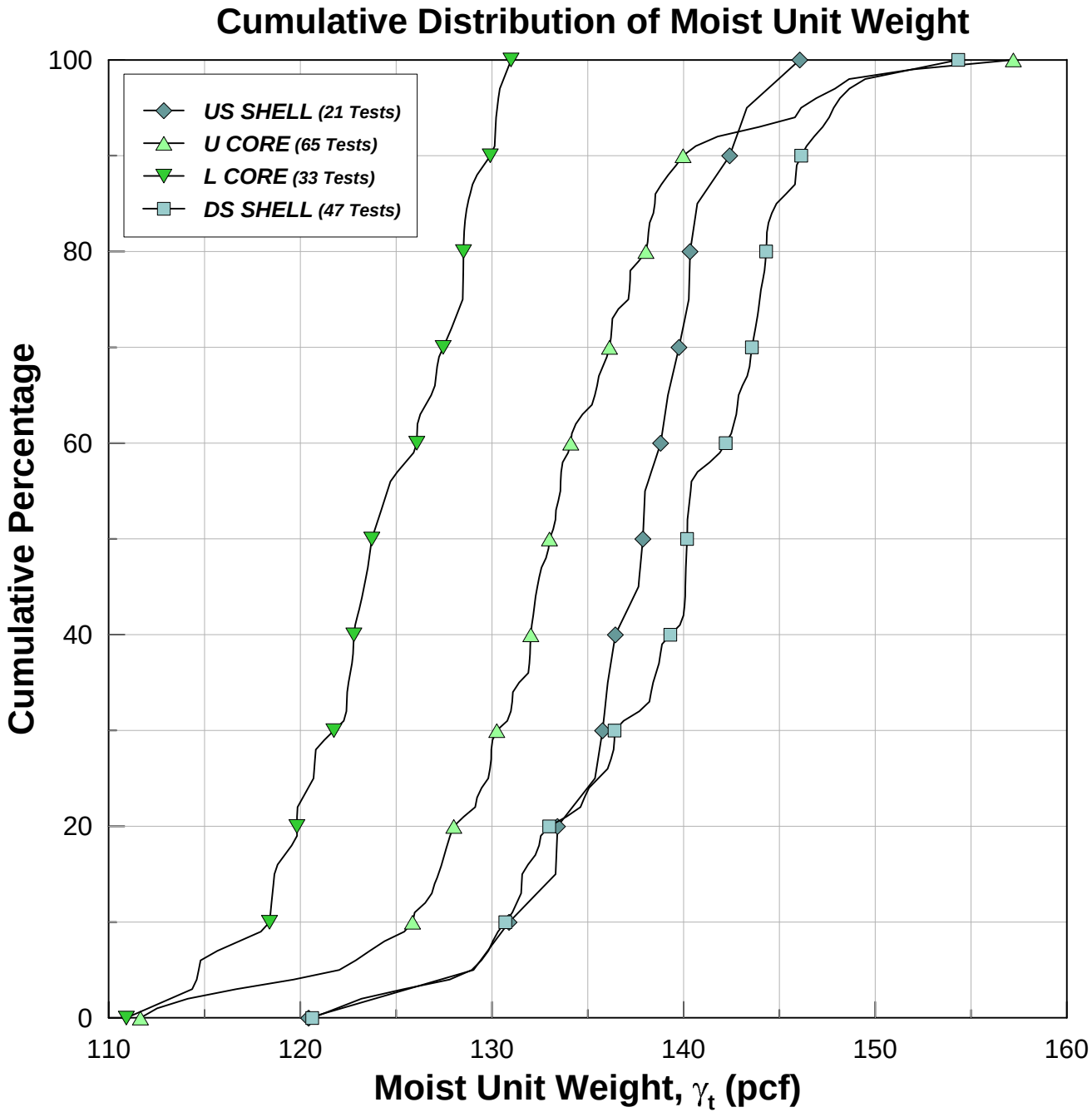

TERRA / GeoPentech a Joint Venture	TOTAL UNIT WEIGHT DATA LENIHAN DAM SEISMIC STABILITY EVALUATIONS (SSE2)	Figure 5-12

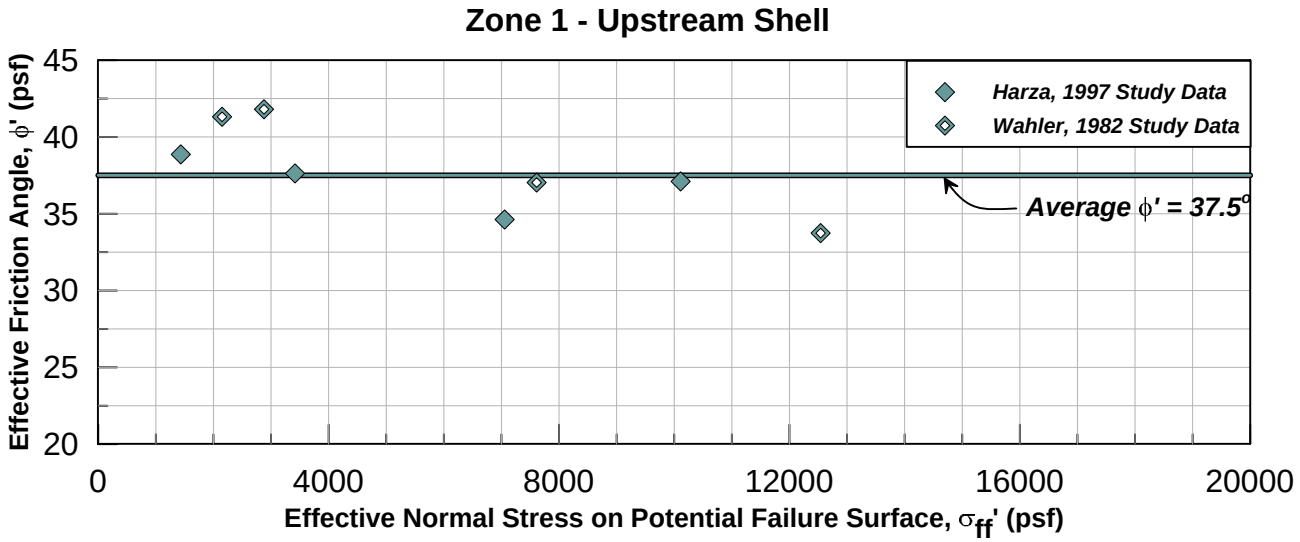
Zone 1 - Upstream Shell
Effective Friction Angle, ϕ' (psf)
45
40
35
30
25
20
0
4000
8000
12000
16000
20000
Effective Normal Stress on Potential Failure Surface, σff' (psf)
Harza, 1997 Study Data
Wahler, 1982 Study Data
Average ϕ' = 37.5°

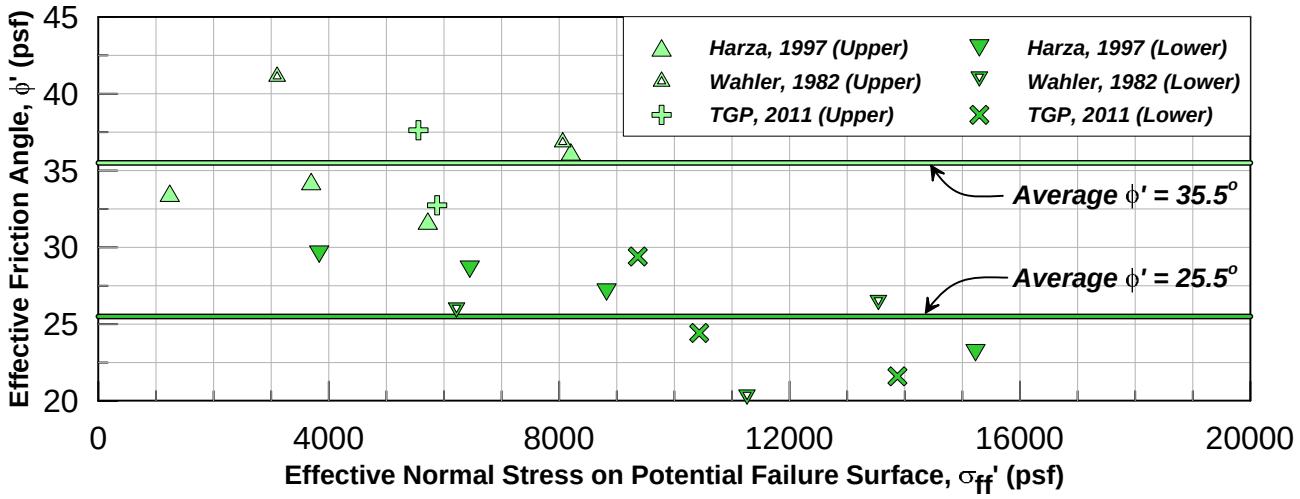
Zone 2U and 2L - Upper and Lower Core
Effective Friction Angle, ϕ' (psf)
45
40
35
30
25
20
0
4000
8000
12000
16000
20000
Effective Normal Stress on Potential Failure Surface, σff' (psf)
Harza, 1997 (Upper)
Wahler, 1982 (Upper)
TGP, 2011 (Upper)
Harza, 1997 (Lower)
Wahler, 1982 (Lower)
TGP, 2011 (Lower)
Average ϕ' = 35.5°
Average ϕ' = 25.5°

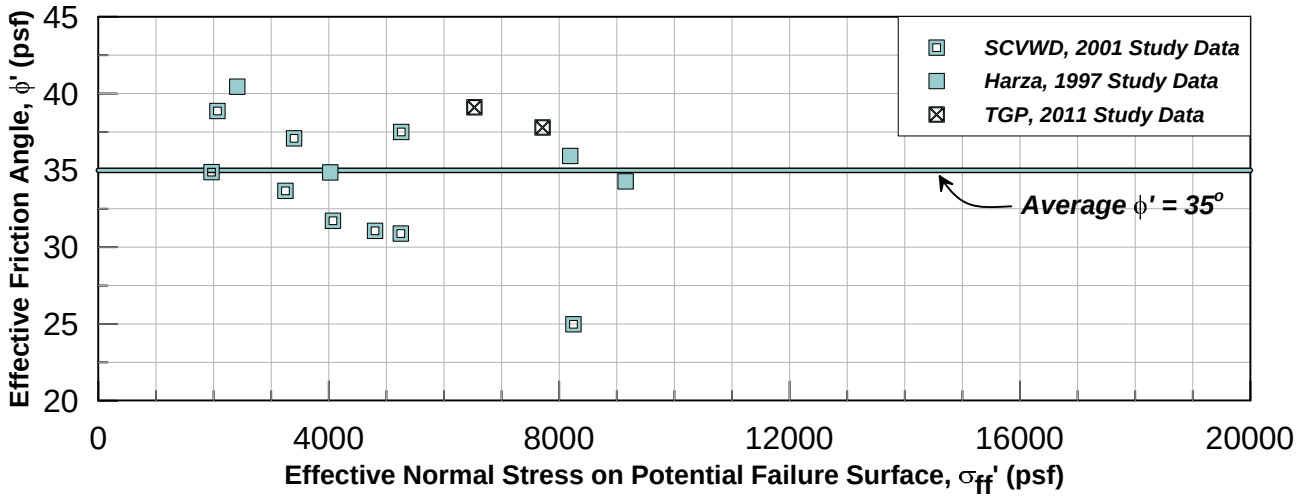
Zone 4 - Downstream Shell
Effective Friction Angle, ϕ' (psf)
45
40
35
30
25
20
0
4000
8000
12000
16000
20000
Effective Normal Stress on Potential Failure Surface, σff' (psf)
SCVWD, 2001 Study Data
Harza, 1997 Study Data
TGP, 2011 Study Data
Average ϕ' = 35°

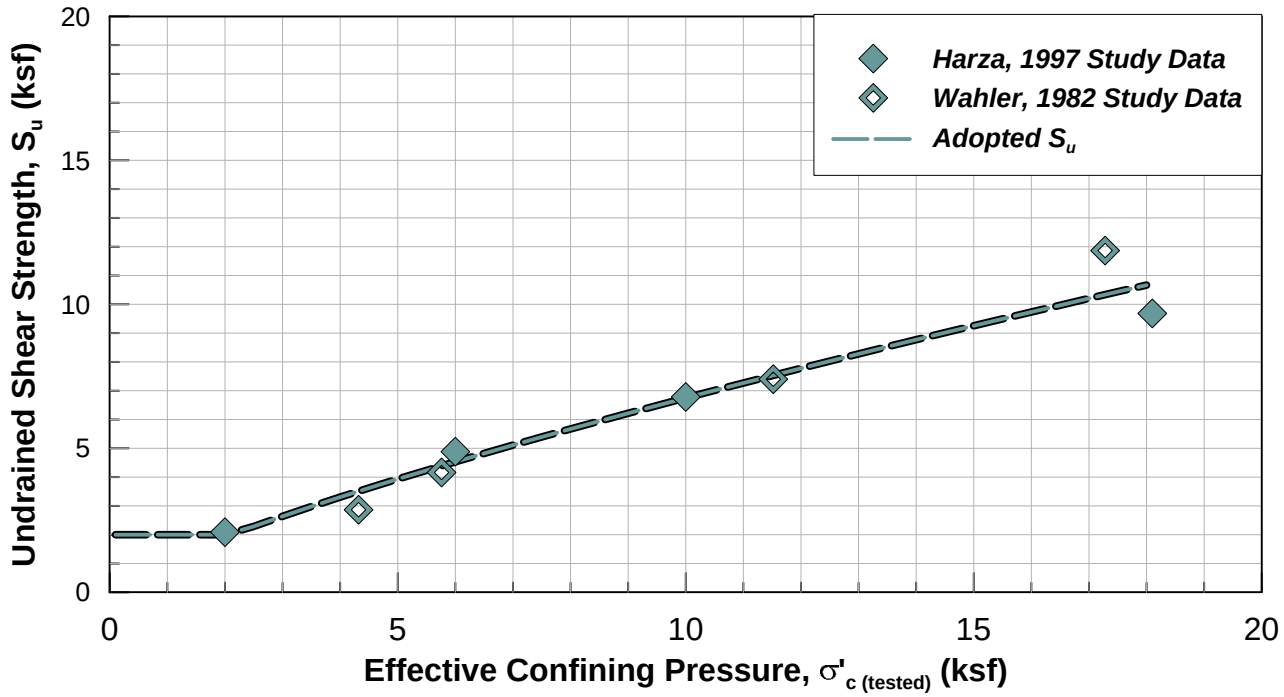

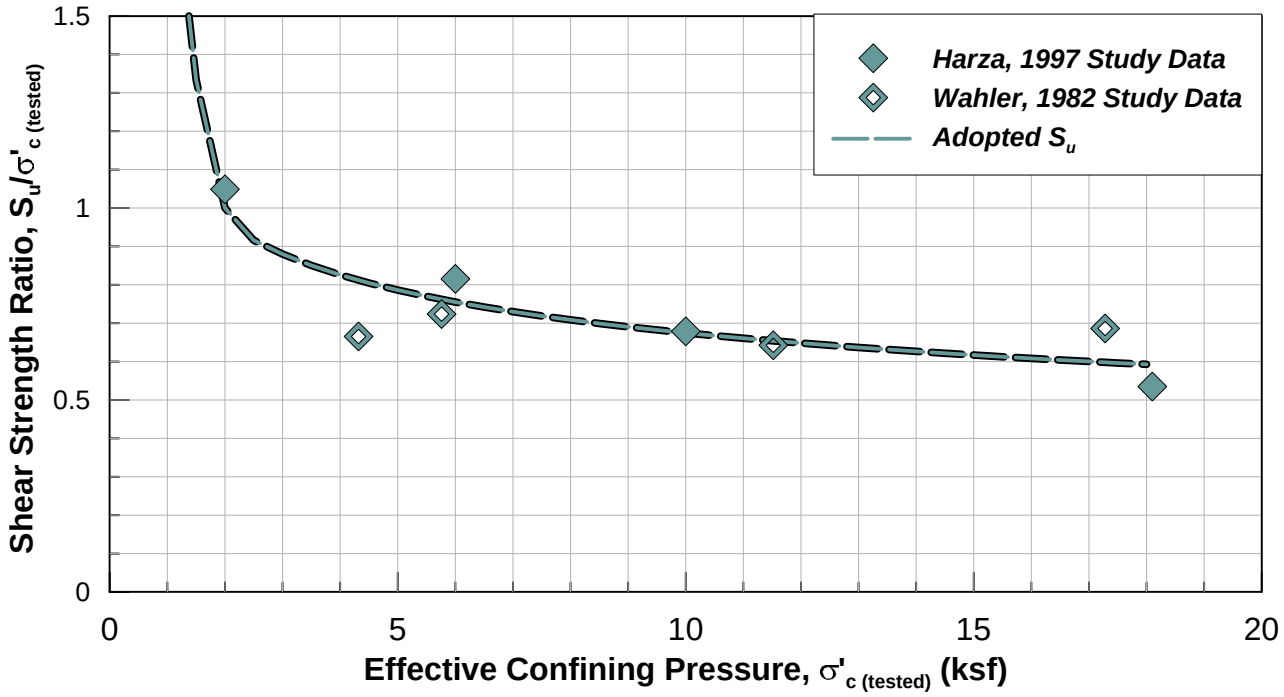

Note: All data from ICU'TXC Triaxial Tests

Adopted Parameter

$$S_u / \sigma_{vc}' = e^{[-0.22*\ln(\sigma_{vc}')+0.12]},\ S_u \geq 2.0\ ksf$$

TERRA / GeoPentech
a Joint Venture

UPSTREAM SHELL UNDRAINED STRENGTH
LENIHAN DAM
SEISMIC STABILITY EVALUATIONS (SSE2)

Figure
5-14

Rev. 1 12/08/2011 SSE2-R-3LN

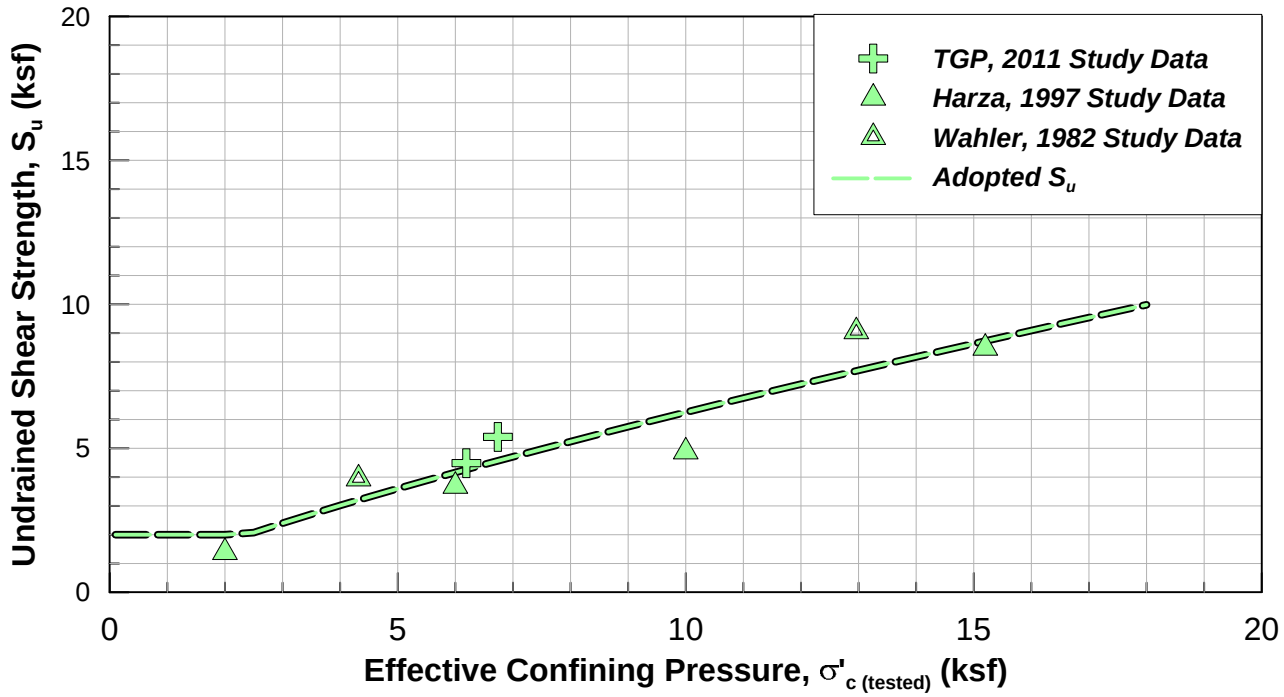

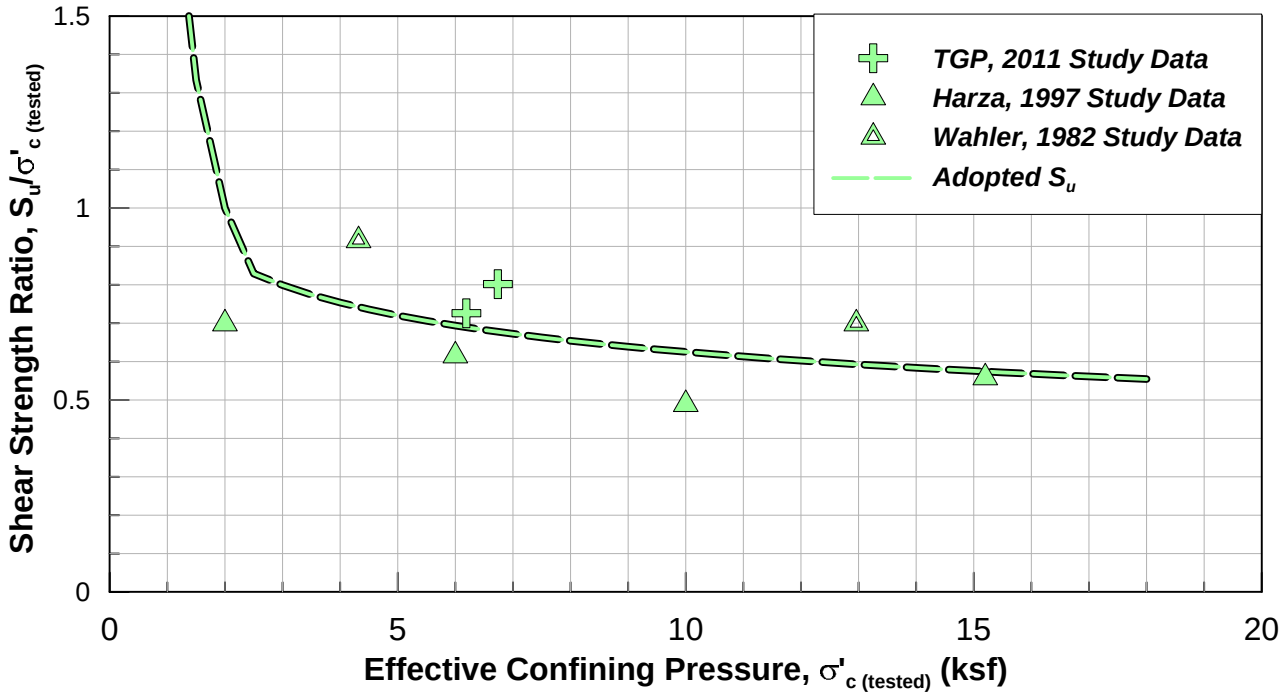

Note: All data from ICU'TXC Triaxial Tests

Adopted Parameter

$S_u / \sigma_{vc}' = e^{[-0.20*\ln(\sigma_{vc}')-0.01]}$, $S_u \geq 2.0$ ksf

TERRA / GeoPentech
a Joint Venture

UPPER CORE UNDRAINED STRENGTH
LENIHAN DAM
SEISMIC STABILITY EVALUATIONS (SSE2)

Figure
5-15

Rev. 1 12/08/2011 SSE2-R-3LN

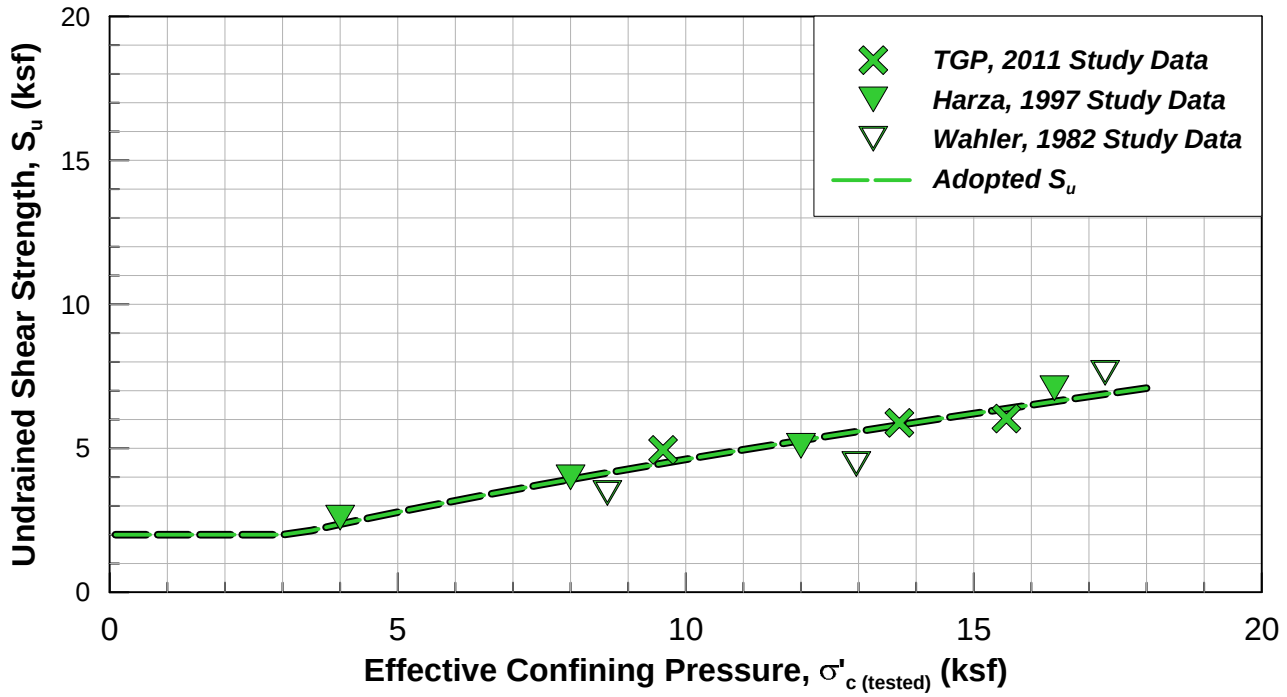

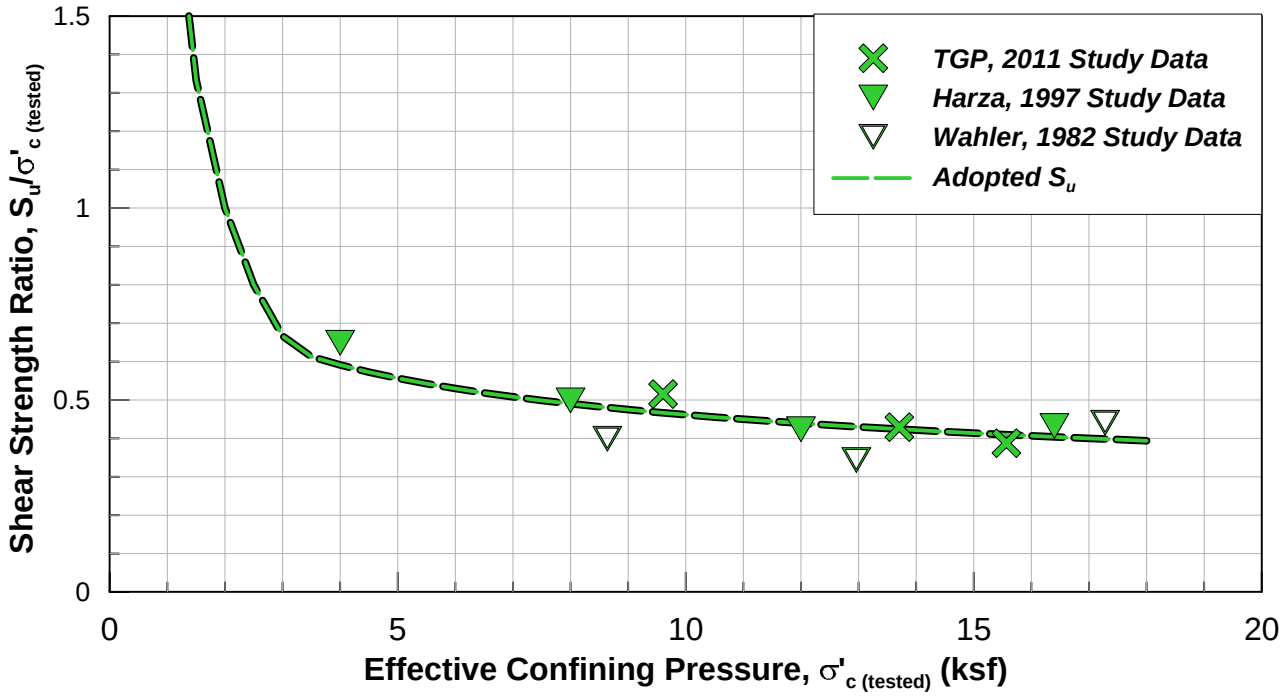

Note: All data from ICU'TXC Triaxial Tests

Adopted Parameter

$S_u / \sigma_{vc}' = e^{[-0.27*\ln(\sigma_{vc}')-0.15]}$, $S_u \geq 2.0$ ksf

TERRA / GeoPentech
a Joint Venture

LOWER CORE UNDRAINED STRENGTH
LENIHAN DAM
SEISMIC STABILITY EVALUATIONS (SSE2)

Figure
5-16

Rev. 1 12/08/2011 SSE2-R-3LN

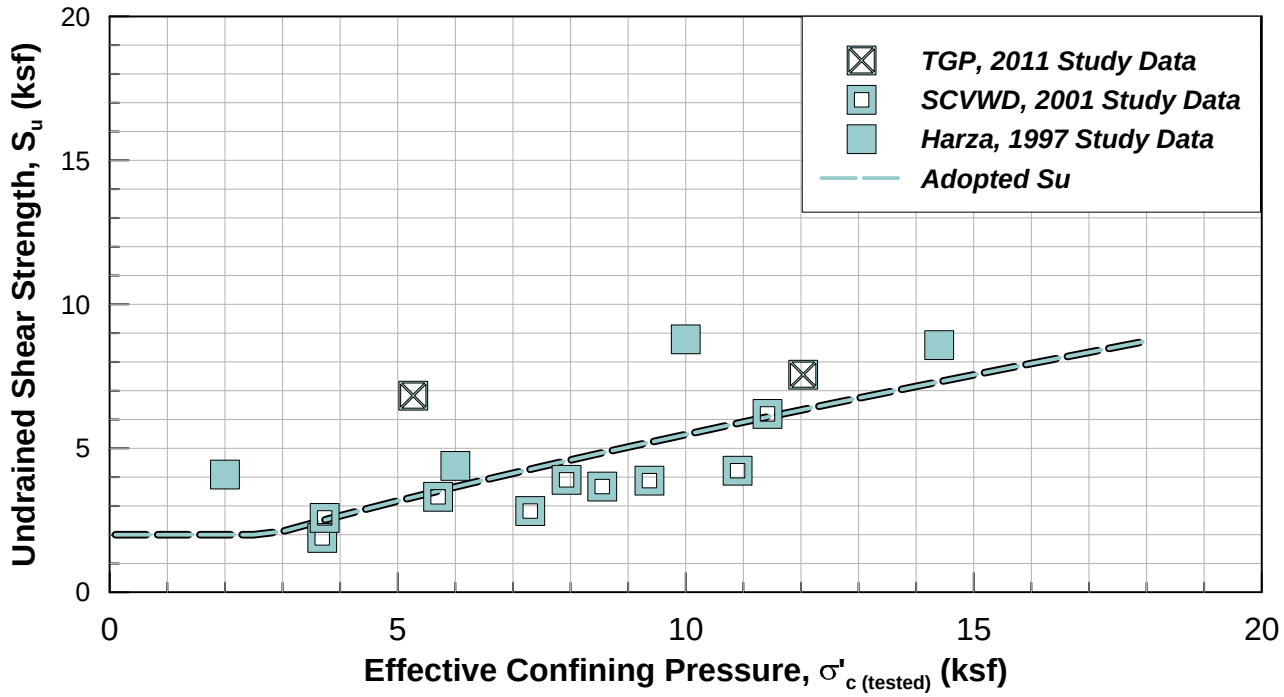

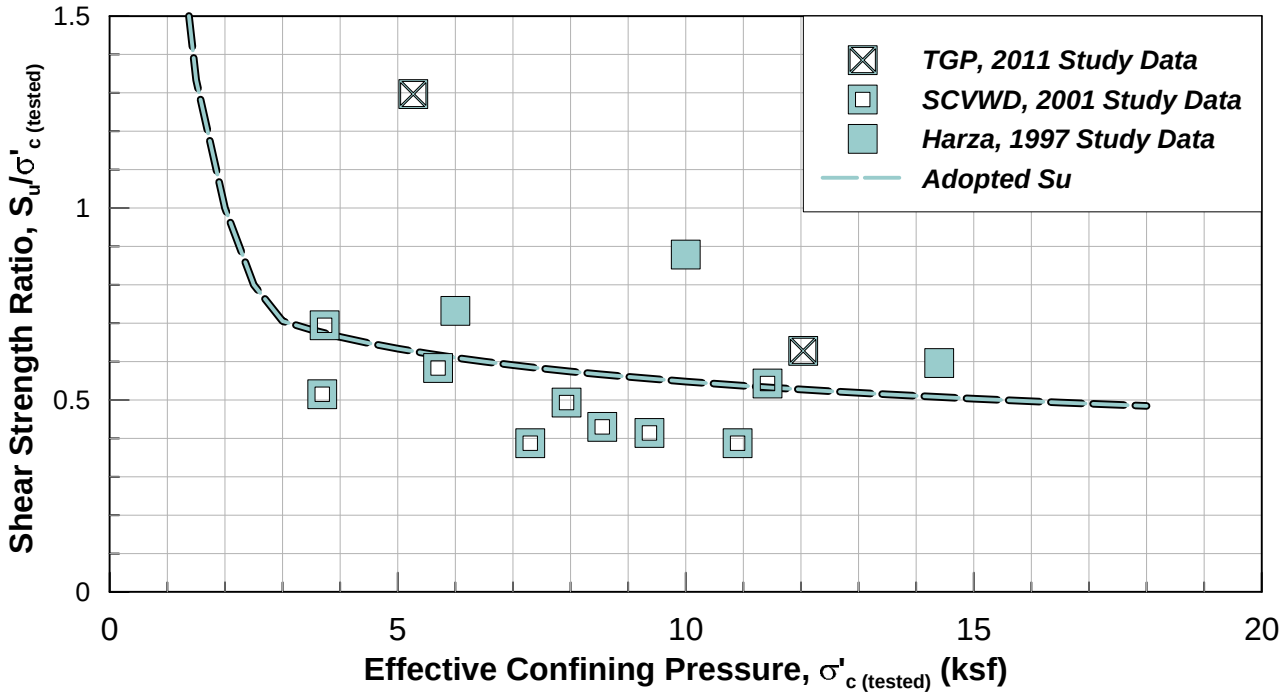

Note: All data from ICU'TXC Triaxial Tests

Adopted Parameter

$S_u / \sigma_{vc}' = e^{[-0.21*\ln(\sigma_{vc}')-0.12]}$, $S_u \geq 2.0$ ksf

TERRA / GeoPentech
a Joint Venture

DOWNSTREAM SHELL UNDRAINED STRENGTH
LENIHAN DAM
SEISMIC STABILITY EVALUATIONS (SSE2)

Figure
5-17

Rev. 1 12/08/2011 SSE2-R-3LN

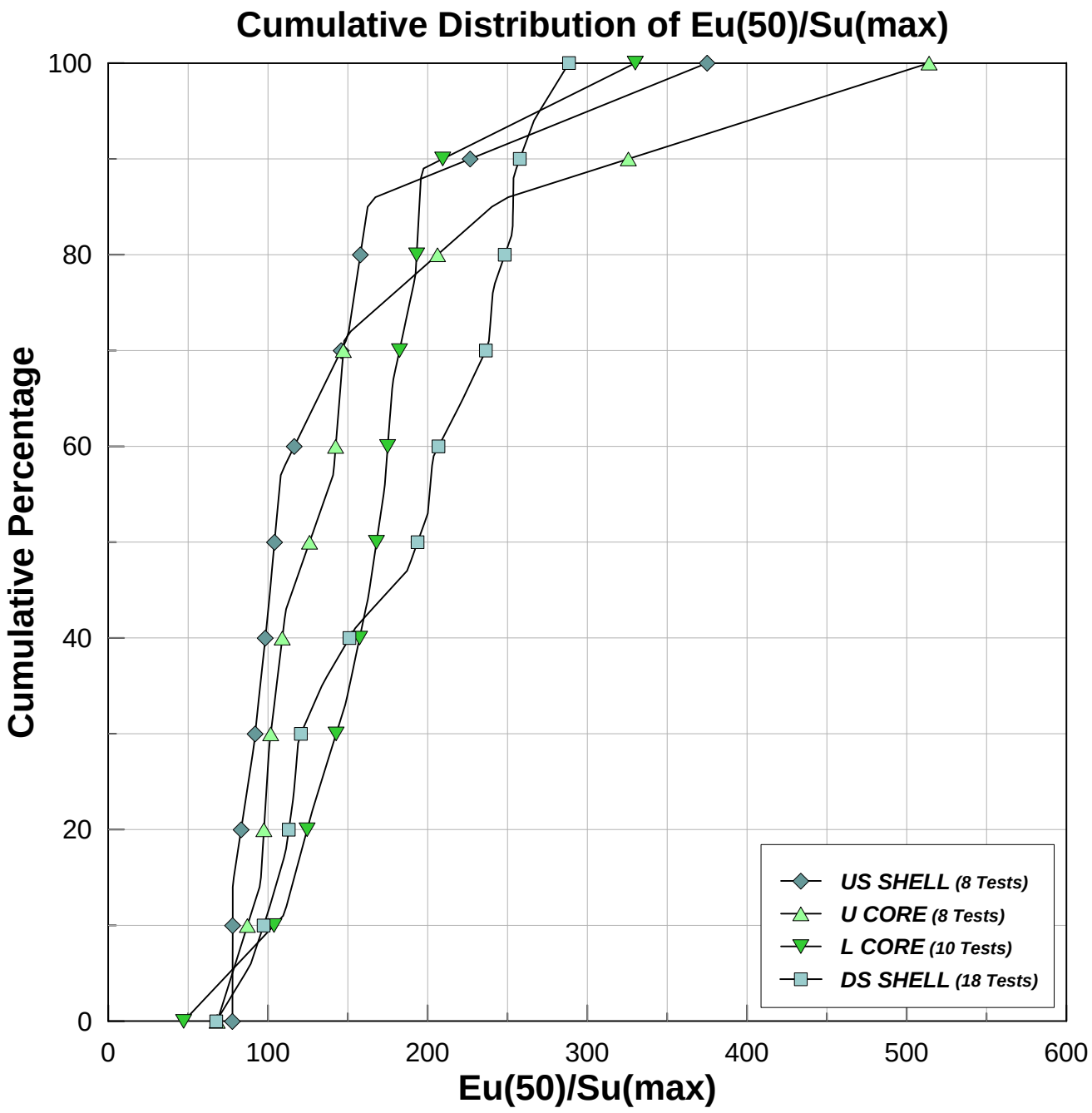

TERRA / GeoPentech
a Joint Venture

DISTRIBUTION OF E_{u50} / S_u
LENIHAN DAM
SEISMIC STABILITY EVALUATIONS (SSE2)

Figure
5-18

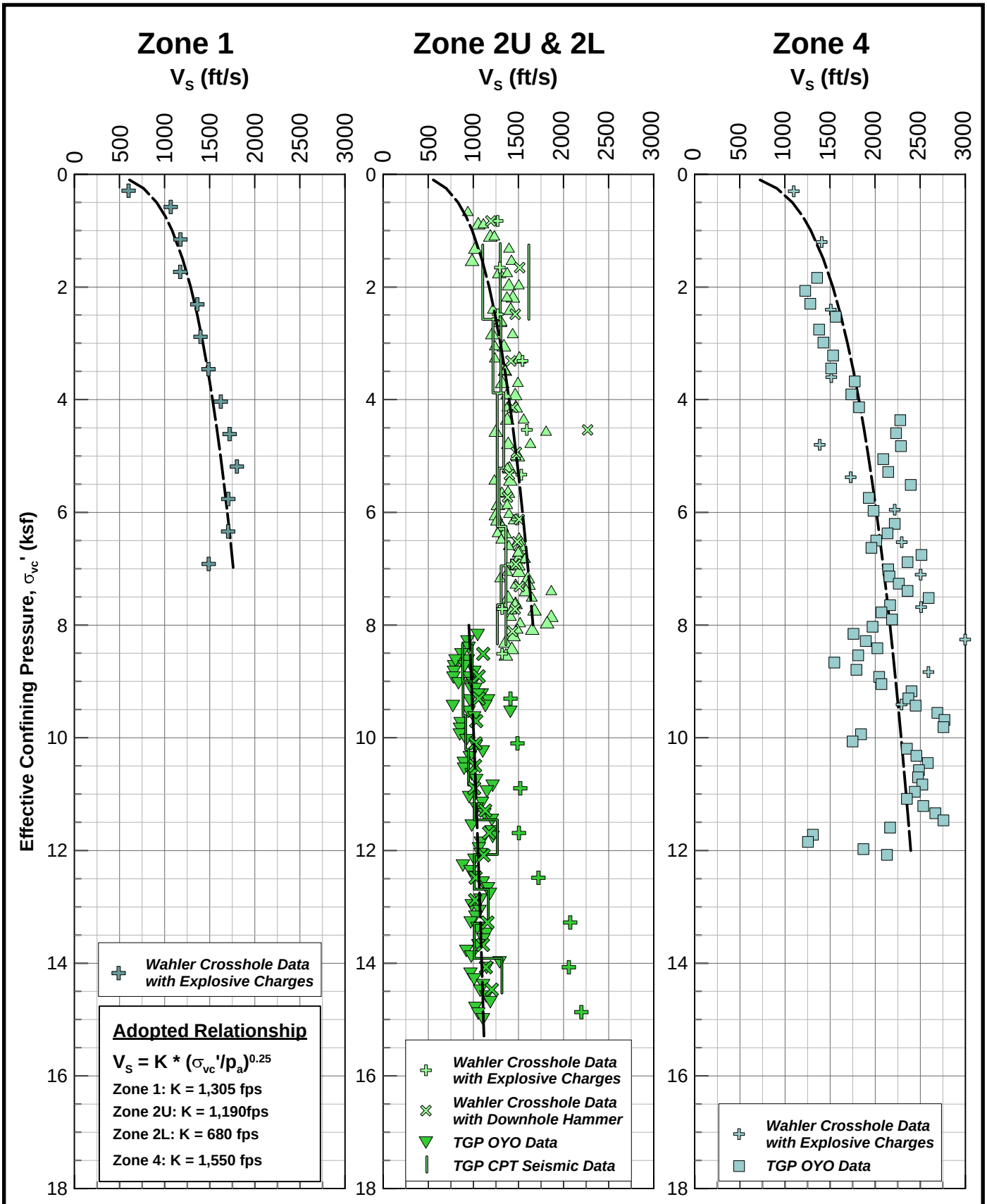

TERRA / GeoPentech
a Joint Venture

SHEAR WAVE VELOCITY DATA
LENIHAN DAM
SEISMIC STABILITY EVALUATIONS (SSE2)

Figure
5-19

Rev. 1 12/08/2011 SSE2-R-3LN

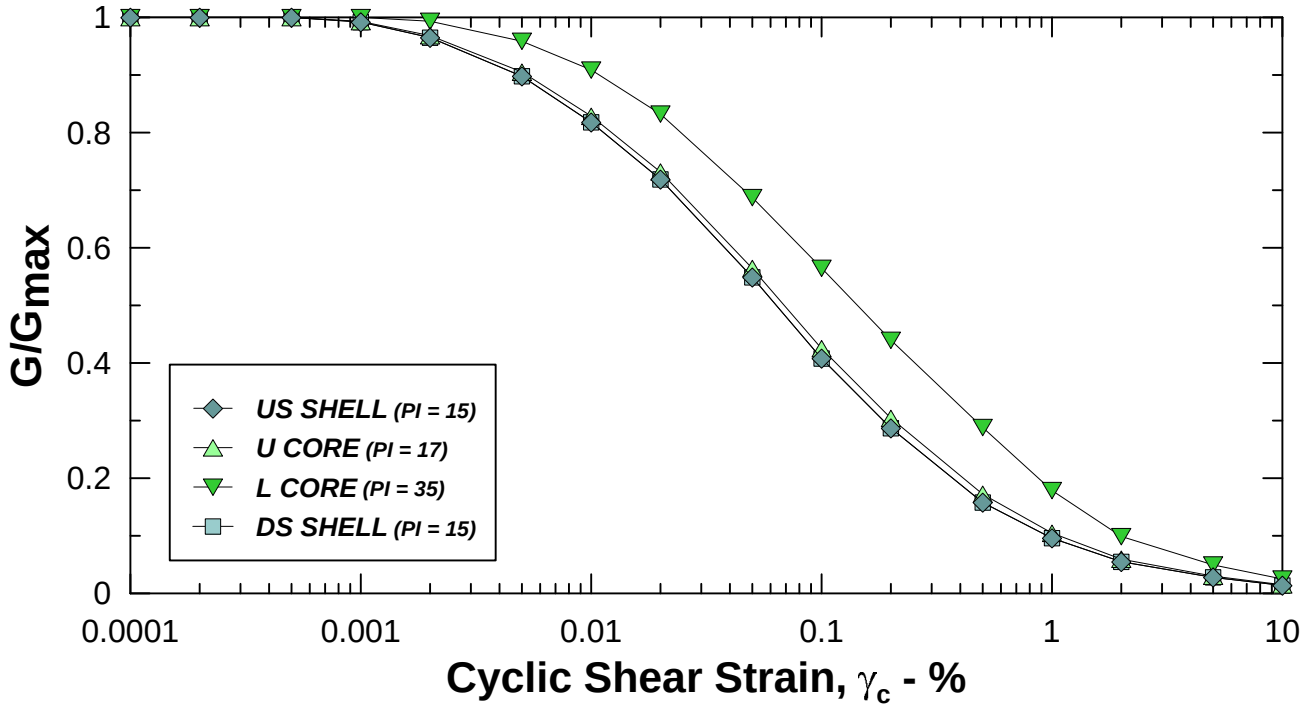

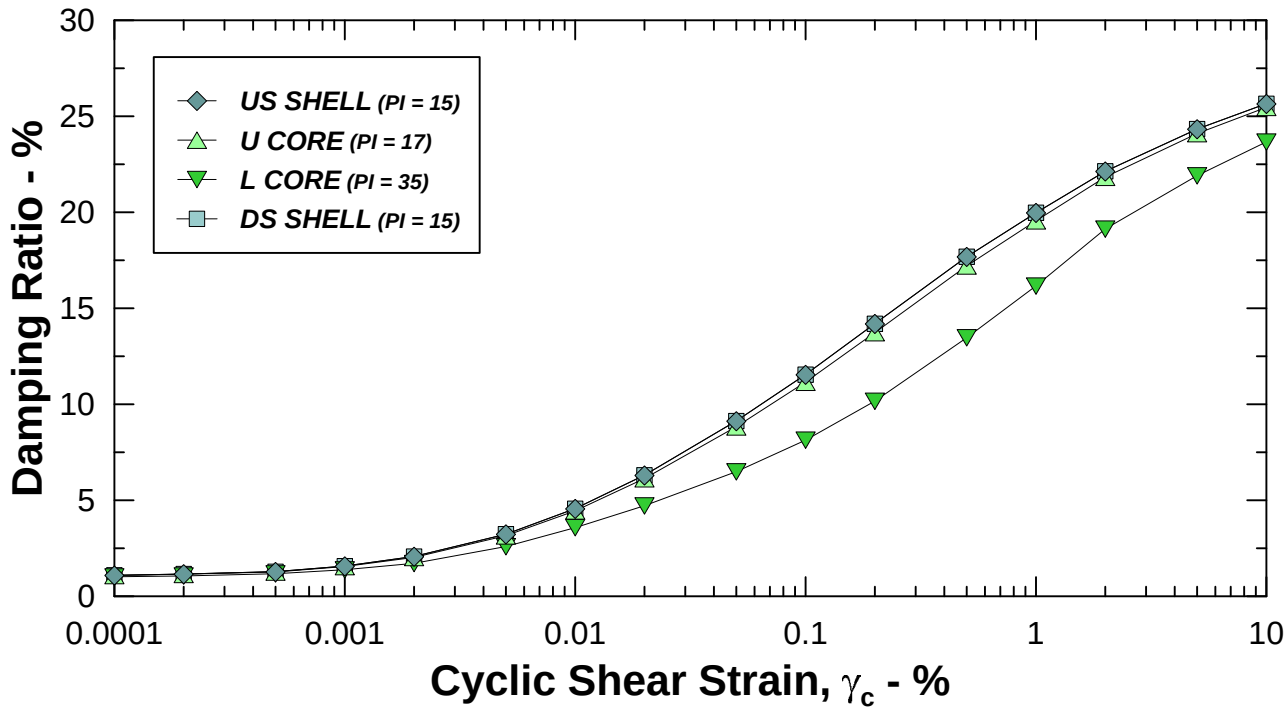

Note: Modulus reduction and damping ratio curves are based on Vucetic and Dobry, 1991

TERRA / GeoPentech a Joint Venture	MODULUS REDUCTION AND DAMPING RATIO CURVES - LENIHAN DAM SEISMIC STABILITY EVALUATIONS (SSE2)	Figure 5-20

TERRA / GeoPentech
a Joint Venture

PLAN LOCATIONS OF SHEAR WAVE VELOCITY MESUREMENTS IN ROCK - LENIHAN DAM
SEISMIC STABILITY EVALUATIONS (SSE2)

Figure
6-1

Rev. 0 11/21/2011 SSE2-R-3LN

Dam Crest Section

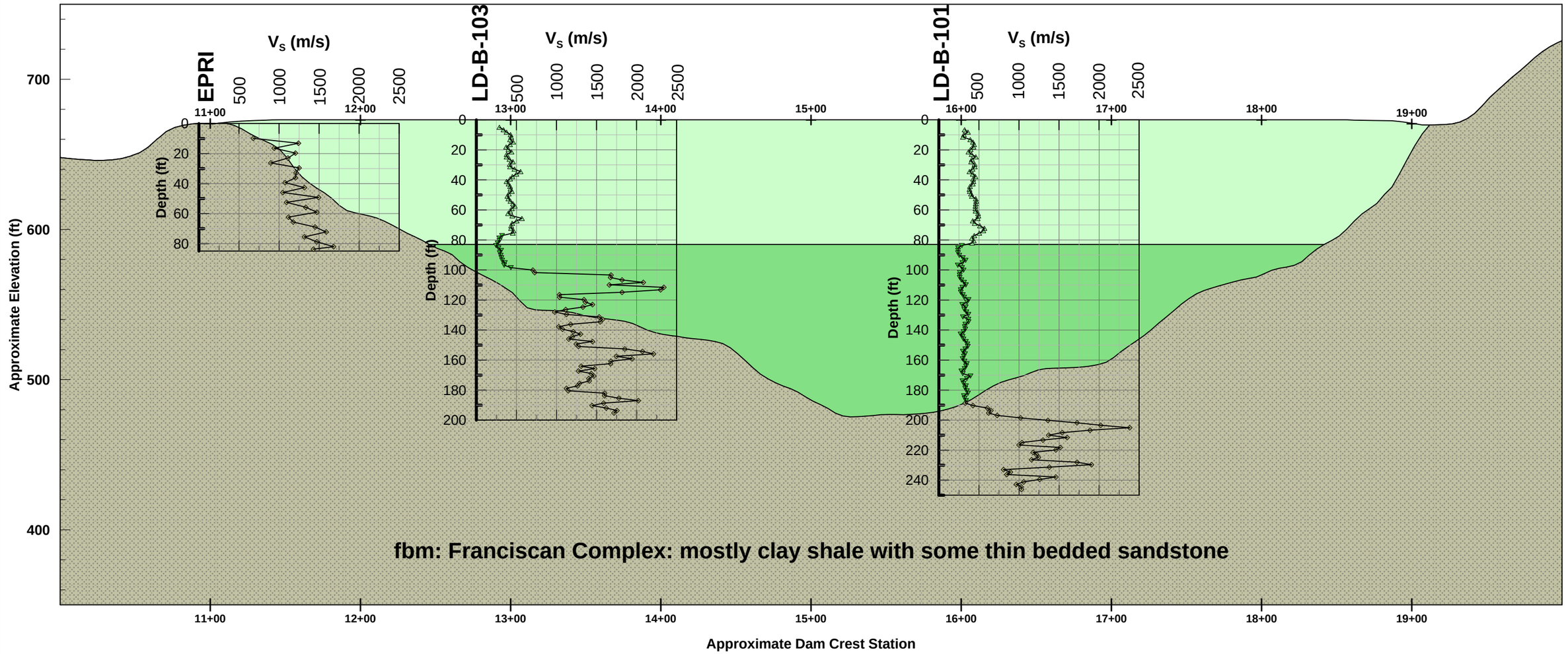

KEY:

- Upper Core
- Lower Core
- Foundation/Franciscan Complex

TERRA / GeoPentech
a Joint Venture

SHEAR WAVE VELOCITY PROFILES
LENIHAN DAM
SEISMIC STABILITY EVALUATIONS (SSE2)

Figure
6-2

Rev. 0 11/22/2011 SSE2-R-3LN

LD-B-101 (Bedrock Only)

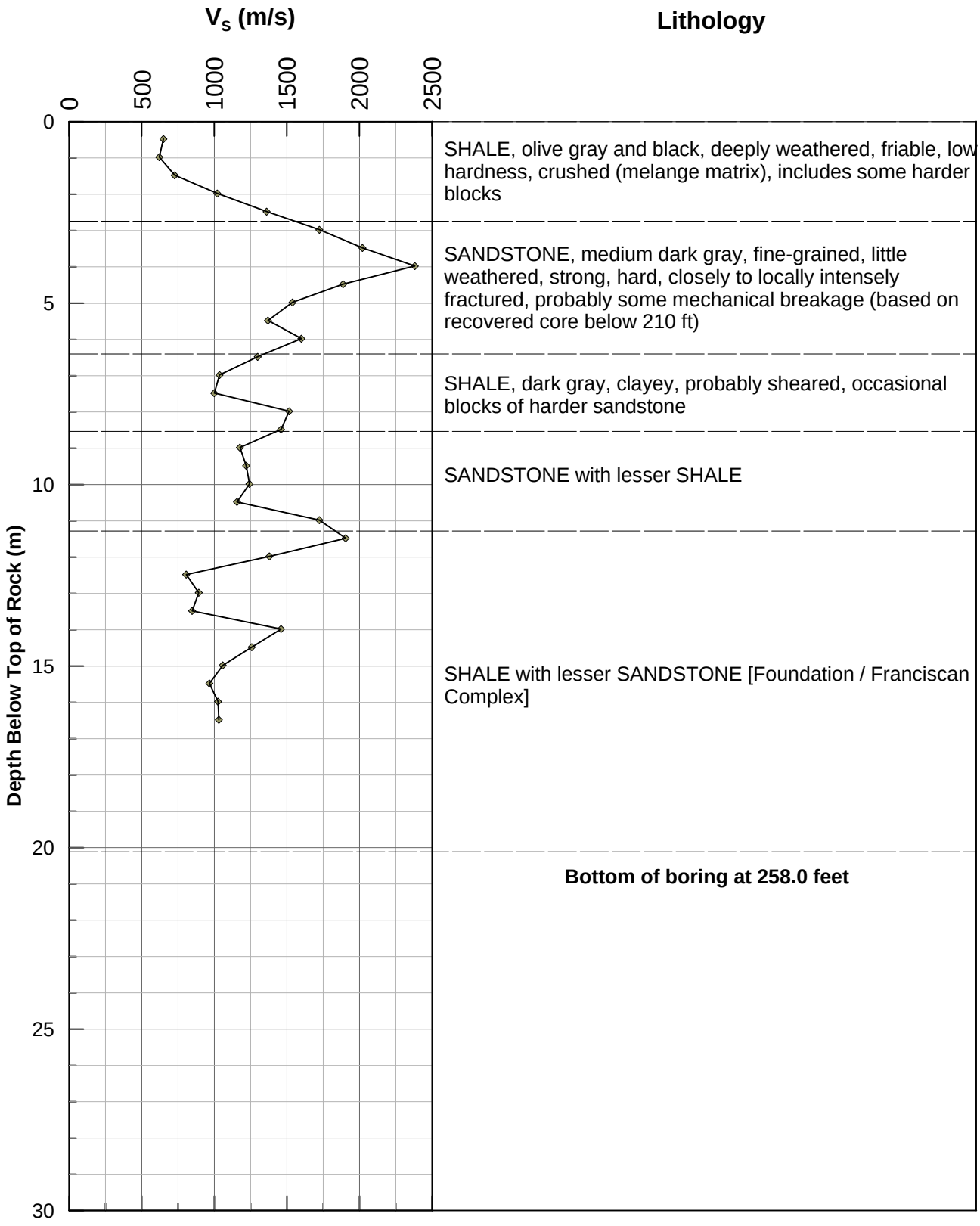

TERRA / GeoPentech
a Joint Venture

SHEAR WAVE VELOCITY LD-B-101
LENIHAN DAM
SEISMIC STABILITY EVALUATIONS (SSE2)

Figure
6-3

LD-B-103 (Bedrock Only)

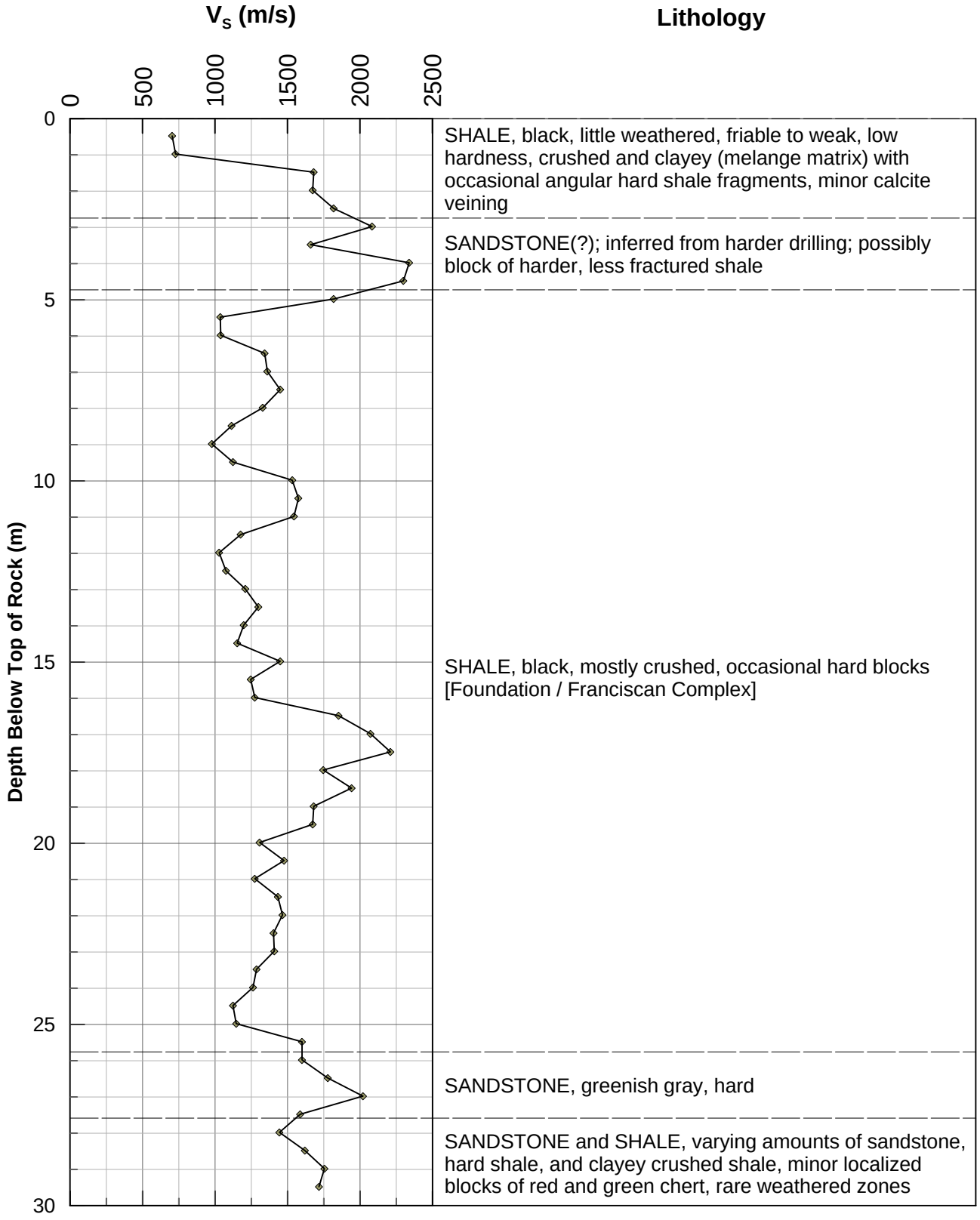

TERRA / GeoPentech
a Joint Venture

SHEAR WAVE VELOCITY LD-B-103
LENIHAN DAM
SEISMIC STABILITY EVALUATIONS (SSE2)

Figure
6-4

Rev. 0 11/22/2011 SSE2-R-3LN

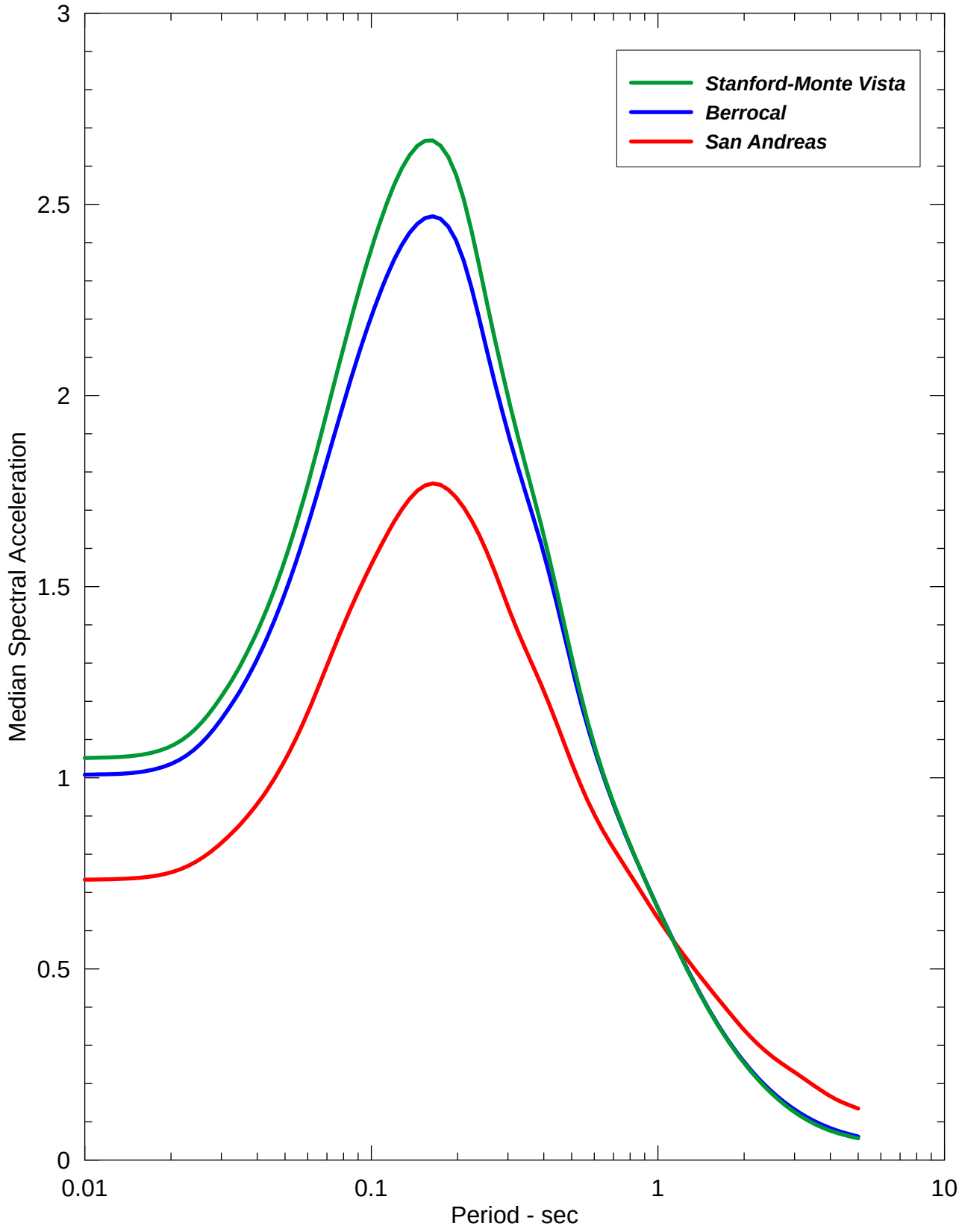

TERRA / GeoPentech
a Joint Venture

FAULT PARALLEL (FP) RESPONSE SPECTRA
LENIHAN DAM
SEISMIC STABILITY EVALUATIONS (SSE2)

Figure
6-5

Rev. 1 12/08/2011 SSE2-R-3LN

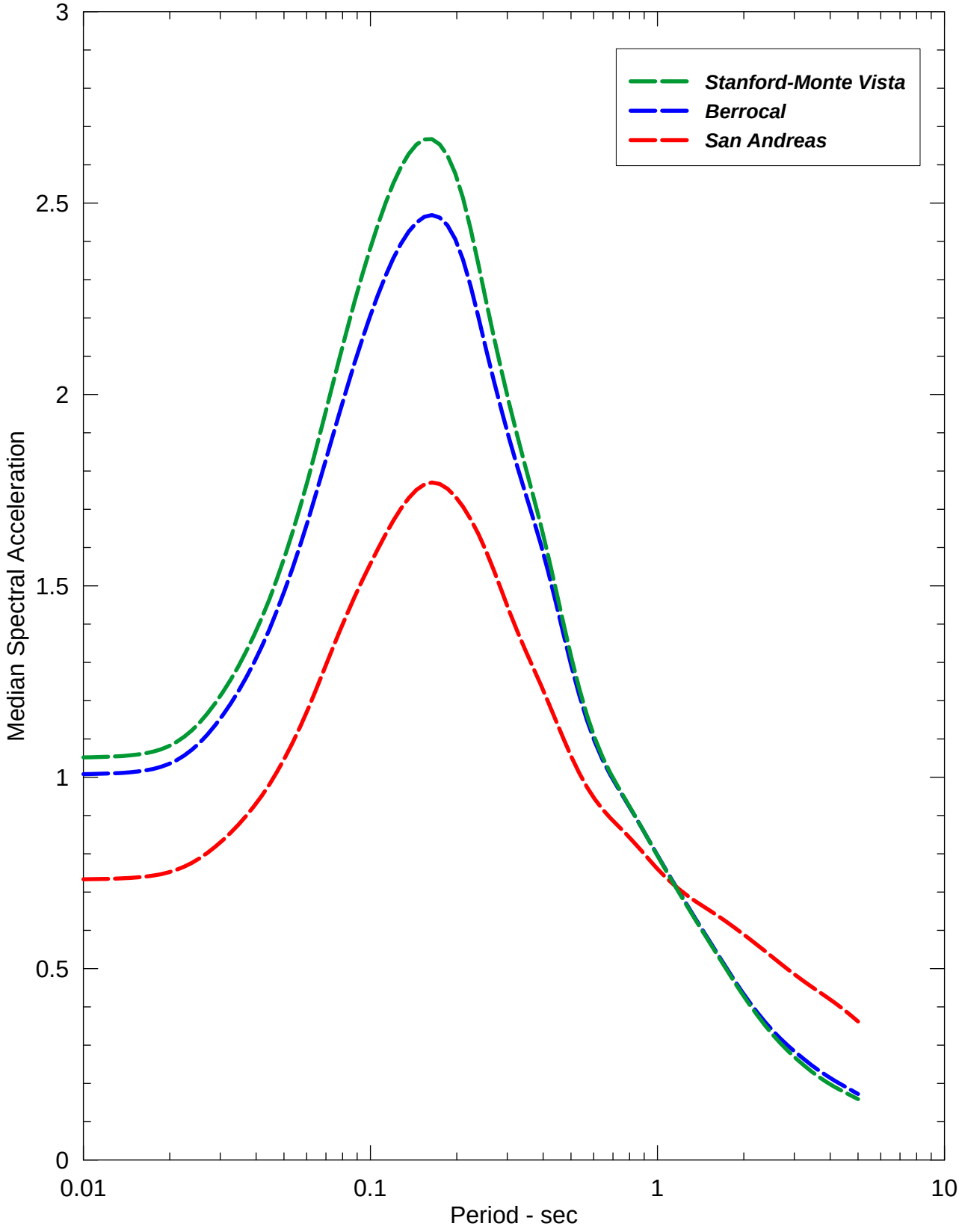

TERRA / GeoPentech
a Joint Venture

FAULT NORMAL (FN) RESPONSE SPECTRA
LENIHAN DAM
SEISMIC STABILITY EVALUATIONS (SSE2)

Figure
6-6

Rev. 1 12/08/2011 SSE2-R-3LN

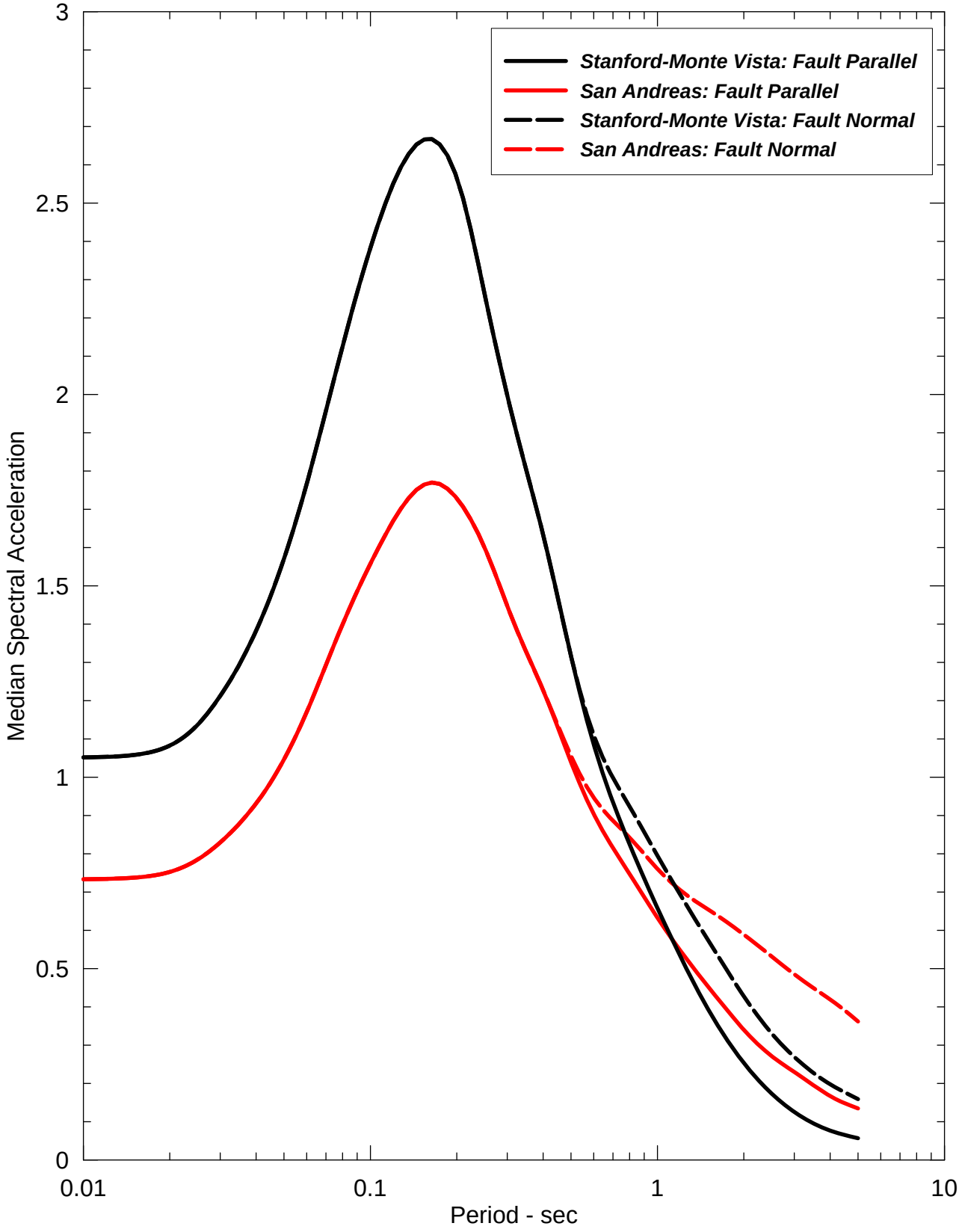

TERRA / GeoPentech
a Joint Venture

RECOMMENDED RESPONSE SPECTRA
LENIHAN DAM
SEISMIC STABILITY EVALUATIONS (SSE2)

Figure
6-7

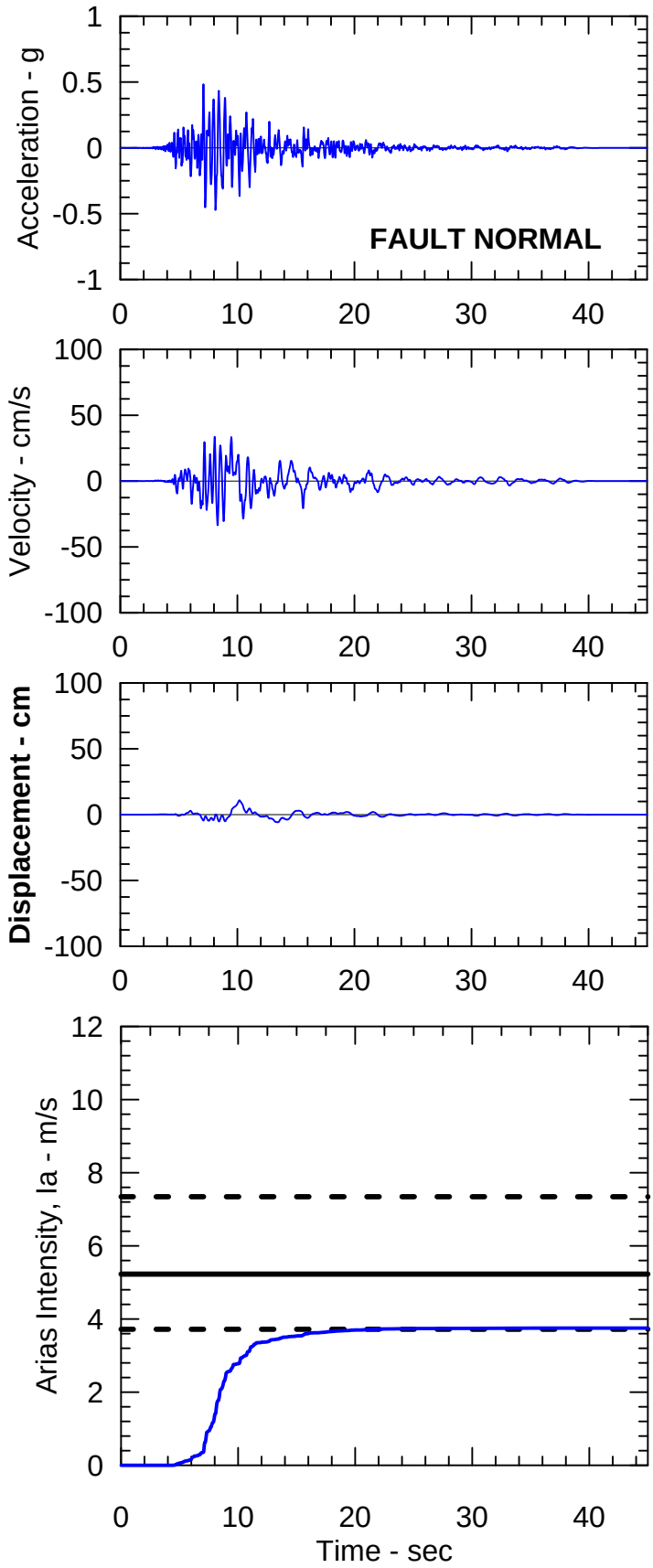

Kobe - Nishi-Akashi
Strike Slip Event
Rotated to Fault Normal

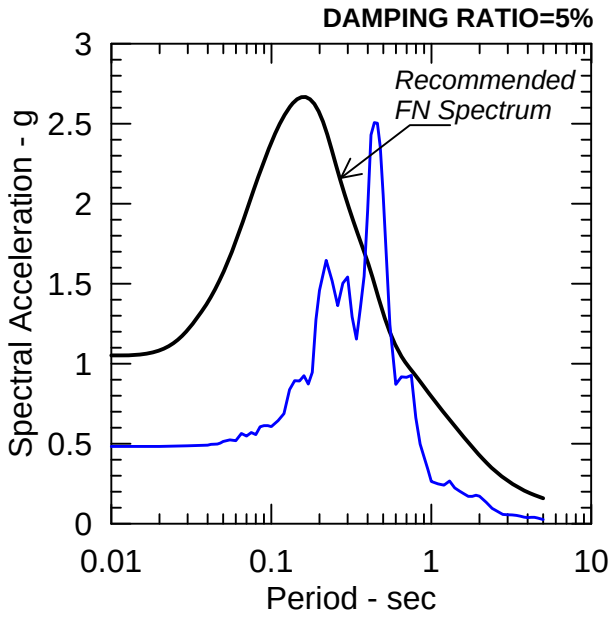

Rev. 1 12/08/2011 SSE2-R-3LN

TERRA / GeoPentech
a Joint Venture

CHARACTERISTICS OF KOBE E/Q,
NISHI-AKASHI (FN) RECORD
SEISMIC STABILITY EVALUATIONS (SSE2)

Figure
6-8

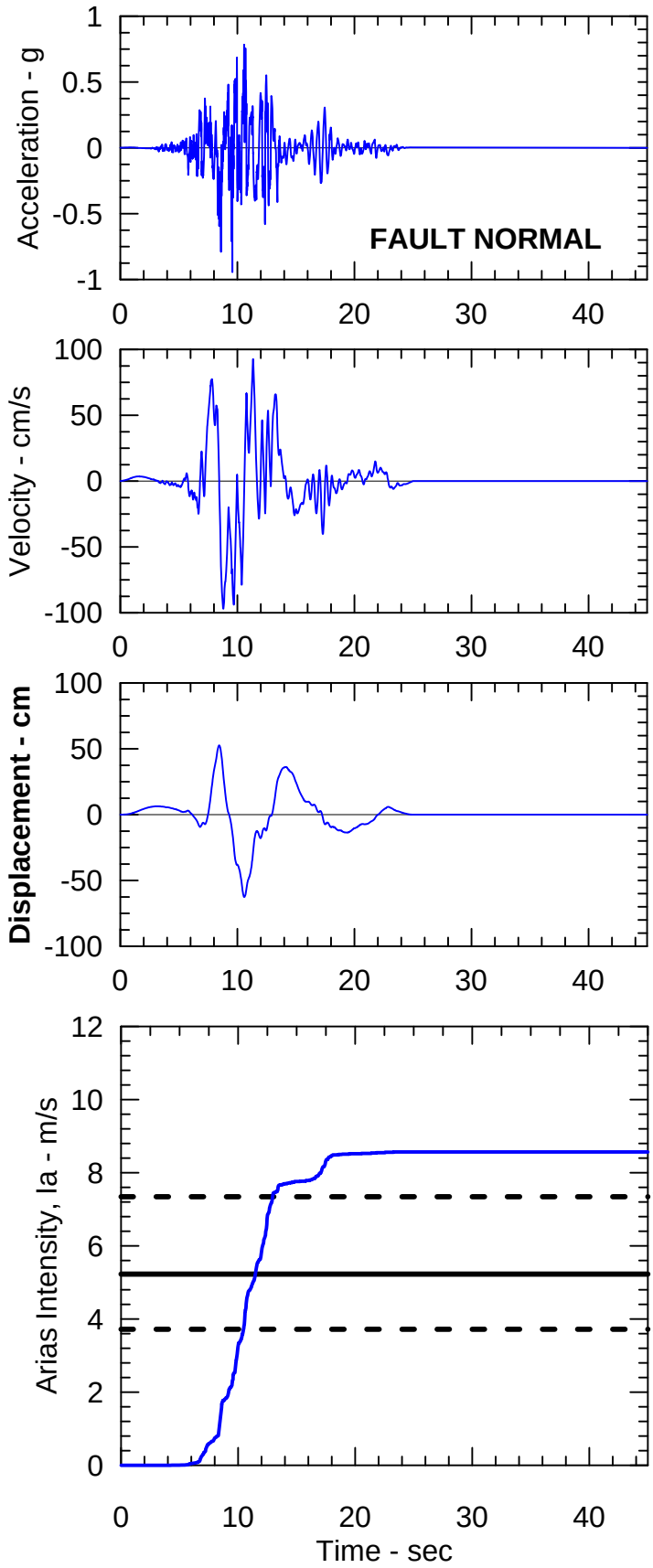

Loma Prieta - LGPC
Reverse Oblique Event
Rotated to Fault Normal

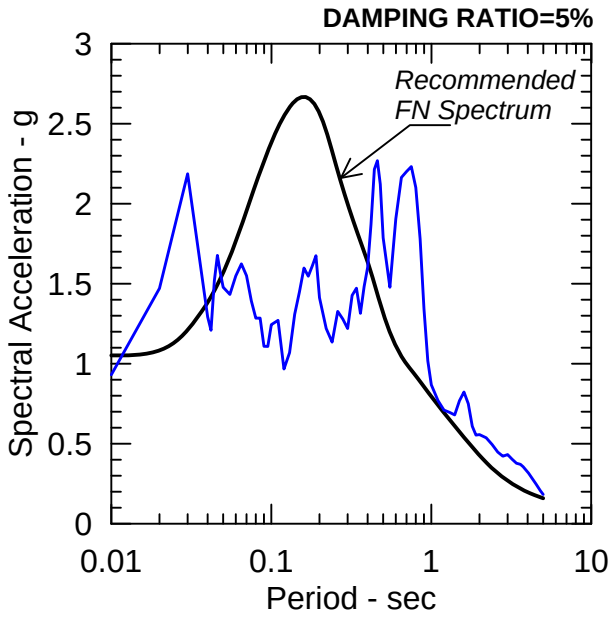

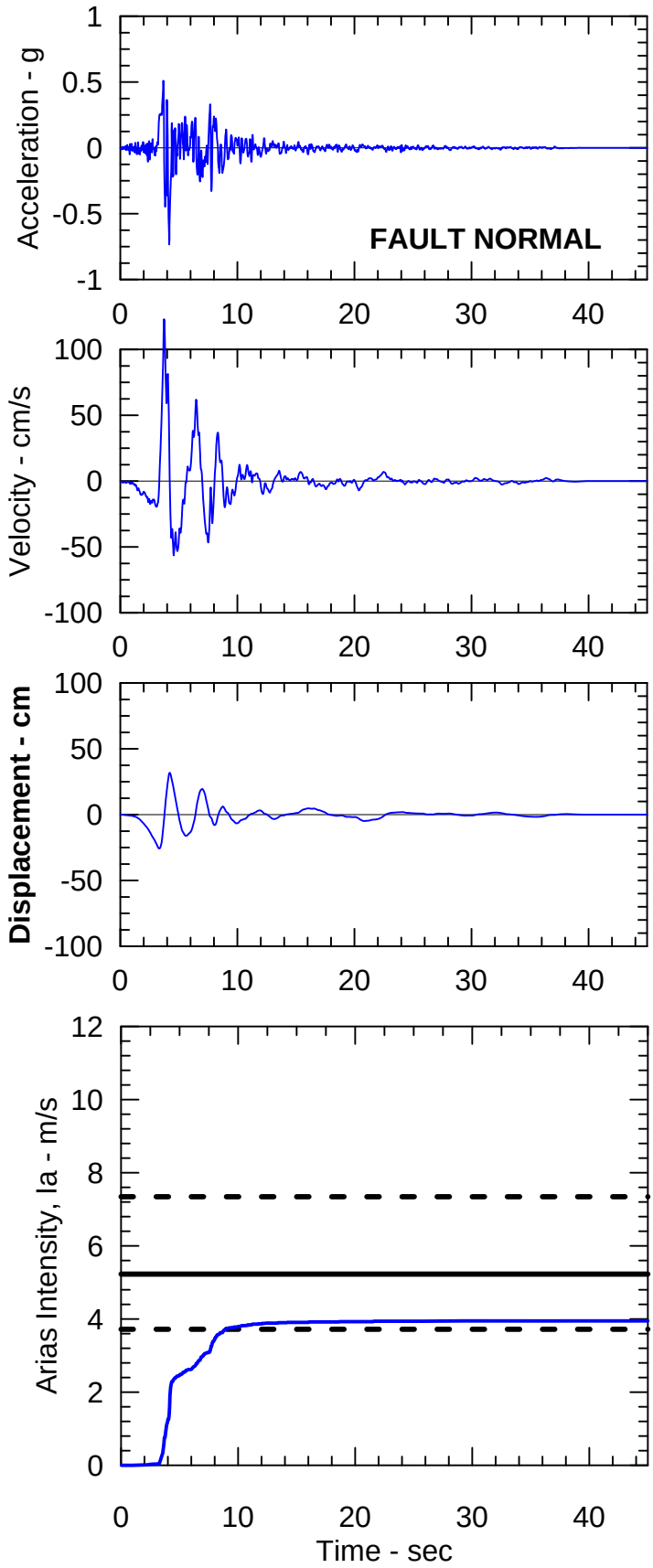

Northrigde - Sylmar
Reverse Event
Rotated to Fault Normal

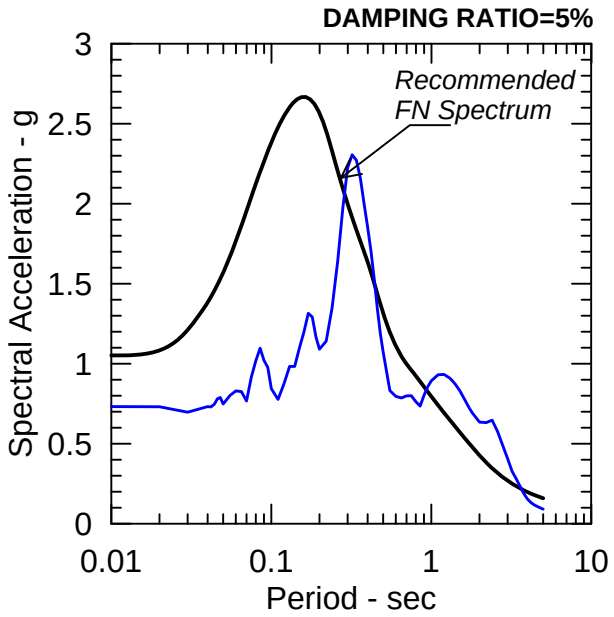

Rev. 1 12/08/2011 SSE2-R-3LN

TERRA / GeoPentech
a Joint Venture

CHARACTERISTICS OF NORTHRIDGE E/Q, SYLMAR (FN) RECORD
SEISMIC STABILITY EVALUATIONS (SSE2)

Figure
6-10

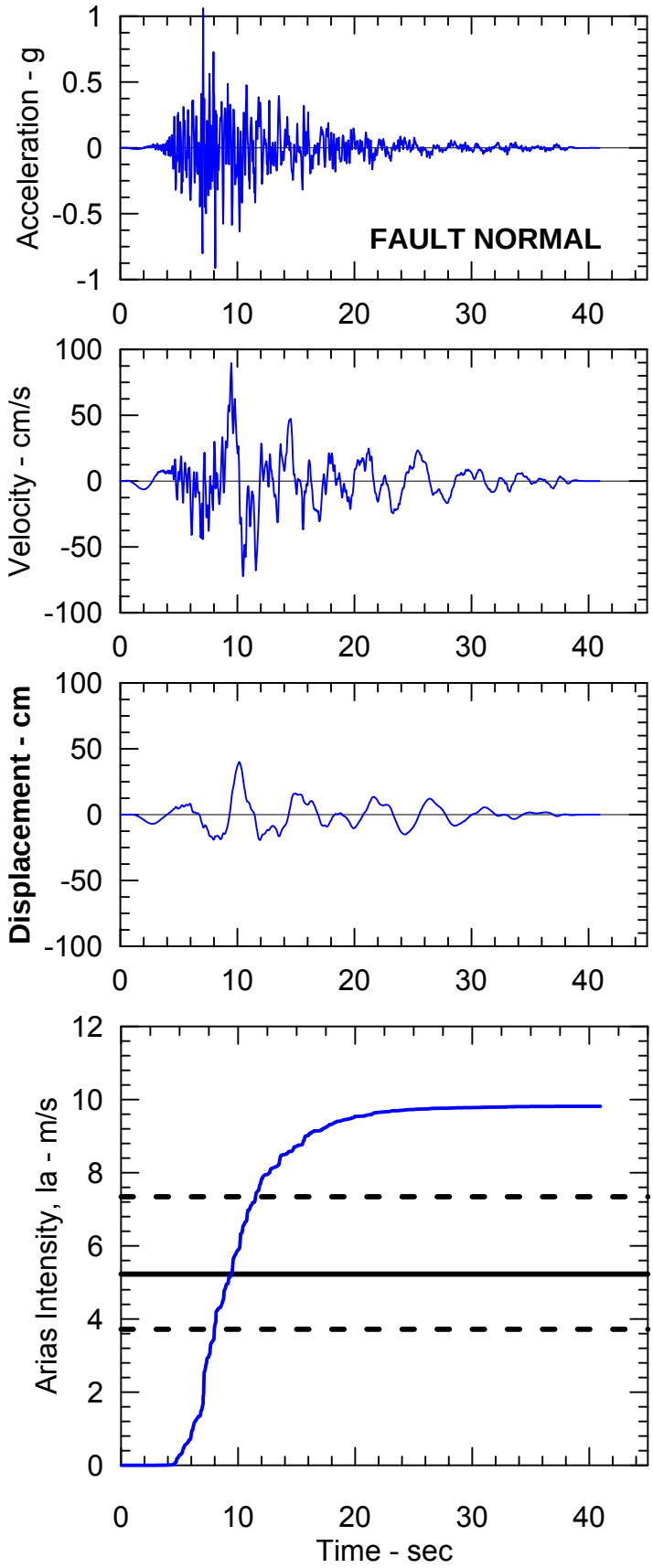

Kobe - Nishi-Akashi
Strike Slip Event
Rotated to Fault Normal
Spectrally Matched to SMV

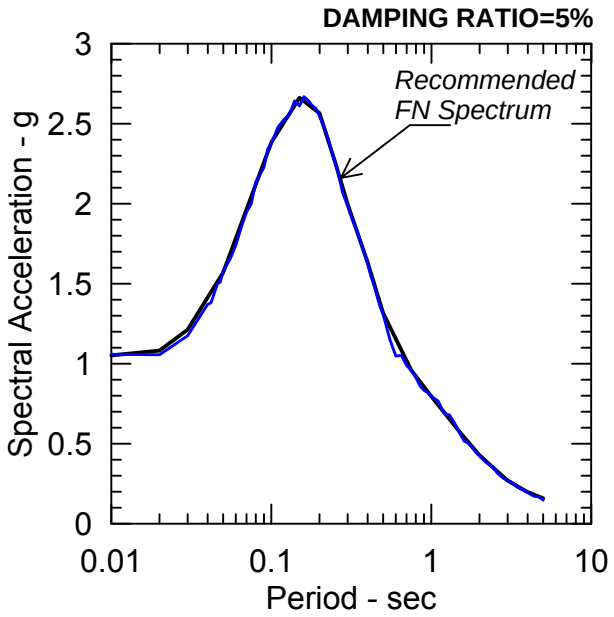

TERRA / GeoPentech a Joint Venture	CHARACTERISTICS OF KOBE E/Q, NISHI-AKASHI (FN) MATCHED RECORD SEISMIC STABILITY EVALUATIONS (SSE2)	Figure 6-11

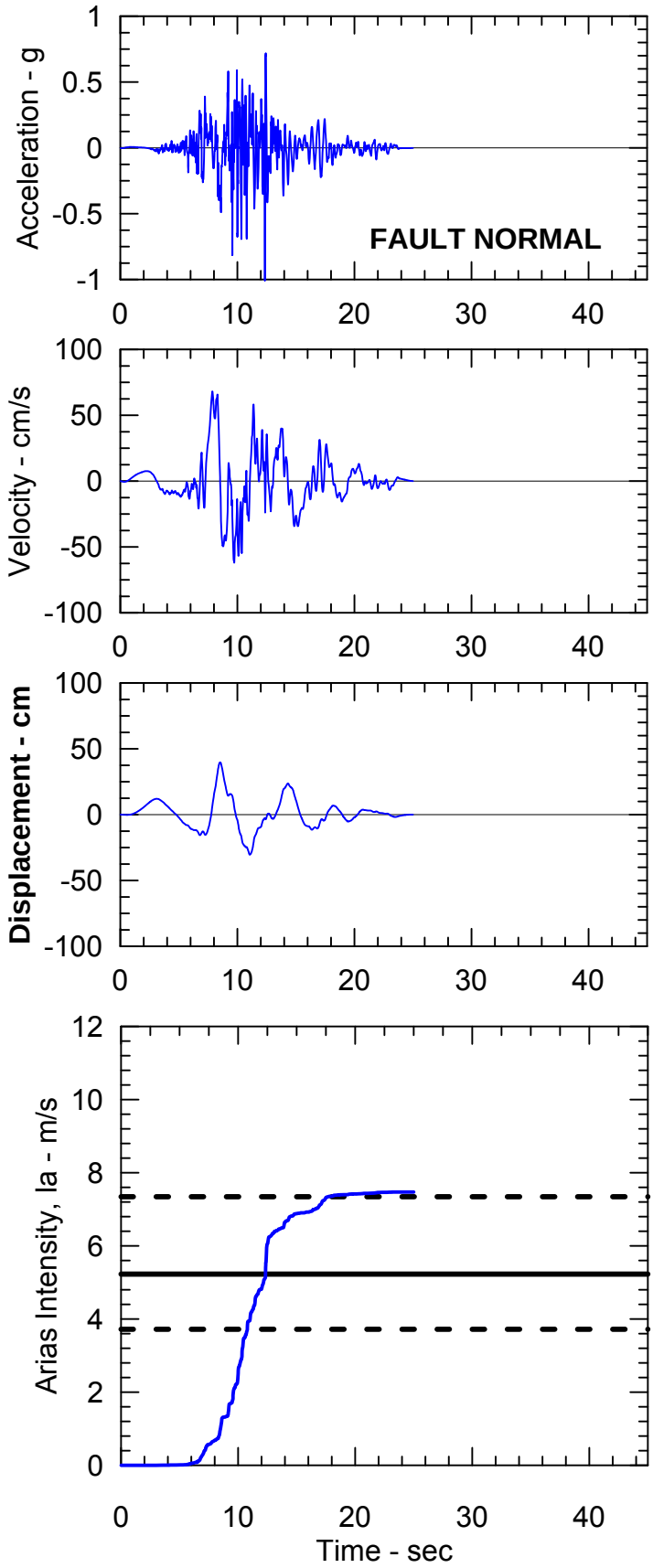

Loma Prieta - LGPC
Reverse Oblique Event
Rotated to Fault Normal
Spectrally Matched to SMV

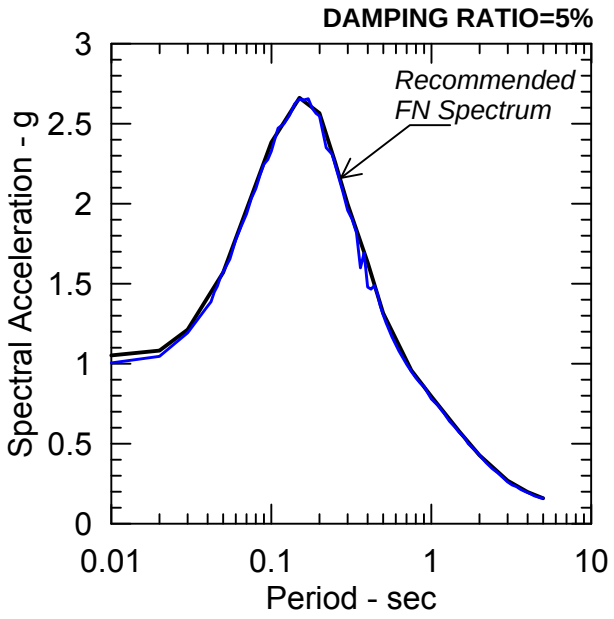

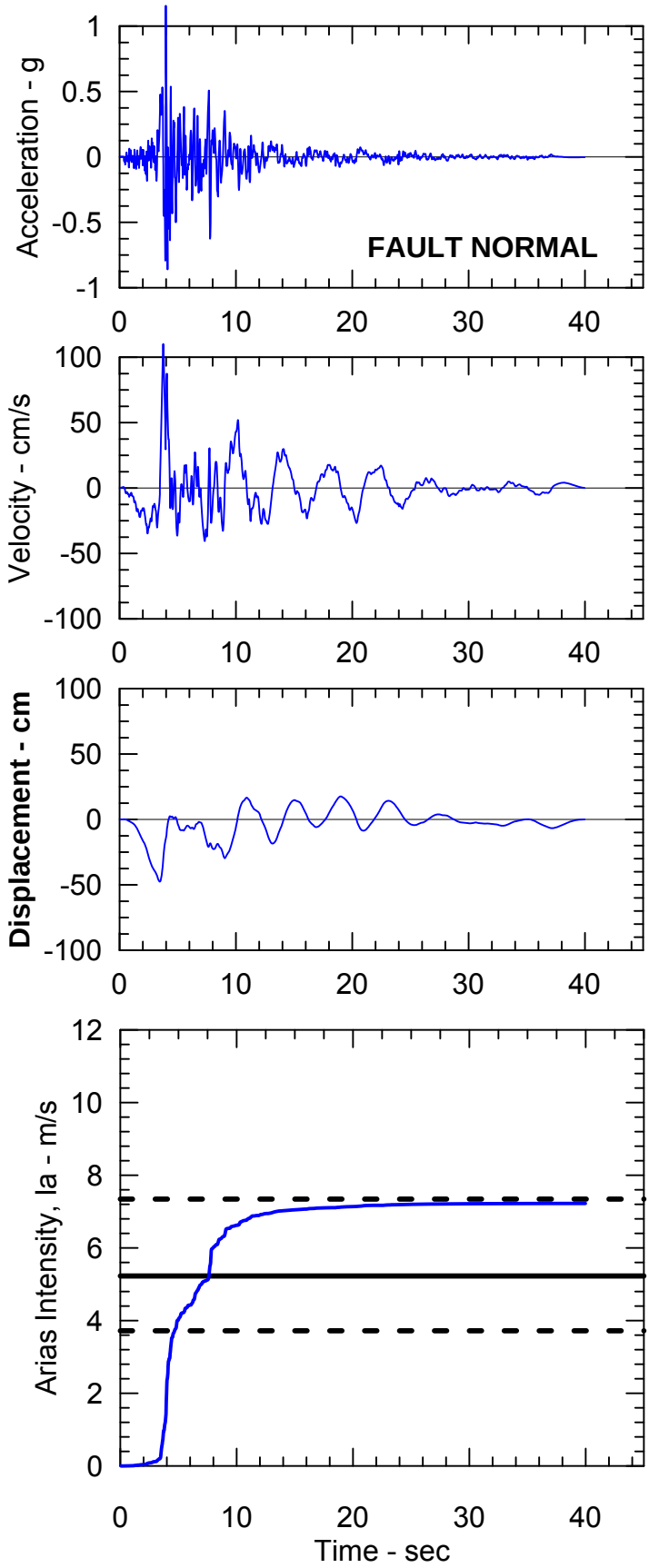

Northridge - Sylmar
Reverse Event
Rotated to Fault Normal
Spectrally Matched to SMV

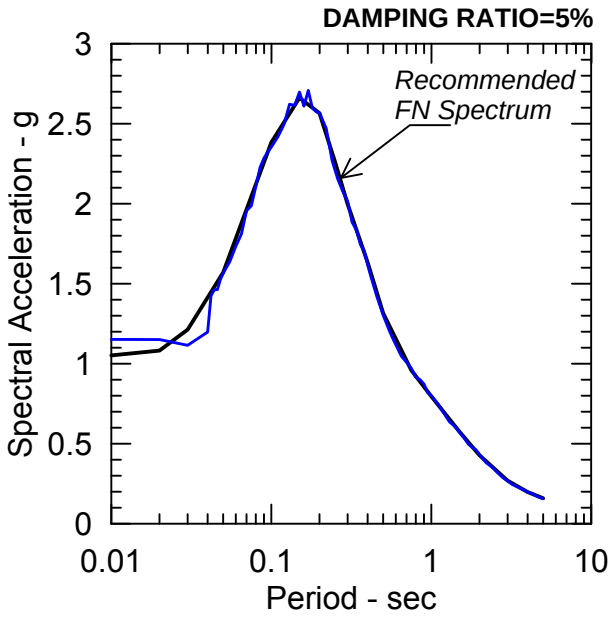

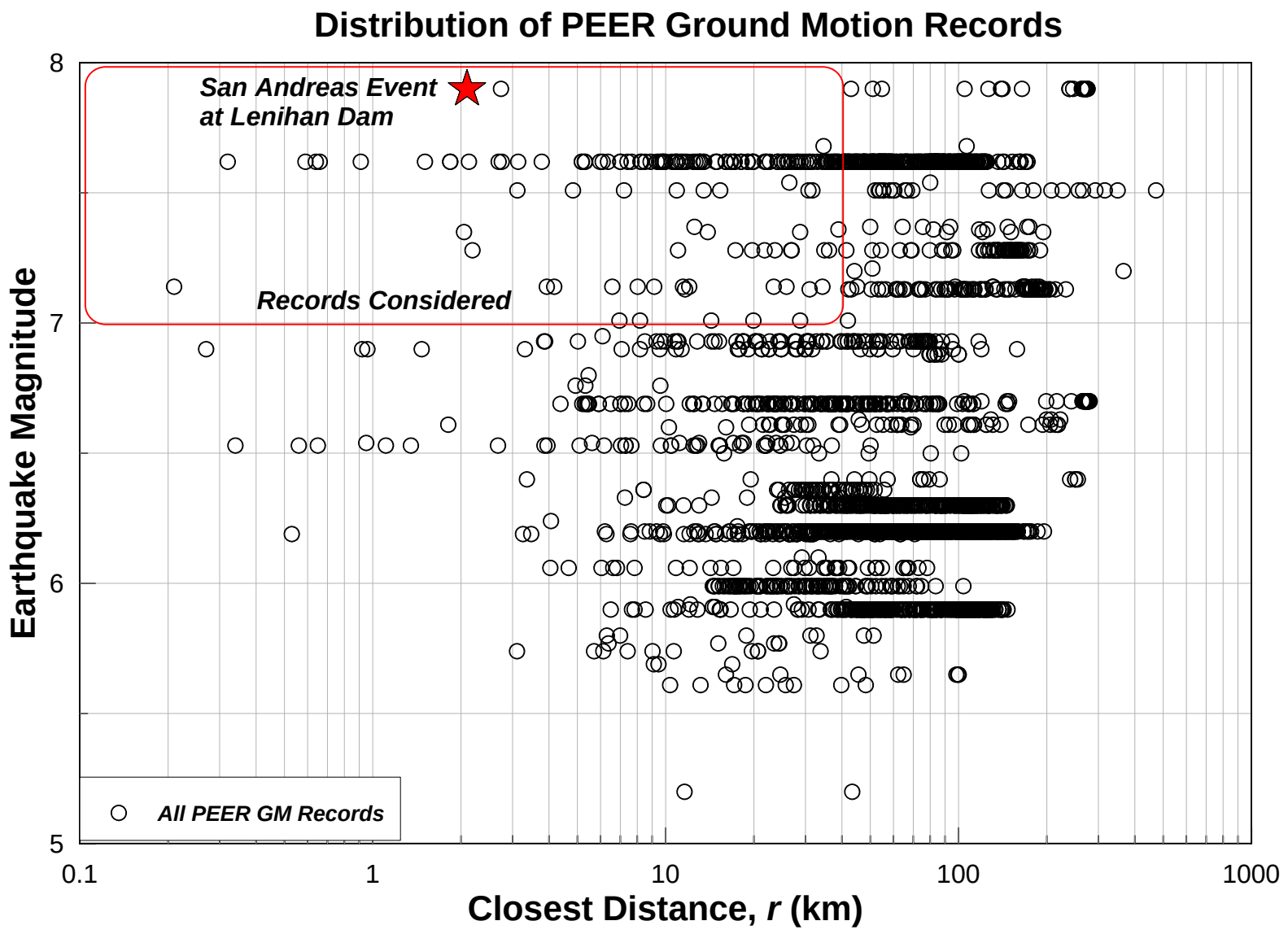

TERRA / GeoPentech
a Joint Venture

SAN ANDREAS MAGNITUDE-DISTANCE SCREENING - LENIHAN DAM
SEISMIC STABILITY EVALUATIONS (SSE2)

Figure 6-14

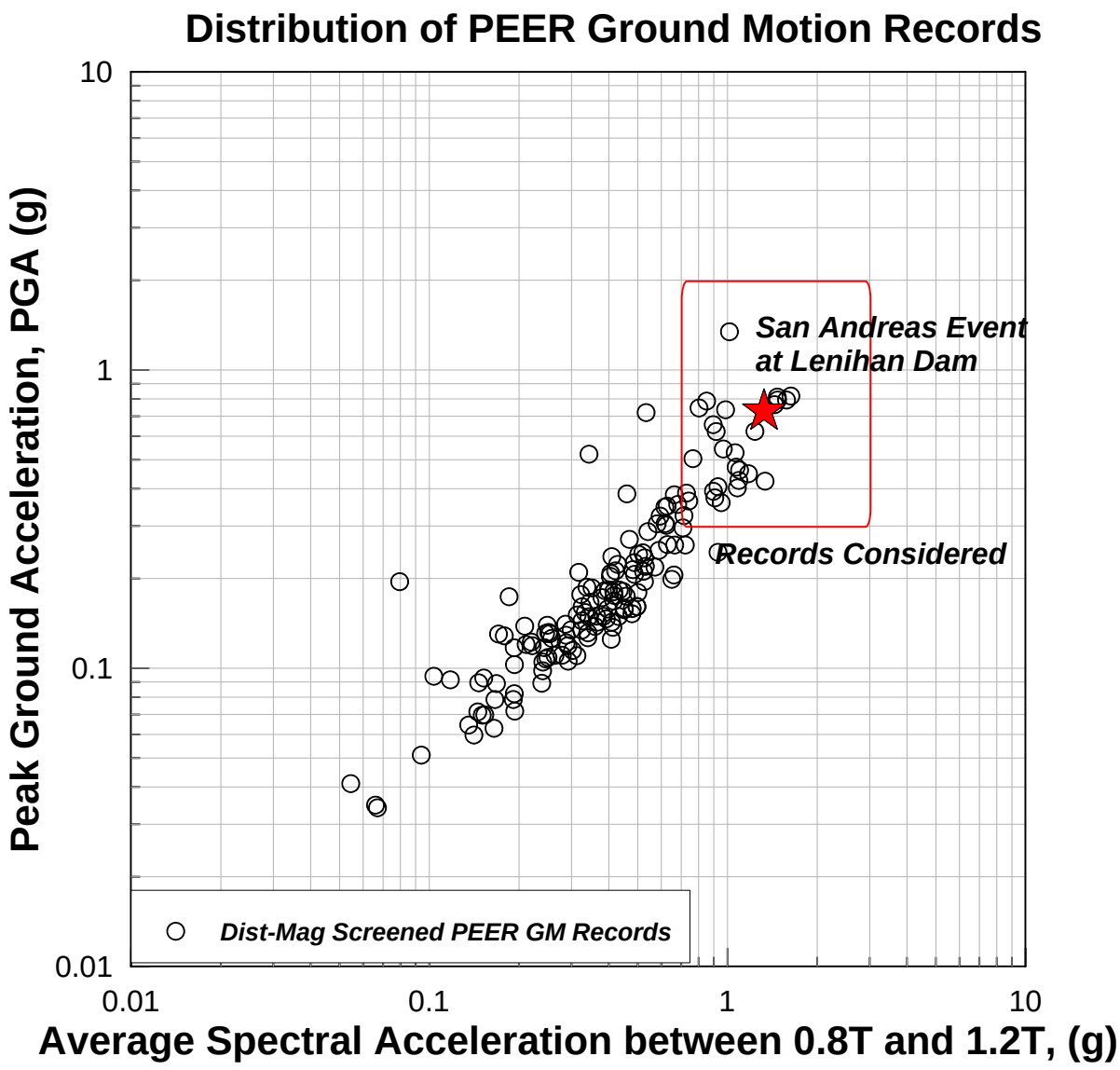

TERRA / GeoPentech
a Joint Venture

SAN ANDREAS PGA-SPECTRAL ACCELERATION SCREENING - LENIHAN DAM
SEISMIC STABILITY EVALUATIONS (SSE2)

Figure
6-15

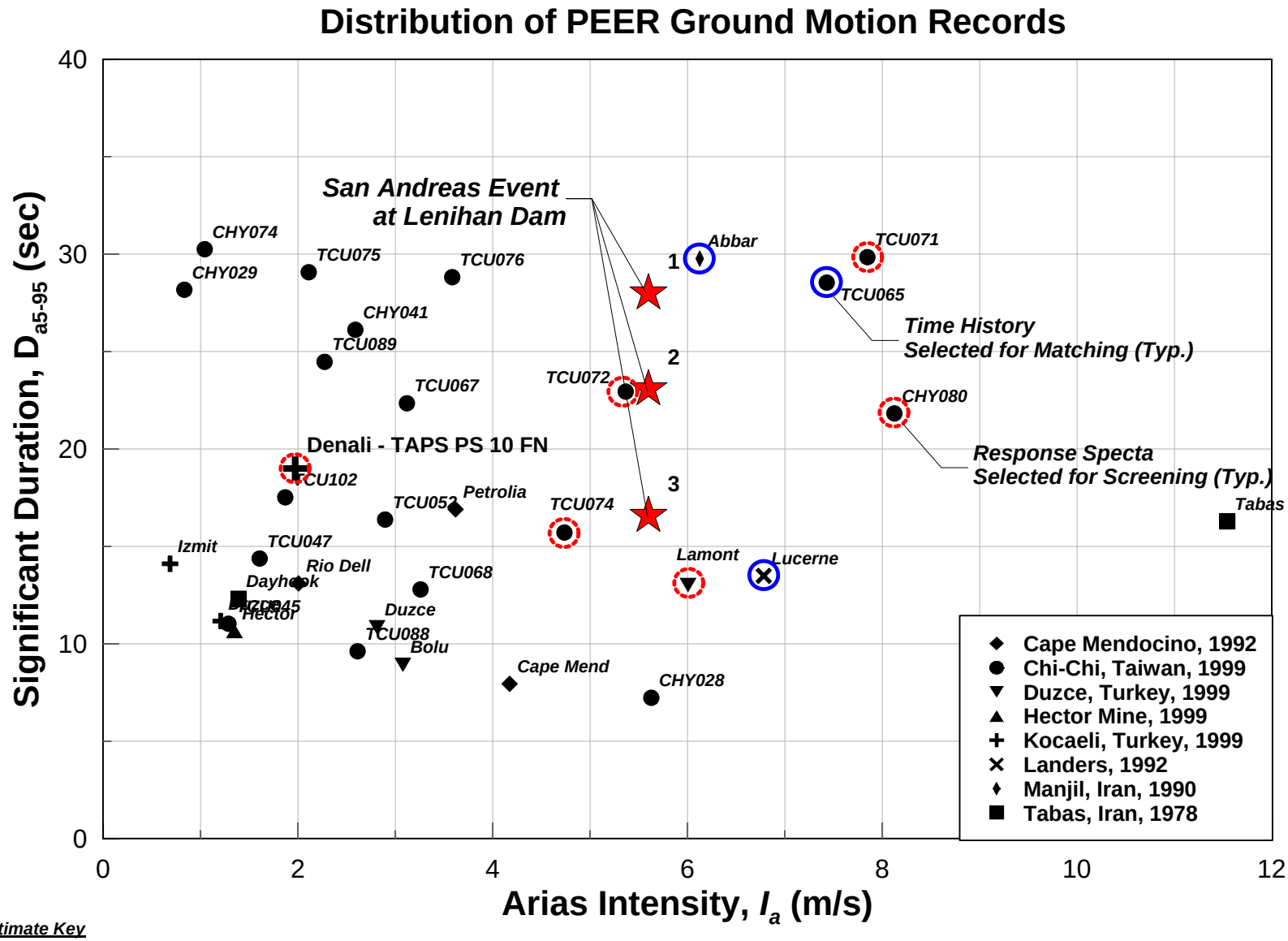

Duration Estimate Key

[1]Kempton and Stewart, 2006 wo/Directivity
[2]Kempton and Stewart, 2006 w/Directivity
[3]Bommer et. al., 2009

TERRA / GeoPentech
a Joint Venture

SAN ANDREAS DURATION-ARIAS INTENSITY SCREENING - LENIHAN DAM
SEISMIC STABILITY EVALUATIONS (SSE2)

Figure 6-16

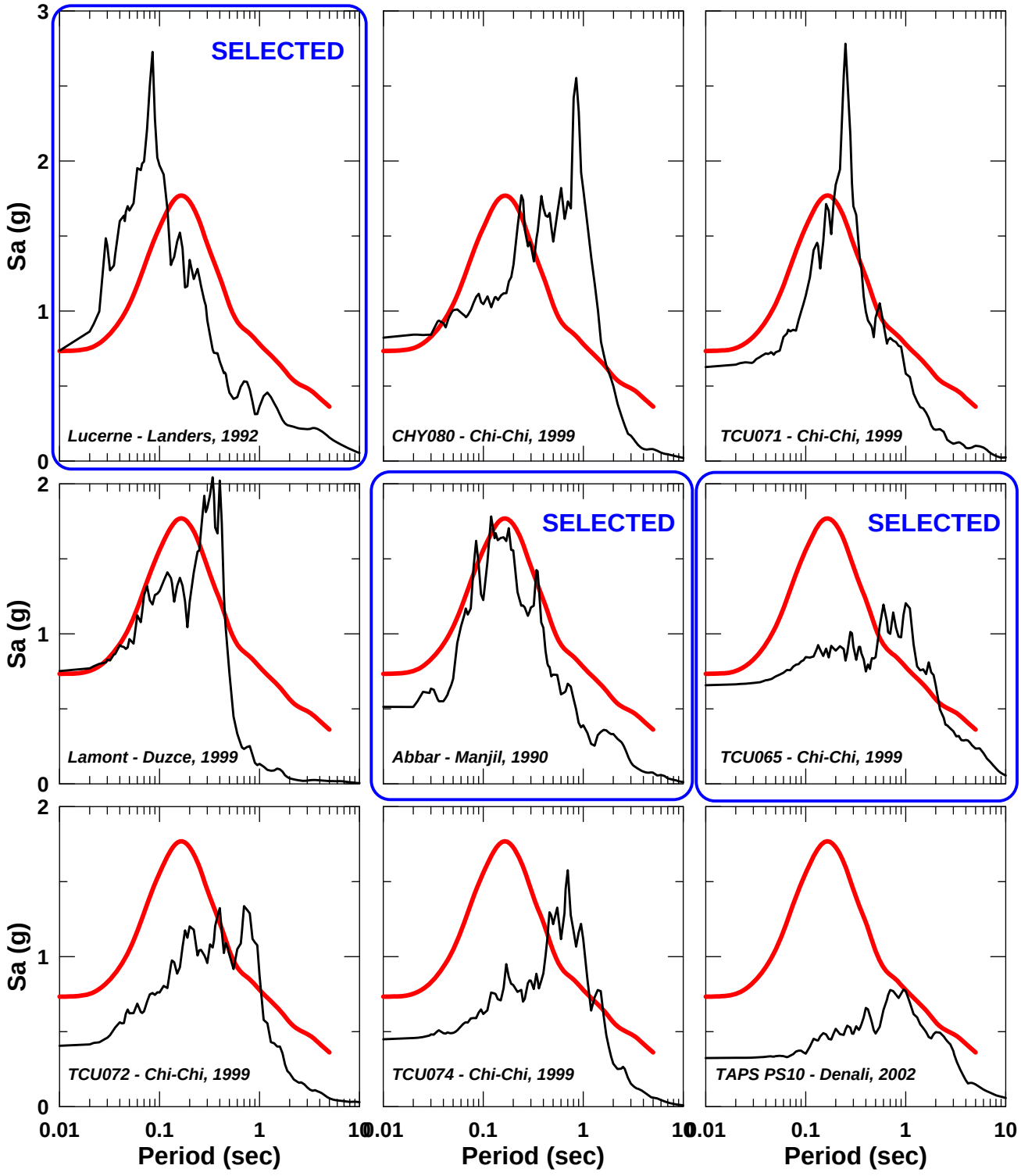

San Andreas Recommended Response Spectra vs.
Geometric Average of Acceleration Response Spectra (5% Damped)

TERRA / GeoPentech a Joint Venture	SAN ANDREAS RESPONSE SPECTRA COMPARISON - LENIHAN DAM SEISMIC STABILITY EVALUATIONS (SSE2)	Figure 6-17

Rev. 1 12/08/2011 SSE2-R-3LN

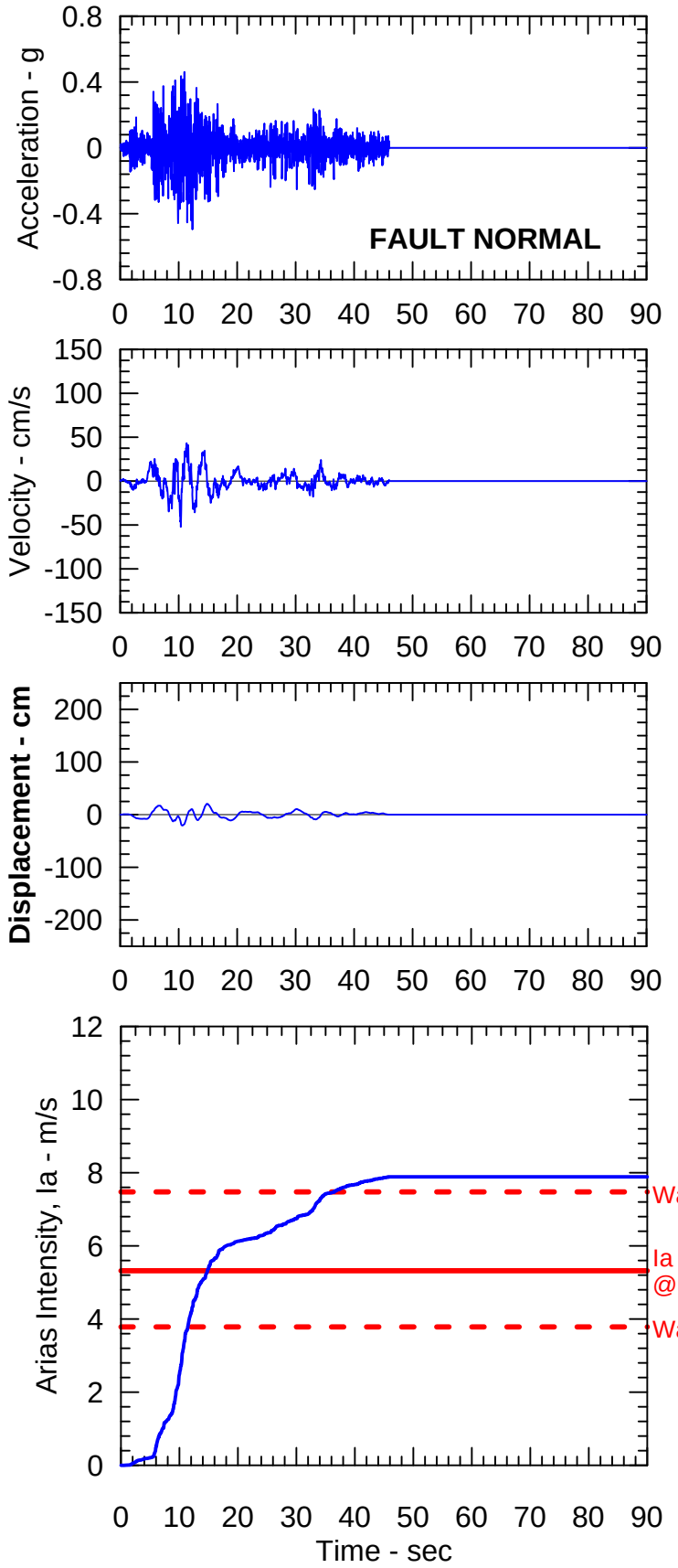

Manjil - Abbar
Strike Slip Event
Rotated to Fault Normal

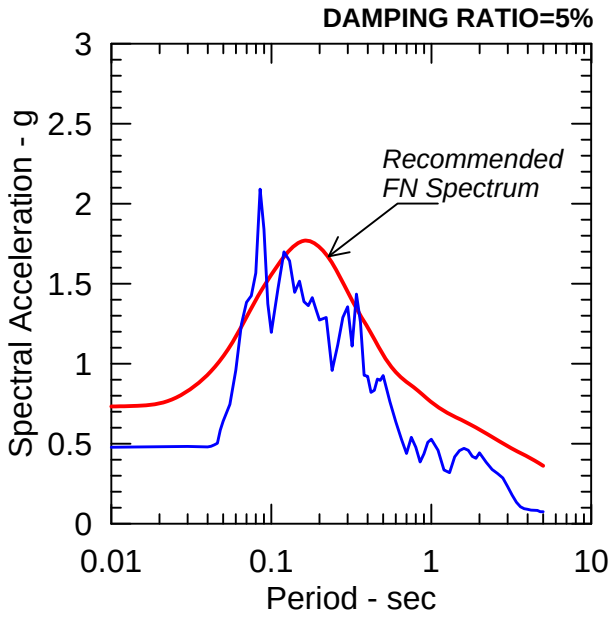

Rev. 1 12/08/2011 SSE2-R-3LN

TERRA / GeoPentech
a Joint Venture

CHARACTERISTICS OF MANJIL E/Q,
ABBAR (FN) RECORD
SEISMIC STABILITY EVALUATIONS (SSE2)

Figure
6-18

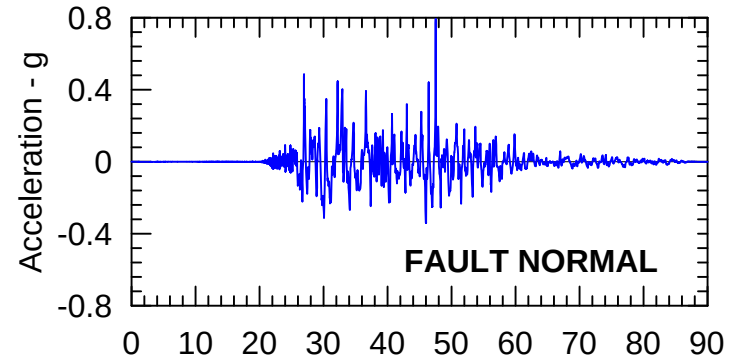

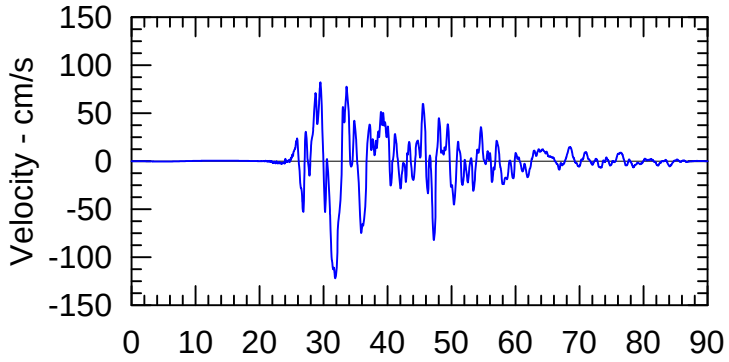

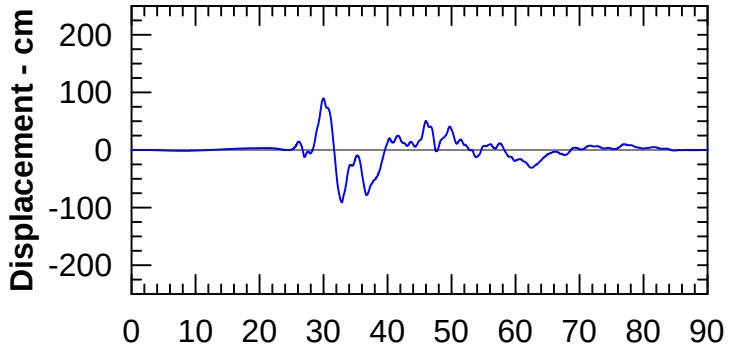

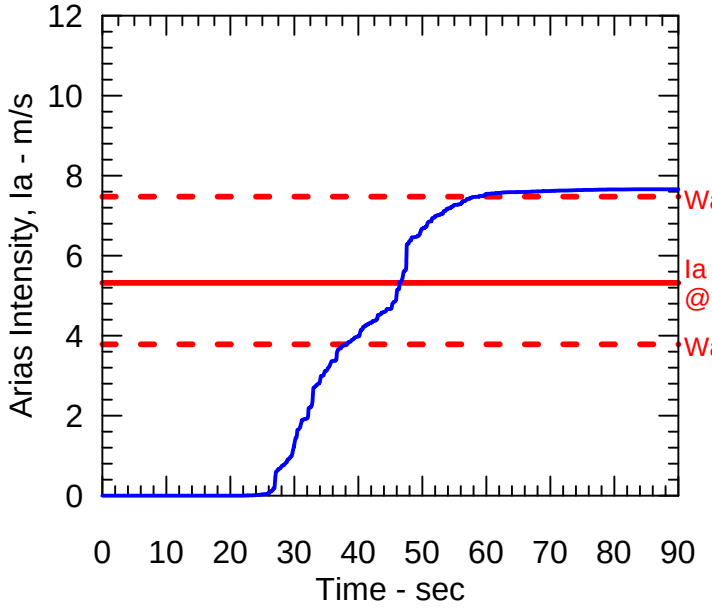

Chi Chi - TCU065
Reverse-Oblique Event
Rotated to Fault Normal

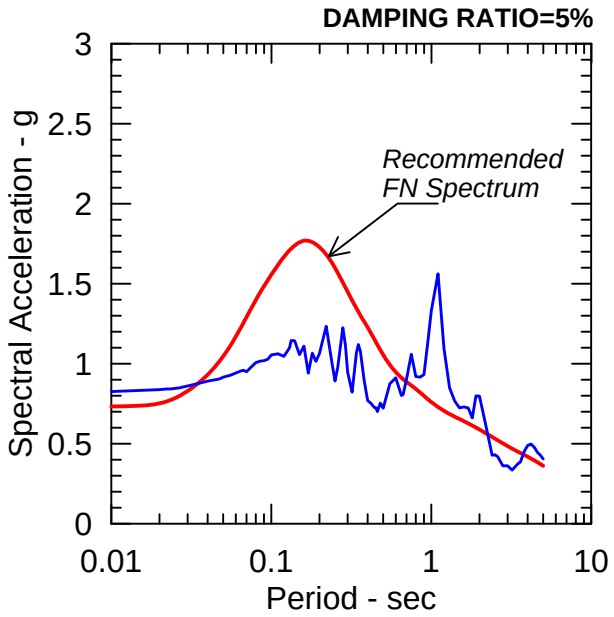

Rev. 1 12/08/2011 SSE2-R-3LN

TERRA / GeoPentech
a Joint Venture

CHARACTERISTICS OF CHI CHI E/Q,
TCU065 (FN) RECORD
SEISMIC STABILITY EVALUATIONS (SSE2)

Figure
6-19

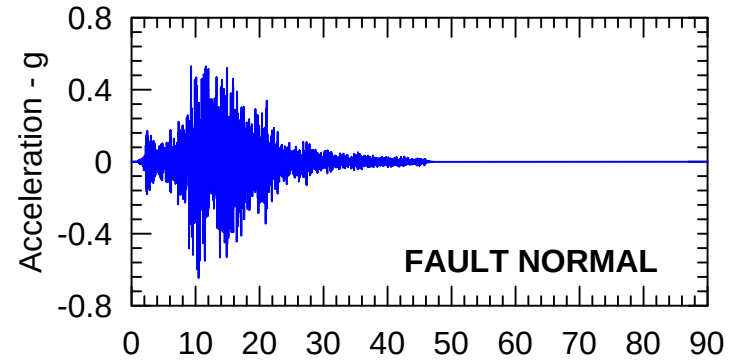

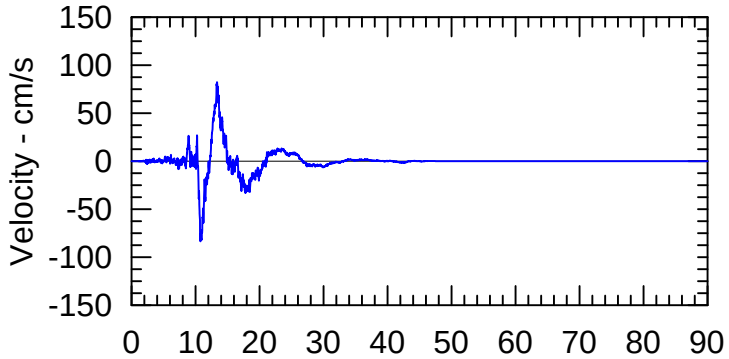

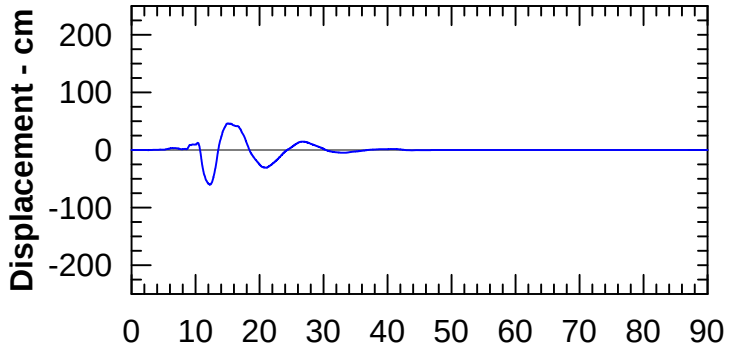

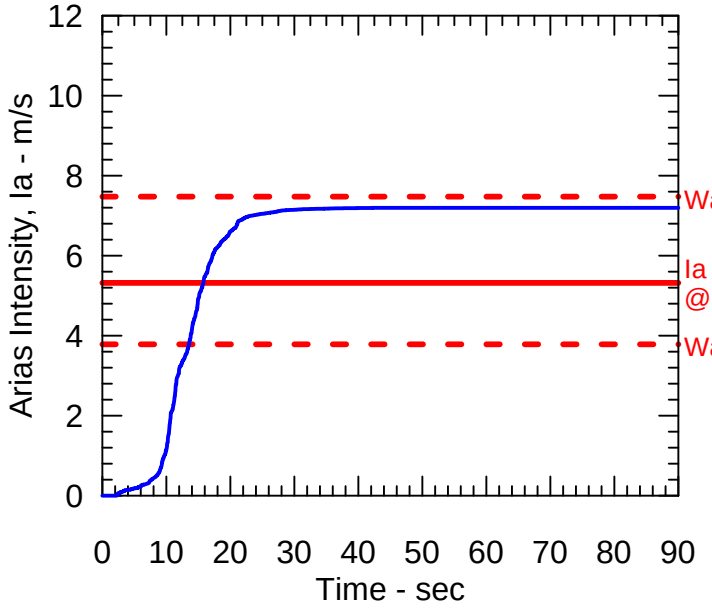

Landers - Lucerne
Strike Slip Event
Rotated to Fault Normal

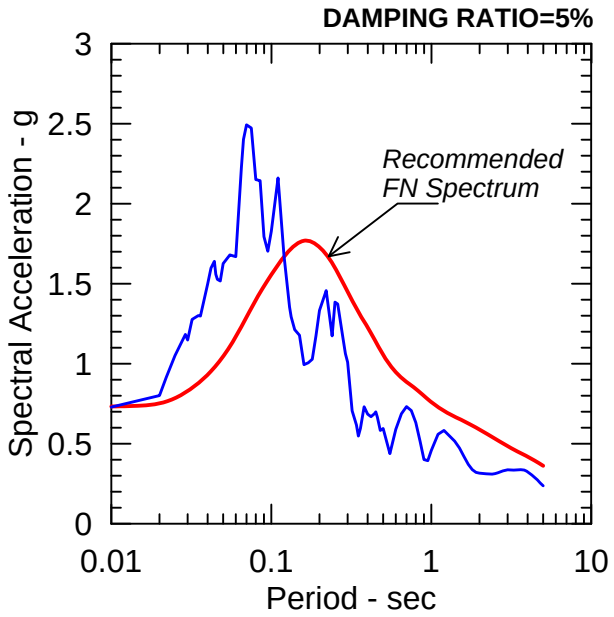

Rev. 1 12/08/2011 SSE2-R-3LN

TERRA / GeoPentech
a Joint Venture

CHARACTERISTICS OF LANDERS E/Q,
LUCERNE (FN) RECORD
SEISMIC STABILITY EVALUATIONS (SSE2)

Figure
6-20

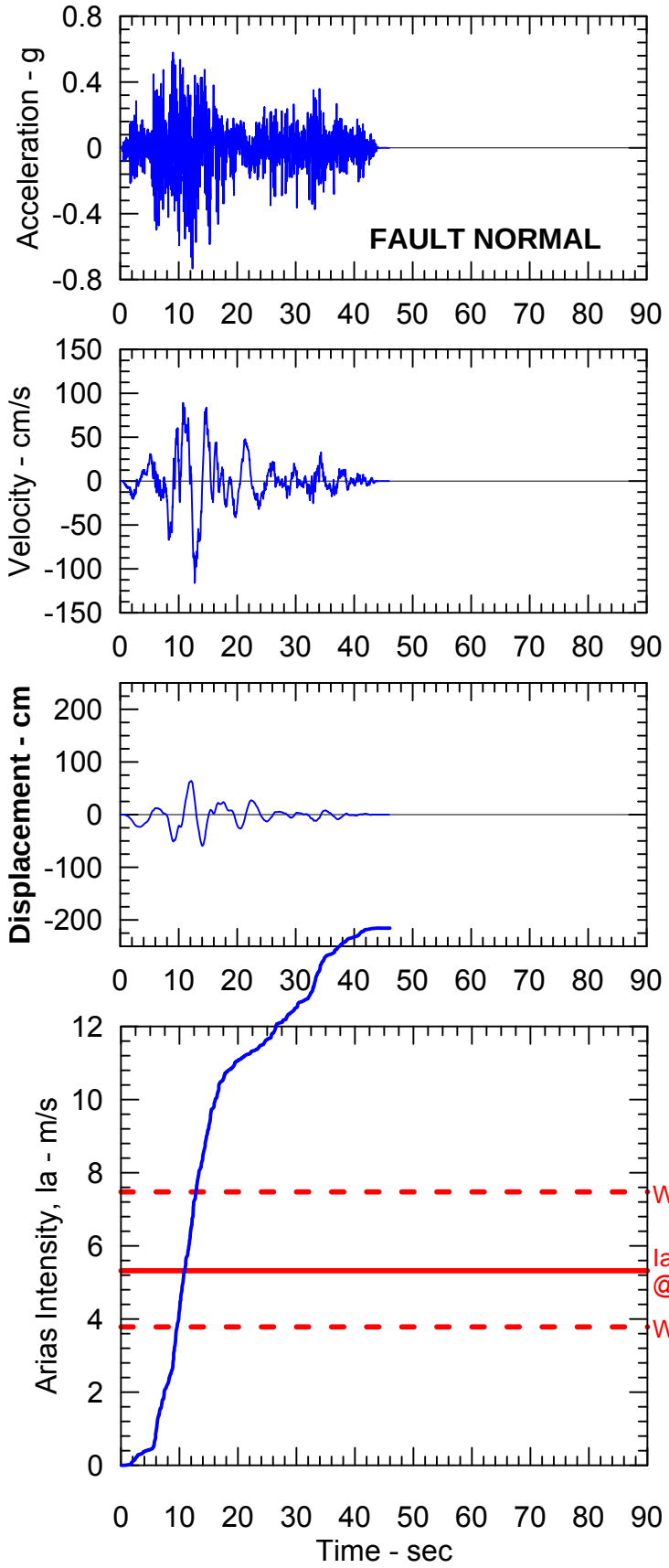

Manjil - Abbar
Strike Slip Event
Rotated to Fault Normal
Spectrally Matched to SA

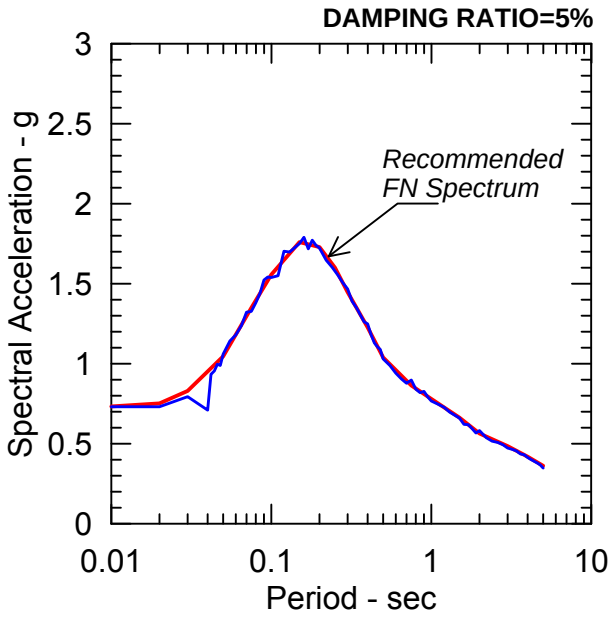

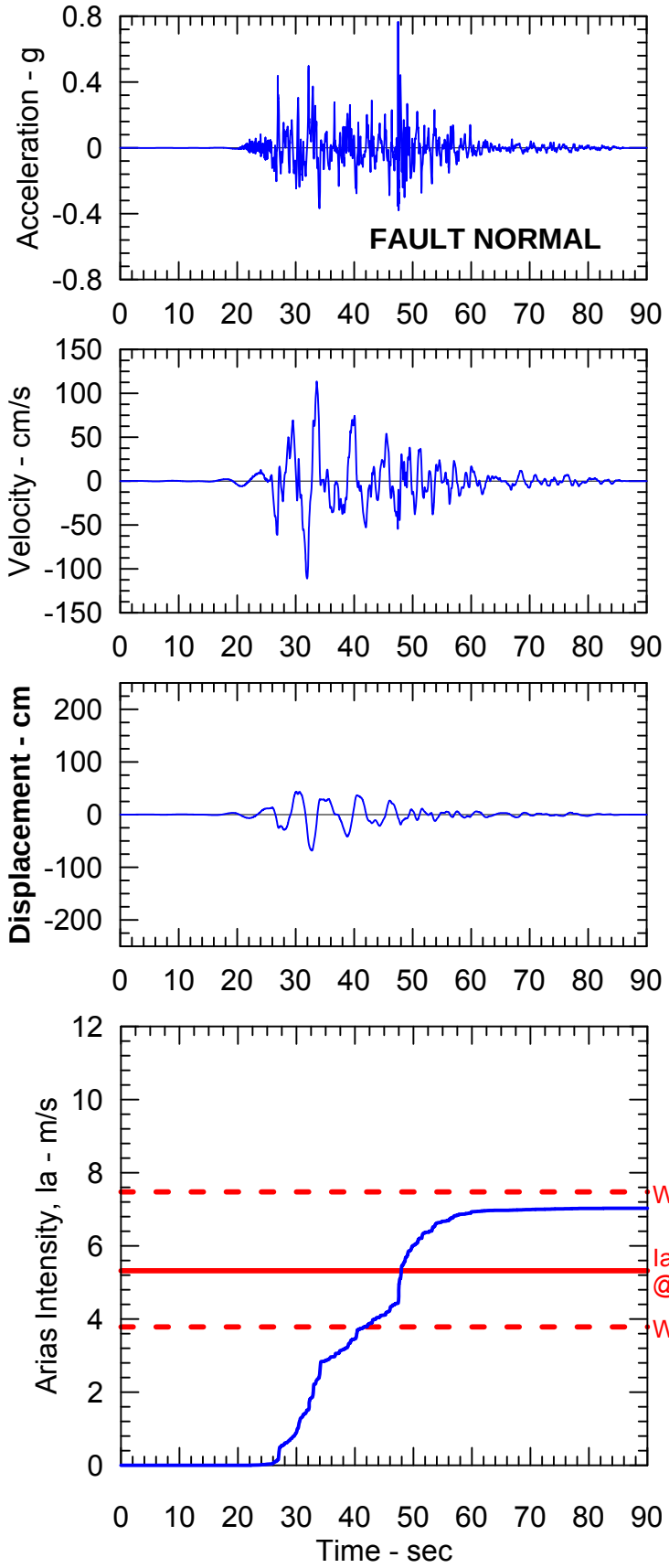

Chi Chi - TCU065
Reverse-Oblique Event
Rotated to Fault Normal
Spectrally Matched to SA

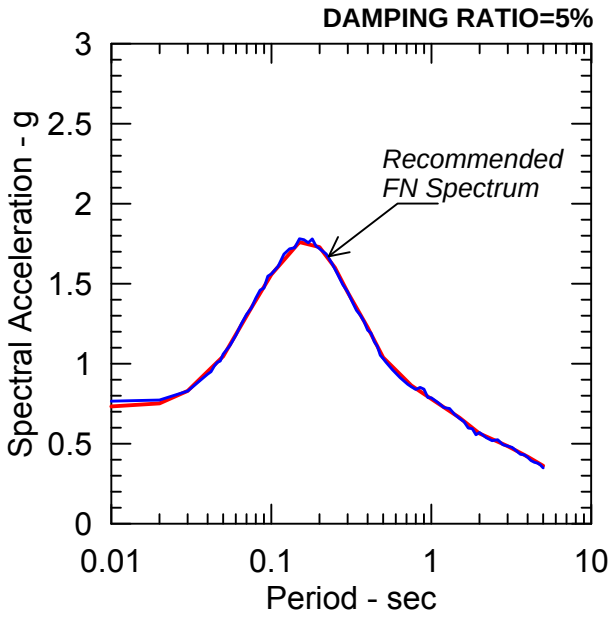

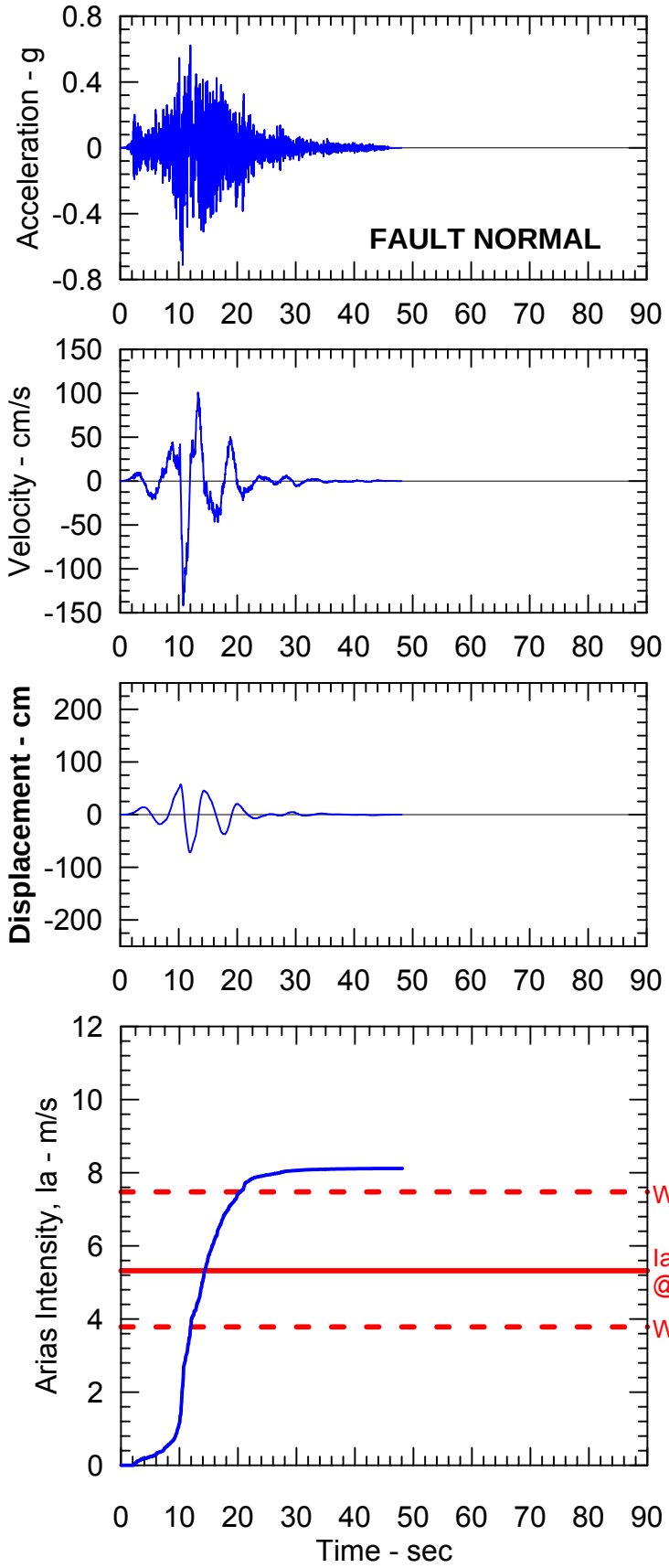

Landers - Lucerne
Strike Slip Event
Rotated to Fault Normal
Spectrally Matched to SA

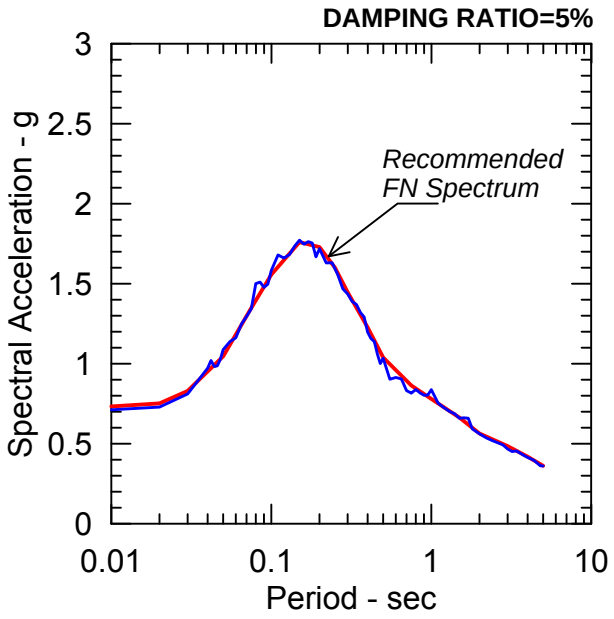

Watson-Lamprey Ia plus σ

Ia from Watson-Lamprey (2007)
@84th Percentile [5.3 m/s]

Watson-Lamprey Ia minus σ

TERRA / GeoPentech a Joint Venture	CHARACTERISTICS OF LANDERS E/Q, LUCERNE (FN) MATCHED RECORD SEISMIC STABILITY EVALUATIONS (SSE2)	Figure 6-23

Rev. 1 12/08/2011 SSE2-R-3LN